L-Glutamate uptake, decarboxylation to Γ-aminobutyric acid and GABA efflux in isolated *Asparagus sprengeri* mesophyll cells

by

Induk Chung

Department of Biological Sciences

(A thesis submitted in partial fulfilmemt of the requirement for the degree of Master of Science)

Brock University

St. Catharines, Ont.

CONTENTS

TITLES OF CONTENTS

ACKNOWLEDGEMENTS

I should like to thank Dr. Alan Walters Bown for his advice, encouragement, and patience over the past two years. His many suggestions and encouragement gave me confidence in my project and allowed me to complete this thesis successfully. I am particularly grateful Dr. Barry J. Shelp, Horticultural Science Department, University of Guelph, for his expertise, thoroughness, and valuable discussion over the last two years at Brock as well as at Guelph. Special thanks go to Lucie Tuin. I am indebted to her for many hours she spent setting up the HPLC and assisting running my samples. Working at Guelph was a different and precious experience in Canada. I thank Dr. Peter Ram, Department of Psychology for using his computer with the area measurement programme. I would like to say thank you to Lesley, Caroline, and Fang who supplied technical assistance and/or encouragement.

My last two years in Canada were the hardest time in my life. My parents, Young Lee's family, and Insook who gave me constant encouragement allowed me to complete this thesis. Thank you all.

November 1989

Induk Chung

LIST OF FIGURES

LIST OF TABLES

LIST OF MODELS

ORGANIZATION OF LITERATURE REVIEW

ORGANIZATION OF MATERIALS AND METHODS

ORGANIZATION OF RESULTS

ORGANIZATOIN OF DISCUSSION

ABSTRACT

Addition of L-glutamate caused alkalinization of the medium surrounding *Asparagus sprengeri* mesophyll cells. This suggests a H^+/L-glutmate symport uptake system for L-glutamate. However stoichiometries of H^+/L-glutamate symport into *Asparagus* cells were much higher than those in other plant systems. Medium alkalinization may also result from a metabolic decarboxylation process. Since L-glutmate is decarboxylated to Γ-amino butyric acid (GABA) in this system, the origin of medium alkalinization was reconsidered.

Suspensions of mechanically isolated and photosyntheically competent *Asparagus sprengeri* mesophyll cells were used to investigate the H^+/L-glutamate symport system, GABA production, GABA transport, and the origin of L-glutamate dependent medium alkalinization.

The major results obtained are summarized as follows :

1. L-Glutamate and GABA were the second or third most abundant amino acids in these cells. Cellular concentrations of L-glutamate were 1.09 mM and 1.31 mM in the light and dark, respectively. Those of GABA were 1.23 mM and 1.17 mM in the light and dark, respectively.
2. Asparagine was the most abundant amino acid in xylem sap and comprised 54 to 68 % of the amino acid pool on a molar basis. GABA was the second most abundant amino acid and represented 10 to 11 % of the amino acid pool. L-Glutamate was a minor

component.

3. A 10 minute incubation with 1 mM L-glutamate increased the production of GABA in the medium by 2,743 % and 2,241 % in the light and dark, respectively.
4. L-Glutamate entered the cells prior to decarboxylation.
5. There was no evidence for a H^+/GABA symport process .
6. GABA was produced by loss of carbon-1 of L-glutamate.
7. The specific activity of newly synthesized labeled GABA suggests that it is not equilibrated with a storage pool of GABA.
8. The mechanism of GABA efflux appears to be a passive process.
9. The evidence indicates that the origin of L-glutamate dependent medium alkalinization is a H^+/L-glutamate symport not an extracellular decarboxylation.

The possible role of GABA production in regulating cytoplasmic pH and L-glutamate levels during rapid electrogenic H^+/L-glutamate symport is discussed.

INTRODUCTION

An electrogenic plasma membrane-located proton pumping ATPase generates a proton electrochemical gradient across the membrane of plant cells (Sze 1985). The favored hypothesis for amino acid uptake into higher plant cells is a H^+/amino acid symport process. Influx of amino acids is coupled to the downhill flux of the proton by means of plasma membrane proteins which bind the protons and amino acids prior to their coupled entry into the cells. The main evidence for a H^+/amino acid symport process includes alkalinization of the medium, specific uptake of amino acids with stoichiometric uptake of protons, and depolarization of the plasma membrane (Reinhold and Kaplan 1984).

Recently on the basis of L-glutamate dependent medium alkalinization and specific uptake of L-glutamate, the presence of a specific H^+/L-glutamate symport system has been proposed in photosynthetically competent *Asparagus sprengeri* mesophyll cells (McCutcheon and Bown 1987). However the H^+/L-glutamate molar stoichiometry obtained was not consistent with those in other plant systems. The molar stoichiometry was 3 to 7 protons per L-glutamate. This is much higher than the 2 protons suggested for H^+/acidic amino acid symport (*e.g.* L-aspartate, L-glutamate) in sugarcane cells (Wyse and Komor 1984).

Medium alkalinization can also arise from a metabolic decarboxylation process (Reinhold and Kaplan 1984). Addition of L-glutamate stimulated CO_2 evolution and analysis of labeled

metabolites of L-glutamate demonstrated the appearance of Γ-amino butyric acid (GABA) and organic acids in the medium (McCutcheon *et al.* 1988). Thus L-glutamate dependent medium alkalinization and the high proton stoichiometries may result from metabolic decarboxylation.

The objective of the present study was to investigate the origin of medium alkalinization. Experiments were designed to answer questions concerning the mechanisms resulting in GABA appearance in the medium.

1. Is ^{14}C labeled L-glutamate decarboxylated by an extracellular enzyme prior to the entry of label into the cell ?
2. Is GABA, the decarboxylated product, transported with H^+ into the cell ?
3. Is GABA produced only in response to exogenous L-glutamate ?
4. What is the biochemical pathway of GABA production ?
5. What is the mechanism of GABA efflux ?
6. What is the physiological role of GABA production ?

LITERATURE REVIEW

I. TRANSPORT AT THE PLASMA MEMBRANE

1. Location of an ATPase at the plasma membrane

The plasma membrane (PM) - bound ATPase has been investigated in a few plant species. The PM fraction isolated from oat roots, probably contaminated with mitochondrial membranes, showed K^+ and other monovalent cation stimulated, oligomycin sensitive ATPase (Fisher and Hodge 1969). Further characterization by Fisher *et al.*(1970) again demonstrated that in oat roots ATPase was associated with membranes. This activity required Mg^{+2}, and was activated by monovalent ions, K^+ and Rb^+. The kinetics of monovalent ion-stimulated ATPase displayed Michaelis-Menten kinetics with increasing Mg^{+2}:ATP.

In plants the initial strong evidence supporting the presence of an ATPase at the PM was obtained by Hodge and colleagues (Hodge *et al.* 1972). Using discontinuous sucrose density gradient centrifugation, they isolated a PM fraction from oat roots. The membrane fraction was identified as PM by the presence of a glucan synthetase, a high sterol to phospholipid ratio, and specific stains for carbohydrate. A correlation between the K^+-stimulated component of the ATPase activity in the PM fraction and K^+ transport rate into intact oat roots was observed. Also this PM-rich fraction showed a higher substrate specificity for ATP than other nucleoside triphosphates. Thus,

on the basis of morphological or cytochemical markers, it has been suggested that plant cells contain ATP hydroyzing activity which might transport cations at the PM of higher plants.

2. Identification of an electrogenic plasma membrane proton translocating ATPase

The K^+-stimulated ATPase associated with the PM was thought to transport K^+ and other monovalent cations in plant cells (Hodge *et al.* 1972). Independent work on fungi and higher plant cells provided evidence for an electrogenic ion transport process. In the cells of oat coleoptiles and of pea epicotyls (Higinbotham *et al.* 1970), the negative inside membrane potentials of cells were higher than the ionic diffusion potential predicted by the Goldman equation. Inhibition of respiration and active ion transport by cyanide, a respiratory inhibitor, and dinitrophenol (DNP), a protonophore, rapidly reduced the membrane potential to -40 to -80 mV from 140 mV. The rapidly inhibited component of membrane potential was not ascribed to ion diffusion but strongly linked to an energy requiring electrogenic process.

Because the uncoupler reduced ATP levels as well as the electropotential, ATP was considered as an energy source for generating the membrane potential. This view was supported by Slayman *et al.* (1970). In *Neurospora crassa*, a correlation between potential and ATP level rather than NADH level suggested that ATP was the energy source for the electrogenic transport. In *Chara* Keifer and Spanswick (1979) demonstrated that uncouplers

such as carbonyl cyanide *m*-chloropheny hydrazone (CCCP) and DNP, and membrane ATPase inhibitors such as dicyclohexylcarbodiimide (DCCD) and diethylstilbestrol (DES) reduced ATP levels as well as causing the depolarization of membrane potential to the diffusion potential. These findings relating ATP levels and membrane potential confirmed that ATP was the energy source for the electrogenic ion pump at the PM.

However the identification of the ion being transported by the electrogenic ion pump still remained. In order to identify the transported ion, much work has been done. The first postulation that protons might be the ion was made by Kitasato using *Nitella* (1968). He found the large difference between the membrane conductance and the sum of conductances of K^+, Cl^- , and Na^+ fluxes. In addition he found that the membrane potential was depolarized as the external H^+ concentration increased. He suggested that the membrane conductance for H^+ might be responsible for the discrepant results with K^+, Cl^-, and Na^+ and that the PM would be permeable to H^+. However clear evidence was difficult to obtain. The assumption that H^+ might be the electrogenically transported ion was confirmed in fungi and algae by Slayman (1973) and Shimmen and Tazawa (1981), respectively. Using inhibitors, transient changes in membrane potential were found to be consistent with the fall and rise of proton efflux and ATP levels in *Neurospora* (Slayman 1973). In perfused cells of *Chara* the net H^+ efflux was stimulated when the perfusing medium containing Mg^{+2}:ATP (Shimmen and Tazawa 1981). The idea

of the presence of an electrogenic H^+ pumping ATPase at the PM is now accepted in algal cells, fungi and higher plants.

3. The Proton electrochemical gradient and solute accumulation

An electrogenic PM proton pumping ATPase generates both an electrical potential and a pH gradient. Relative to the outside the interior of the cell has a high pH and a negative charge. The pH gradient and membrane potential have been measured in PM inside-out vesicles. Labeled weak acids, weak bases, or optical probes for pH gradient have been used to demonstrate that intravesicular acidification is correlated with ATP hydrolysis. Also a positive interior membrane potential was examined by accumulation of labeled permeable anions across the vesicle (O'Neill and Spanswick 1984a, Rasi-Caldogno *et al.* 1985).

The energy content of the proton electrochemical gradient is expressed by the proton electrochemical potential difference, $\Delta\tilde{\mu}_H+$. The total energy available in such a proton electrochemical gradient in units of millivolts at 30° C is described by

$$\Delta\tilde{\mu}_H+ = \Delta\psi - 0.06\ \Delta pH$$

where $\Delta\psi$ is the membrane potential in volts, and ΔpH is the pH difference. *i.e.* a proton concentration gradient (ΔpH) and an electrical gradient ($\Delta\psi$) are two related terms that comprise the electrochemical gradient generated by a proton translocating ATPase. This proton motive force or proton electrochemical gradient generated by the proton pump provides the driving force

for transport of solutes as well as their accumulation into the cells (Nicholls 1982).

4. Characterization of the electrogenic plasma membrane ATPase

A proton translocating ATPase has been well characterized in isolated membrane vesicles as well as reconstituted proteoliposomes from red beet, radish seedling, and corn leaf mesophyll cells. Properties of the PM bound H^+-ATPase of membrane vesicles and of the reconstituted enzyme show similarities with respect to K^+-stimulation, monovalent cation specificity, optimum pH, substrate specificity, and inhibitor sensitivity. The H^+-ATPase consists of a peptide of 100 Kdalton which contains the phosphorylation and ATP binding sites. The H^+-ATPase is Mg^{+2}-dependent, and cation-stimulated. The order of monovalent cation stimulation is $K^+ > Rb^+ > Na^+ > Li^+ > Cs^+ >$ $choline^+$, and divalent cation requirement is $Co^{+2} > Mg^{+2} > Mn^{+2} > Zn^{+2} > Ca^{+2}$. There is no synergistic stimulation by K^+ and Na^+ unlike the Na^+ / K^+ ATPase found at the PM of animal cells. The optimum temperature and pH are 40°C, and 6.5 respectively. The kinetics with increasing Mg^{+2}:ATP obeyed Michaelis-Menten kinetics with a Km of 0.3 mM. The enzyme activity is inhibited by vanadate, DCCD, and DES, and is insensitive to oligomycin, azide, ouabain, molybdate, and anions (Perlin and Spanswick 1981, Harvastein and Nissen 1981, Briskin and Poole 1983, 1984, O'Neill and Spanswick 1984b, Serrano 1984, Rasi-Caldogno *et al.* 1985).

5. H^+ / Amino acid symport

Living plant cells are able to accumulate nutrients, such as inorganic ions, amino acids, and sugars to greater concentrations than their surrounding environment. The chemiosmotic theory developed by Peter Mitchell to explain energy transduction in mitochondria, chloroplasts, and bacteria emphasized the importance of the proton gradient in energy transduction at biological membranes. After the chemiosmotic theory was developed, many researchers tried to explain the transport mechanisms of these nutrients in fungi, algae, and plants in terms of proton movements. As a result it is suggested that the active transport of many nutrients involves the operation of a H^+ symport (Nicholls 1982).

The proton electrochemical gradient generated by ATP dependent proton pumping provides the driving force for transport of solutes. The influx of substrate is coupled to the downhill flux of the proton by means of a carrier system which binds the protons and the substrates prior to their coupled entry into the cell. The favored hypothesis to account for amino acid uptake into higher plant cells is a H^+/amino acid symport system.

A proton symport system for amino acids is indicated by general criteria which include (1) alkalinization of the medium surrounding the cells, (2) depolarization of the membrane potential, (3) specificity of uptake, and (4) saturation kinetics (Reinhold and Kaplan 1984). In algae there seems to be a common carrier transporting all amino acids with low specificity. This

common carrier system is supported by a demonstration of the mutual competitive inhibition of transport between amino acids. Evidence suggesting several carriers have also been published (Kinraide and Etherton 1980, Wyse and Komor 1984, Borstlap *et al.* 1986). Sugarcane suspension cells show competitive uptake between neutral amino acids, basic amino acids, or acidic amino acids, suggesting three different carrier systems for neutral, basic, and acidic amino acids (Wyse and Komor 1984). Each system has a different molar stoichiometry for protons. *i.e.* 1 H^+ per neutral amino acids, 2 H^+ per acidic amino acids, and a uniport for basic amino acids.

The specificity of H^+/amino acid symport might vary from species to species and tissue to tissue. A free living algae or cultured cells may be adapted to take up all amino acids from their bathing medium. Conversely cells exposed to a defined constant medium such as xylem fluid may have specific uptake system appropriate to the solute presented to the cell.

6. H^+ / Amino acid symport and accumulation ratio

An accumulation ratio is expressed as

$$\log \frac{[X^m]_o}{[X^m]_i} = \frac{\Delta\psi (m + n)}{0.06} - n\Delta pH$$

where m is the ion charge of the amino acid, n is the number of protons symported, $\Delta\psi$ is the membrane potential in volts, ΔpH is

the pH gradient across the plasma membrane, and $\log ([X^m]_o/[X^m]_i)$ is the accumulation ratio (Nicholls 1982). This mathematic equation indicates that when the ratio of external to internal concentration is maintained constant, the progress curve of solute uptake gradually decreases and reaches a plateau.

A progress curve for amino acid uptake showing a maximal uptake has been obtained in algae (Sauer *et al.* 1983), and higher plants (Cheung and Nobel 1973, Rubinstein and Tatter 1980, Suzuki 1981). The rate of [^{14}C]Leucine (Leu) in *Vinca* protoplast was linear for 20 minutes then reached a plateau after 80 minutes (Suzuki 1981). [^{14}C]Glycine (Gly) uptake into leaf segments of *Pisum* increased linearly for 2 hours then attained a plateau at 3 hours. Under aerobic conditions, the rate of Gly uptake was the same in the light and dark. When N_2 was supplied, Gly uptake in the dark ceased whilst that in the light was 50 % of uptake under aerobic conditions, suggesting the involvement of metabolism of Gly (Cheung and Nobel 1973). In *Chlorella* cells, the time curves of arginine (Arg) and proline (Pro) accumulation showed plateaus after 2 hours. Both plateaus resulted from a decrease of influx rather than an increase of efflux. Accumulation ratios were calculated at three different initial external concentrations of both amino acids. The accumulation ratios decreased with increasing external concentration of amino acids. After 2 hours, the internal concentrations of free Pro were 55, 56 and 54 mM with an initial external concentration of

1, 5 and 20 mM, respectively. The corresponding accumulation ratios were 277-, 13- and 2.8-fold. The concentrations of inside free Arg were 64, 65 and 92 mM with 1, 5 and 20 mM initial outside concentrations and with corresponding accumulation ratios of 1294, 4 and 4.9. Since this accumulation ratio of 1200-fold was much higher than that expected from the electrical potential of -130 mV, H^+/Arg symport was suggested (Sauer *et al.* 1983). An effort has been made to obtain theoretical accumulation ratios in leaves and protoplasts of oat mesophyll cells (Rubinstein and Tatter 1980). Assuming a pH gradient of 1.5, and a membrane potential of 0.065 volt, they obtained a theoretical accumulation ratio of 400 in leaves which is close to the experimental value of 300 in protoplasts.

Obtaining the theoretical accumulation ratio is often impeded by several factors such as the difficulty in measuring internal pH, the non-homogeneous distribution of lipophilic cations in measuring $\Delta\psi$, the metabolism of transported amino acids, and possible cell aging before attaining a steady state (Rubinstein and Tatter 1980). In addition it is possible that failure to attain theoretical accumulation ratios indicates control by the internal concentration.

7. H^+ / L-Glutamate symport in isolated *Asparagus* cells

Evidence for H^+/L-glutamate (L-Glu) symport has been suggested in both bacteria and the higher plants (Mitchell *et al.* 1979, Chapman and Meeks 1983, McCutcheon and Bown 1987,

McCutcheon *et al.* 1988).

Mitchell and colleagues reported accumulation of L-Glu in *Staphylococcus aureus* when the electrical potential gradient was collapsed using valinomycin. The accumulation of L-Glu was increased by decreasing the pH of the cell suspension medium. When L-Glu was added to the surrounding medium of cells, slight medium alkalinization could also be detected. Comparison of the initial rate of proton uptake and that of L-Glu uptake over 15 minutes at pH 6.5 gave a stoichiometry of 2 protons per 1 L-Glu transported (Mitchell *et al.* 1979). A kinetic study of L-Glu uptake was performed in a dinitrogen-fixing cyanobacterium *Anabaena variabilis* (Chapman and Meeks 1983). Using the L-Glu structural analogs, L-glutamine (L-Gln) and L-methionine-D,L,-sulfoximine (L-MSO), the kinetics of L-Glu transport could be characterized in terms of kinetic parameters. In competitive uptake experiments with L-Glu, L-Gln, and L-MSO, it was shown that L-Glu and L-Gln are transported by low and high affinity systems and MSO is transported by a high affinity system. Thus L-Glu may be transported by more than one system. It is unclear from the evidence whether the high and low affinity systems represent separate transport proteins or a single system which can undergo conversion to a low affinity system as the concentration increases.

Recent evidence indicates the presence of highly specific H^+/L-Glu symport system in the higher plant, *Asparagus sprengeri* (McCutcheon and Bown 1987, McCutcheon *et al.* 1988).

Upon addition of many different amino acids to suspensions of mechanically isolated *Asparagus* mesophyll cells, only L-Glu and L-MSO caused immediate and transient medium alkalinization. The uptake of L-Glu was not inhibited by L-aspartate (L-Asp) and D-Glu but was inhibited by an excess of L-MSO. The transport of L-Glu was further characterized by varying the proton motive force. When the pH gradient and membrane potential gradient were collapsed by CCCP, L-Glu dependent medium alkalinization and uptake of L-Glu were significantly decreased. As the pH_o was decreased from 6.5 to 5.5, L-Glu dependent medium alkalinization and uptake were increased. Also L-Glu dependent medium alkalinization and uptake of L-Glu were stimulated when cells were exposed to fusicoccin (FC). FC stimulated H^+ efflux in *Asparagus* cells and has been shown to cause hyperpolarization in other tissues (Marre 1979). Similarly high concentration of K^+ which is known to depolarize membrane potentials inhibited L-Glu dependent alkalinization and uptake. The results obtained indicate a highly specific electrogenic H^+/L-Glu symport in *Asparagus* mesophyll cells (McCutcheon and Bown 1987).

Several results obtained with *Asparagus* cells are not consistent with those in bacteria or other plant systems. The molar stoichiometry of H^+/L-Glu symport into *Asparagus* was estimated to be 3 to 10 protons which is far higher than 2 protons reported in *Staphylococcus* and sugarcane (Mitchell *et al.* 1979, Wyse and Komor 1984). Often experimental H^+/solute stoichiometries in symport systems are less than 1 because of

export of H^+ by the plasma membrane (Hutchings 1978, Robinson and Beevers 1981). Although 3 to 10 protons were apparently taken up into the cells for every L-Glu, there was no evidence for a repolarizing K^+ efflux. Therefore questions arise concerning the fate of the 3 to 10 protons transported, maintenance of electroneutrality and the possibility of overestimation of the stoichiometry resulting from the loss from the cells of radioactive L-Glu metabolites. In addition Reinhold and Kaplan (1984) have suggested that medium alkalinization may arise from a metabolic decarboxylation process.

$$RCOO^- + H^+ \text{------>} RH + CO_2$$

Consequently the origin of the medium alkalinization should be reconsidered. Perhaps L-Glu dependent alkalinization and the unusually high stoichiometries result from metabolism not symport.

Recent studies were carried out to elucidate the origin of L-Glu dependent medium alkalinization by *Asparagus* cells through simultaneous measurement of L-Glu dependent medium alkalinization and CO_2 evolution (McCutcheon *et al.* 1988). Upon addition of L-Glu to the cell suspension medium, medium alkalinization was immediate and reached a maximum pH value after 45 minutes. However CO_2 evolution exhibited a lag period before its release and continued in a linear manner for upto 100 minutes. This separation of alkalinization from decarboxylation was supported using the analog L-MSO. This has been already shown to be transported by carriers which recognize L-Glu

(Chapman and Meek 1983, McCutcheon and Bown 1987). L-MSO and L-Glu both caused alkalinization. However L-Glu stimulated CO_2 evolution but L-MSO did not. Thus it appears that the origin of alkalinization is not a decarboxylation process (McCutcheon *et al.* 1988).

II. L-GLUTAMATE METABOLISM

1. L-Glutamate and the photorespiratory nitrogen cycle

In photosynthetic cells of C_3 plants NH_4^+ is assimilated into organic nitrogen by the combined action of glutamine synthetase (EC.6.3.1.2)/glutamate synthase (EC.1.4.7.1) (glutamine : 2-oxoglutarate aminotransferase (EC 1.4.7.1.)) (GS/GOGAT) and glutamate dehydrogenase (GDH) (EC.1.4.1.3) (Miflin and Lea 1980). The majority of this NH_4^+ is released in photorespiration by the mitochondrial glycine decarboxylase enzyme.

GS ; L-Glutamate + NH_4^+ + ATP

------> L-Glutamine + ADP + Pi + H^+

GOGAT ; L-Glutamine + 2 ferredoxin $_{red}$ + α-ketoglutarate

<------> 2 L-Glutamate + 2 ferredoxin $_{ox}$

GDH ; α-Ketoglutarate + NH_4^+ + NAD(P)H

<------> L-Glutamate + $NAD(P)^+$ + H_2O

In chloroplasts, GS catalyses an ATP-dependent incorporation of NH_4^+ into L-Gln. L-Gln and α-ketoglutarate (α-KG) are converted into two L-Glu molecules by ferredoxin-linked GOGAT. In mitochondria, GDH may be involved in NH_4^+ assimilation into L-Glu (Yamaya *et al.* 1984, 1986).

Although the flux of NH_4^+ in photorespiration is very high, it does not accumulate. The Km of GS for NH_4^+ is much

lower than that of GDH, consequently GDH is unlikely to assimilate significant amounts of NH_4^+. Therefore, the chloroplastic GS/GOGAT pathway rather than GDH seems to be major route for assimilating NH_4^+ into L-Glu (Hartman and Ehmke 1980, Nauen and Hartman 1980, Wallsgrove *et al.* 1987).

2. Glutamate decarboxylase (GAD)

L-Glu catabolism to GABA involves a decarboxylation reaction catalyzed by GAD (EC.4.1.1.15).

L-Glutamate ------> GABA + CO_2

GAD is widely distributed in higher plants (Wickremasinghe and Swain 1965, Spedding and Wilson 1968, Streeter and Thompson 1972b, Chou and Splittsoesser 1972, Koiwai and Noguchi 1972, Collins and Wilson 1975, Jordan and Givan 1979, Walker *et al.* 1984, Melcher 1986, Satyanarayan and Nair 1985, Tsushida and Murai 1987). It has also been purified and characterized from embryos and roots of barley (Inatomi and Slaughter 1975), potato tubers (Satyanarayan and Nair 1985) and tea leaves (Tsushida and Murai 1987).

GAD activity appears to be highly pyridoxal phosphate (PLP) dependent. In crude extracts of barley embryos and tea leaves, the activity of GAD was activated 2.5 to 3.5 times by saturating concentrations of PLP (Inatomi and Slaughter 1975, Tsushida and Murai 1987). In the absence of added PLP, the purified GAD from potato extract absorbed strongly at 388 nm, a value identical with the absorption maximum for authetic PLP. It

was also calculated that at least 2 molecules of PLP are bound per molecule of isolated enzyme (Satyanarayan and Nair 1985).

The Km values for barley embryos are approximately 22 mM (Inatomi and Slaughter 1975) and 25 mM for wheat (Cheng *et al.* 1960). The values of Km for mature tissues are 3.1 mM for barley root (Inatomi and Slaughter 1975), 5.6 mM for potatos (Satyanarayan and Nair 1985), 8.3 mM for tea leaves (Tsushida and Murai 1987), and 9.1 to 9.6 mM for sunflower cotyledons (Smith and Waygood 1961). Thus the Km values for L-Glu in GAD activity seems to be higher in embryos than mature tissues.

The optimal pH value for the purified GAD was between 5.7 and 6.2 in sunflower cotyledons (Smith and Waygood 1961), barley tissues (Inatomi and Slaughter 1975), potatos (Satyanarayan and Nair 1985), and tea leaves (Tsushida and Murai 1987). This optimum is lower than that for many other enzymes.

Sulfhydryl directed reagents (*p*-hydroxymercuribenzoate, N-ethylmaleiimide, dithionitrobenzoate) and heavy metal ions (Mg^{+2}, Cu^{+2}, Fe^{+2}) inhibit the GAD activity of potato. One mM Hg^{+2}, Cu^{+2}, and Fe^{+2} inhibited the GAD by 100 %, 75 %, and 55 %, respectively. Also *p*-hydroxymercuribenzoate inhibited activity by 96 %, indicating that -SH groups are required for activity. Thiol acids (3-mercaptopropionic acid, L-thiomalic acid, thioglycollic acid) completely inhibited the GAD activity. Inhibition was increased 45-fold by substituting an -SH group on propionate, suggesting that -SH groups are important in binding the inhibitor to the enzyme-PLP complexes. D-Glu, GABA, D-Asp,

L-cysteic acid, 2-mercaptoethanol, reduced glutathione, δ-aminolevulinic acid, α,ε-diaminopimelate, succinic semialdehyde, ATP, pyruvate, lactate, maleate, fumarate and 18 L-amino acids at concetrations 10 times higher than the L-Glu concentration did not inhibit L-Glu decarboxylation. Similarly the GAD activity of potato shows substrate specificity for L-Glu. When 18 L-amino acids, Γ-methylene Glu, D-Glu, and Gly were used as substrates for GAD, decarboxylation was not detectable (Satyanarayan and Nair 1985).

3. L-Glutamate and GABA metabolism

GAD is generally present in higher plants and GABA has been detected in a wide variety of plant species at high levels (Lahdesmaski 1968, Spedding and Wilson 1968, Lane and Stiller 1970, Missen and Wilson 1970, Streeter and Thompson 1972b, Inatomi and Slaughter 1975, Satyanarayan and Nair 1985, Selman and Cooper 1978, Desmaison and Tixier 1986, Tsushida and Murai 1987).

Studies on the metabolism of L-Glu and GABA in leaves of *Vicia faba* and wheat were carried out by Jordan and Givan (1979) and Walker *et al.* (1984). Illuminated leaves of *Vicia faba* and wheat mainly metabolized L-Glu to L-Gln via the GS reaction in the chloroplast. However in the dark or in the presence of L-MSO, a GS inhibitor, L-Glu was metabolized to CO_2, GABA, malate, and succinate. Metabolism of [1-^{14}C]L-Glu in the presence of L-MSO shows that the carbon-1 is rapidly converted to

CO_2. It is suggested that the CO_2 is produced when L-Glu is decarboxylated to form GABA by loss of carbon-1. Alternatively CO_2 may result from decarboxylation of the α-KG in the Krebs cycle. Studies with tobacco cells also support the production of GABA and CO_2 from L-Glu (Mizusaki *et al.* 1964, Koiwai and Noguchi 1972).

The labeling pattern resulting from the metabolism of [^{14}C]GABA indicates that succinate, malate, L-Asp, and L-Gln are rapidly labeled. Only slight radioactivity was found in L-Glu. There is no evidence for the direct formation of L-Glu from GABA by reversal of GAD (Streeter and Thompson 1972b). With longer incubation periods appreciable incorporation was observed in L-Gln, L-Asp, L-asparagine (L-Asn), succinate and malate (Satyanarayan and Nair 1986b). The authors suggest that some L-Glu is converted to GABA which is converted to succinate. The succinate enters the Krebs cycle and is further metabolized to intermediates of the cycle and related compounds *e.g.* L-Gln, L-Glu. The metabolism of L-Glu and GABA by the Krebs cycle is clearly supported by treatments with malonate. In leaves of *Vicia faba*, malonate caused the accumulation of labeled succinate on incubation with both [^{14}C]L-Glu and [^{14}C]GABA (Jordan and Givan 1979). It is suggested that L-Glu may enter the Krebs cycle after conversion to α-KG by transamination and/or oxidative deamination. Alternatively GABA from L-Glu can be converted to succinic semialdehyde by GABA-pyruvate transaminase (EC.2.6.1.19) via a transamination reaction.

GABA + Pyruvate <------> Succinic semialdehyde + Alanine

Succinic semialdehyde can then be converted to succinate by succinic semialdehyde dehydrogenase (EC.1.2.1.16).

Succinic semialdehyde + $NAD(P)_{ox}$ ------> Succinate + $NAD(P)_{red}$

This pathway is called the GABA shunt and represents a different route for entry of L-Glu carbon into the Krebs cycle (Dixon and Fowden 1961, Misusaki *et al.* 1964, Streeter and Thompson 1972b, Vandewalle and Olsson 1983, Satyanarayan and Nair 1986b).

GABA transaminase activity was assayed in pea nut seedling (Dixon and Fowden 1961), radish leaves (Streeter and Thompson 1972b), soybean leaves (Wallace *et al.* 1984) and potato tubers (Satyanarayan and Nair 1986b). The activity of GABA pyruvate transaminase was ten times of that of GABA-α-KG transaminaserminase.

GABA + α-KG <------> Succinic semialdehyde + L-Glu

In potato, the activity of GABA-pyruvate transaminase was approximately twice that of GABA-α-KG transaminase. Thus the transaminase appears to utilize pyruvate most readily as the accepter thereby generating alanine (Ala). However GABA transaminase isolated from clover roots nodule tissue (Freney and Gibson 1975), mushroom *Agaricus bisporus* (Baldy 1976) was found to be highly specific for α-KG rather than pyruvate.

Succinic semialdehyde levels were 8 nmol/gm fresh wt. in potato tubers (Satyanarayan and Nair 1986b) and 30 nmol/gm fresh wt. in radish leaves (Streeter and Thompson 1972b). These low levels indicate that free succinic semialdehyde does not

accumulate in the cells, presumably due to its rapid conversion to succinate by succinic semialdehyde dehydrogenase (Streeter and Thompson 1972b, Satyanarayan and Nair 1986b).

The cellular location of the GABA shunt enzymes was studied in peanut seedling (Dixon and Fowden 1961), soybean leaves (Wallace *et al.* 1984), and potato tubers (Satyanarayan and Nair 1986b). The GAD activity is exclusively present in the cytosolic phase without association with any organelle or membrane component. In soybean leaves approximately 37 % of the total GABA transaminase activity was localized in the mitochondria (Wallace *et al.* 1984). GABA transaminase and succinic semialdehyde dehydrogenase in potato tubers appear to be in the mitochondria and the cytosolic phase in a 1 : 3 ratio (Satyanarayan and Nair 1986b). The *in vitro* enzyme ratios indicate that most GABA transaminase is cytosolic whereas a part of its activity is located in the mitochondria. Therefore, the location of GABA transaminase in both the mitochondria and the cytosol of higher plant cells indicates alternate locations for the incorporatiion of L-Glu carbon into succinate. However there is no convincing *in vivo* evidence for either the cytosolic or mitochondrial location of enzymes involved in directing GABA carbon into the Krebs cycle.

In conclusion, it is suggested that L-Glu in leaves can be metabolized to produce Krebs acids via a transamination reaction and/or an oxidative deamination reaction catalysed by GDH in the mitochondria. Alternatively L-Glu may be

decarboxylated to GABA in the cytosol. Further metabolism of GABA involves transamination to yield succinic semialdehyde. This is then converted to succinate which can enter the Krebs cycle.

III. THE REGULATION OF GABA ACCUMULATION AND STORAGE

1. GABA accumulation in response to environmental stress

GABA production in response to environmental stress has been studied in a wide variety of plants. It is known that a number of plants accumulate GABA under stress such as anoxia (Effer and Ranson 1967, Streeter and Thompson 1972a, Tsushida and Murai 1987), low temperature (Wallace *et al.* 1984), mechanical damage (Wallace *et al.* 1984, Melcher 1986), aging (Khavkin 1964, Lahdesmaki 1968), viral infection (Singh and Smalley 1969, Cooper and Selman 1974).

(a) Anaerobiosis

Seeds experience a brief period of natural anaerobiosis due to rigid seed coats. The influence of anaerobiosis on the metabolism of higher plants has been studied using tissues from different species. Reports suggest lactic acid and ethanol accumulation followed by an increase in GABA and Ala and a decrease in L-Glu and Asp when leaves or germinating seeds are incubated in anaerobic conditions (Cossins 1964, Effer and Ranson 1967, Cossins and Cameron 1967, Spedding and Wilson 1968, King 1969, Sherwin and Simon 1969, Missen and Wilson 1970, Leblova *et al.* 1976).

These results can be understood as a consequence of the fall in cytoplasmic pH. With the onset of anaerobiosis, glycoysis leads to a continuous production of lactic acid by

lactate dehydrogenase (EC.1.1.1.27) with a corresponding fall in cytoplasmic pH by 0.3 to 0.5 pH units (Roberts *et al.* 1984, Wray *et al.* 1985). An anaerobiosis induced lactate accumulation is also found in other plant tissues. Maize root tips perfused with deoxygenated medium also showed lactate accumulation.

It is suggested that the decline in pH activates GAD and the production of GABA from L-Glu. Many data favor this proposal. When tritiated water was used to study the anaerobic metabolism of *Sinapis alba* seeds, large amounts of tritiated lactate were accumulated. Upon transferring the seeds to aerobic conditions, the tritium in the lactate was reduced (Missen and Wilson 1970). In anaerobic maize and *Phaseolus* seeds, first lactate and later ethanol were formed during seed swelling with a molar ratio of 1 lactate to 10 ethanol (Leblova *et al.* 1976, Sherwin and Simon 1969). The biochemical reactions taking place during lactate and ethanol metabolism in subsequent aerobic conditions were investigated (Cossins 1964, Effer and Ranson 1967, Cameron and Cossins 1967, Spedding and Wilson 1968, Collins and Wilson 1975). The addition of [^{14}C]lactate to slices of aerobic pea cotyledons for 5 min resulted in L-Glu and L-Asp containing five times as much radioactivity as the CO_2 released. Also a small amount of radioactivity was detected in malate. When aerobic pea cotyledons were fed [^{14}C]ethanol, label was rapidly incorporated into citrate, L-Glu, and CO_2 (Cossins 1964, Cameron and Cossins 1967). Thus when aerobic conditions return, lactate and ethanol decrease and are metabolised via the Krebs

cycle and transamination reactions to produce citrate, malate, succinate, L-Glu, and L-Asp.

The decline in pH with anaerobiosis also stimulated GAD and the decarboxylation of L-Glu to GABA. Some GABA is then transaminated with pyruvate produced from glycolysis, as the amino group acceptor, to produce Ala. This view is supported by *in vitro* studies on GAD and GABA-pyruvate or GABA-α-KG transaminase from radish leaves (Streeter and Thompson 1972b) and tea leaves (Tsushida and Murai 1987). The pH optima for GAD and GABA transaminase are 5.9 and 8.9, respectively. The fall in cytoplasmic pH mediated by anaerobiosis may activate GAD. Therefore an increased rate of GABA production and a decreased rate of GABA transamination may increase the GABA level in the cells (Streeter and Thompson 1972b, Tsushida and Murai 1987).

(b) Low temperature and mechanical stress

Various studies on the influence of temperature on nitrogen metabolism in plant tissues suggest that the nitrogen content in the amino acid pool increases at low temperature. It has been reported that low temperature stress causes accumulation of Ala, L-Glu, Pro, and GABA in higher plants (Wilding et al. 1960, Draper 1972, Wallace *et al.* 1984).

Cold treated *Lolium perenne* leaves exhibited, on a fresh weight basis, an almost three fold increase in total amino acids. In particular Ser, L-Glu, Gly, L-Gln, and Pro increased (Draper 1972). Amino acid anaylsis of alfalfa grown at low

temperature showed a 20 % increase in free amino acids (Wilding *et al.* 1960). Accumulation of GABA and Ala in response to low temperature was also reported for soybean leaves. Compared to detached leaves which were maintained at 22°C, a large increase of GABA and Ala occurred in detached leaves exposed to 6°C, 15 minutes on ice or 2 minutes in liquid nitrogen followed by 15 minutes on ice (Wallace *et al.* 1984). It is possible that increased solute concentration depresses the freezing point of the cytoplasm and therefore protects cells from injury caused by ice crystals.

GABA accumulation after a low temperature stress may be analogous to its accumulation after mechanical stress in rolled or crushed soybean leaves (Wallace *et al.* 1984) and cut slices of pea cotyledon, root, and shoot (Melcher 1986). An increase in GABA level in soybean leaves under low temperature or mechanical stress may result from a change in intracellular compartmentation (Wallace *et al.* 1984). In tissues exposed to L-Glu far more GABA production was observed in cut pea cotyledons, roots, and shoots than in intact tissue. This may also be due to damage and breakdown of intracellular compartmentation (Melcher 1986). Damage or breakdown of intracellular compartments may increase the exposure of L-Glu to GAD. If more L-Glu is exposed to GAD, more GABA may result. In addition if cytosolic pyruvate acts as an efficient acceptor of amino groups from GABA, more Ala will result under these conditions (Wallace et al. 1984).

The breakdown of compartmentation may result from

disruption of cellular transport processes or a physical rupture of the membrane dividing compartments. At present, however, the mechanism of low temperature induced amino acid accumulation, including GABA, is poorly understood.

(c) Pathogens

An increase in the total amino acid content in infected plant tissues has been demonstrated. Singh and Smalley (1969) reported that GABA, Ala, L-Glu, Pro, L-Gln, Asn, and ammonia increased in the xylem fluid of *Ceratocystis ulmi*-infected *Ulmus americana* during the susceptible period (Singh and Smalley 1969). In *Radopholus similis*-infected grapefruit leaves the total amino acid content increased 18 % to 81 % (Hanks and Feldman 1966). In wheat species infected with stem rust, there was a significant increase in total nitrogen content and an increase in the ratio of soluble nitrogen content to insoluble nitrogen. GABA, L-Glu, and Tyr in particular increased (Shaw and Coletelo 1961). Tobacco mosaic virus infected tomato leaves and viral infected cherry and peach leaves also showed marked increase in GABA and Ala (Diener 1960, Cooper and Selman 1974).

This general increase in organic nitrogen in infected plants appears to be a common result of pathogenesis. Such an increase may be due to a physiological disturbance of export and/or import of photosynthates of leaves or amino acids synthesized in roots (Singh and Smalley 1969). Alternatively it may be due to a temporary decline in protein synthesis in the

leaves as viral multiplication begins (Cooper and Selman 1974).

(d) Age

The amount of GABA increases in proportion to the age of leaves of *Salvinia natans*, *Medicago sativa*, *Datura suaveolens*. In the case of *Salvinia*, the amount of GABA in old leaves is about twice that of young leaves. GAD activity parallels the GABA level in leaves of different ages, and increases rapidly in aging leaves (Lahdesmaki 1968). In legume leaves it was also found that the amount of both L-Gln and GABA was increased with aging. In growing leaves, more than 50 % of the total amino nitrogen was in Asn, Gln, and Asp. In mature leaves α-aminobutyric acid, GABA, Ala, and Ser were predominant (Khavkin 1964). GABA is generally regarded as an important temporary reserve of amino group and carbon for protein synthesis. When the rate of protein synthesis is low, a decrease in the utilization of GABA for protein synthesis may cause its accumulation.

(e) GABA accumulation as a response to differential synthesis and utilization

The GABA shunt suggests that GABA is formed by decarboxylation of L-Glu and that it is metabolized to succinate via succinic semialdehyde (Dixon and Fowden 1961, Streeter and Thompson 1972b, and Satyanarayan and Nair 1986b). Thus the rate of formation of GABA and its degradation can regulate the GABA

level in the cells, i.e. an increased rate of GABA formation and/or a decreased rate of GABA breakdown may lead to an accumulation of GABA (Streeter and Thompson 1972b, Tsushida and Murai 1987). The activity of GAD is much higher than that of GABA-pyruvate transaminase in a number of plant leaves, *e.g.* 20 times for radish (Streeter and Thompson 1972), 36 to 66 times for soybean, 7 times for cowpea, 22 times for alfalfa, 61 times for tomato, 12 times barley, 26 times for yellow foxtail (Wallace *et al.* 1984), and 23 times for potato (Satyanarayan and Nair 1986b). Root nodules formed by *Rhizobium* strain TA1 had little GABA whereas nodules with strain NA30 contained large amounts of GABA. Enzyme assays demonstrated that nodules with TA1 could transaminate GABA to succinic semialdehyde with α-KG upto seven times more rapidly than those with NA30. This suggests that GABA accumulates because of low rates of transamination (Freny and Gibson 1975). Furthermore the optimum pH for GAD from plants is approximately 5.9, whereas the corresponding value for GABA transaminase is 8.9. Therefore, the *in vivo* accumulation of GABA from L-Glu may reflect the differential *in vitro* activity of these two enzymes.

In conclusion it appears that GABA accumulates in response to various stress such as anaerobiosis, mechanical injury, low temperature and infection. Fundamental mechanisms which activate GABA accumulation are considered to be breakdown of intracellular compartmentation and acidification of cytoplasm resulting from acidosis. Thus in the response to stress, GABA

accumulation may play a role to (i) adjust osmoticum and protect cells by decreasing the freezing point, (ii) regulate cytoplasmic pH by consuming protons.

2. The storage pool of GABA

In mature plant cells, there are two major compartments, they are referred as the cytosol and the vacuole. A vacuole in plants cells appears to be important because the vacuole constitutes approximately 90 % of the volume of a mature plant cell and has static and dynamic properties. Vacuoles can sequester or immobilize cytoplasmic products or foreign materials, and thereby function as a storage site for metabolites or colored or toxic secondary products. Vacuoles are also dynamic. The vacuoles store or release metabolites according to the requirements of the cytoplasmic activities *e.g.* the seasonal deposition and remobilization of oligosaccharides in storage organs and the diurnal accumulation and release of organic acids in crassulacean acid metabolism plant (Matile 1978, Boller and Wiemken 1986).

Efforts have been made to identify the localization of compounds in intracelluar compartments and the flow of metabolites between different compartments. Methods used include the kinetic analysis of the efflux of labeled compounds and the anaysis of the composition of compounds in isolated compartments. Different kinetics of efflux may indicate different pools. The existence of two separate pools of metabolites is indicated by a

rapid efflux process and a slow efflux process. Slow efflux is from an inaccessible internal organelle which could be the vacuole. Rapid efflux is assumed to be from the cytosol. However it is difficult to interpret this indirect data.

A direct approach for obtaining information concerning the contents of organelles and the transport properties of organelles involves organelle isolation. Gentle osmotic rupture of isolated protoplasts have been used as the starting point in organelle separation. The use of isolated vacuoles has provided considerable information concerning the composition of vacuoles and the energization of the tonoplast and transport systems located in this membrane. Information concerning the intracellular distribution of amino acids may be obtained from an amino acid analysis of plant protoplast and their vacuoles (Wagner 1979, Yamaki 1982). For most amino acids the largest proportion is located in a compartment separated from the metabolically active cytosol (Wagner 1979, Yamaki 1982). Experiments with isotonically isolated vacuoles from *Hippeastrum* petals, *Tulipa* petals and leaf protoplasts demonstrated that they contained a large fraction of the intracellular amino acids. In contrast L-Gln, L-Glu, and GABA concentrations were much higher in the cytosol (Wagner 1979). In apple cotyledons, the greater proportion of amino acids were also located primarily in the vacuole (50 to 80 %). Again GABA, L-Glu, and Ala occurred primarily outside the vacuole (Yamaki 1982). The ability to export amino acid into the surrounding medium was studied with

isolated soybean mesophyll cells. GABA and Ala were the major constituents of the total intracellular amino acid pool in isolated cells. Analyses of the amino acid contents of the cells and bathing medium indicated that amino acids were exported at different rates. After 210 min, 82 % of the total amount of leucine (Leu) was outside the cell, whereas only 26 % of the GABA was outside the cells. Addition of CCCP and 3(3,4-dichlorophenyl)-1,1-dimethylurea (DCMU) or changes of pH and K^+ concentration in the medium did not significantly change the rate of efflux of amino acids, suggesting that amino acids are exported by an energy independent diffusional process. Although the concentration gradient of GABA favored efflux, GABA did not exhibit a high efflux rate. The authors suggested that GABA may be sequestered within a cell compartment and may not be in ready equilibrium with the rest of the cell (Secor and Schrader 1984). The efflux of GABA however was stimulated specifically by *p*-chlorophenyl sulfonic acid, a non-permeant protein reactive reagent, suggesting a plasma membrane protein specific for GABA efflux. Thus compartmental analysis suggests a non-vacuolar possibly cytosolic location for GABA. In contrast efflux analysis suggests that GABA is sequestered within an organelle.

IV. LONG-DISTANCE TRANSPORT OF ORGANIC NITROGEN

The growth and physiology of higher plants require the integration of the absorption and translocation of water, minerals and organic nutrients. Both minerals and nutrients are translocated over long distances through the vascular system which is composed of two specialized tissues, the xylem and the phloem. The xylem is the primary pathway of mineral and water flow from root to leaves. The movement of organic nutrients is primarily from leaves to non-photosynthetic cells via the phloem. Minerals and organic nutrients may also move in the phloem and xylem respectively. Although studies have been made of long distance translocation, the determination of translocate composition in the vascular system was difficult. Recent developments in methods and techniques available for collecting and analyzing small volumes of xylem sap and phloem exudate have made these studies possible.

Techniques available and resulting identification of organic nutrients moving in xylem and phloem will be discussed with regards to the upward transport of nutrients from root to leaves through xylem, the downward export of nutrients from leaves to roots and the lateral exchange of nutrients between the ascending xylem stream and descending phloem stream. In particular the transport and utilization of N-containing metabolites in a whole plant will be discussed.

1. Identity of transported solutes

(a) Techniques

A direct method of examining long distance transport of solutes in plants is to identify and measure the amounts of the compounds present. Thus analysis of xylem and phloem sap is fundamental for understanding the process of xylem and phloem transport. This approach has been applied to a number of plants using several techniques for collecting sap. In addition when these techniques are coupled to isotope studies, information on entry of solutes into specific transport pathways and the manner in which they move within the plant body can be obtained. Although every technique carries some problems, the techniques to be discussed below are still generally accepted and have provided a fairly accurate picture of the solute composition and transport in xylem and phloem.

(a-1) Techniques for collecting xylem sap

To identify the compounds translocated from the root toward the leaves through xylem, several techniques have been employed. Techniques include vacuum extraction of tracheal sap from freshly detached shoot segments and release of xylem sap under root pressure from stems decapitated at ground level (Bollard 1960).

Several problems with these techniques are reviewed as follows (Pate 1983). (i) The vacuum extraction technique may release solutes from surrounding tissues or compartments other

than xylem elements and thereby may contaminate the xylem fluids. This particularly applies to the first drop. (ii) Starvation reactions or changes in water flux following cutting may change the solute composition. To minimize contamination, the first drop to be exuded should be discarded. Also the collection period should be short to avoid starvation reactions and microbial contamination.

It is possible to collect xylem fluid in sugarcane by the direct insertion of a microcapillary tube into a single xylem vessel (Waldron 1976). However it is not easily used to study most herbaceous plants.

(a-2) Techniques for collecting phloem exudate

A variety of methods are available for collecting phloem exudate. Techniques employed rely on turgor pressure and the consequent exudation of the sieve tube contents upon cutting or puncturing.

The first technique involves making shallow incisions in the outer bark of trees or cutting the stem and the inflorescence stalk. Possible artifacts may arise (Pate 1983). (i) Protein level may be high in phloem exudate because pressure release causes non-mobile (*e.g.* P-protein) and structural constituents to exude. (ii) Osmotic attraction of water from neighboring tissues or loss of water from damaged tissue surface may cause a more dilute or more concentrated drop of exudate. (iii) Exchange of solutes with a damaged tissue surface is

another general source of artifacts. (iv) Change and loss of phloem function upon cutting may also cause an artifact. Upon cutting pressure release causes escape of solutes from sieve elements at rate much faster than the rate of translocation *in vivo*. Insolule content of phloem tissue (*e.g.* slime, callose) may block the sieve plate and translocation. These artifacts can be avoided by shortening the collection period or discarding the first drop of phloem exudate.

The second technique utilizes aphids which feed on phloem sap. Aphids are allowed to feed on an exposed region of the plant. Upon penetration into a sieve element, the aphid apparently relies on the turgor pressure of the punctured cell to force sap through the mouth parts. The aphids are then anasthetized in a stream of CO_2 into the gut. After excising the bodies phloem exudate is collected from the mouth parts using microcapillaries. This technique has been verified by sectioning and electron microscope observations showing that the stylet tips actually penetrate sieve elements (Evert *et al.* 1973). Hence this exudate is likely to be a more concentrated and reliable sample. However the volume to be obtained from a single aphid is obviously less than that from a cut or shallow incision. Also this technique is limited by the dearth of suitable large aphids and by their selection of feeding locations on the plants.

Recently the chelating agent, ethylenediamine tetraacetic acid (EDTA) has been employed to collect phloem sap. This technique includes simple immersion of excised tissue in an

EDTA solution and subsequent analysis of the EDTA solution bathing excised tissue. There is much evidence for a stimulation of phloem sap flow by EDTA solutions. ^{14}C-Feeding studies show that EDTA greatly increases phloem exudation of labeled assimilates into a solution bathing its petioles (King and Zeevaart 1974). Also an EDTA solution bathing soybean stylar tip stimulates the leakage of solutes into the solution (Fellow *et al.* 1978). This technique may be usefully applied for collecting phloem sap from species or sites which do not readily bleed *e.g.* the petiole of a translocating leaf, the distal tip of a fruit. Problems with this technique may result from the toxic effect of EDTA on plant tissue and difficulties in analysing the exuded solutes. For example, GABA is usually present in xylem at higher relative level than in phloem (Pate *et al.* 1974, Sharkey and Pate 1975, Pate *et al.* 1981). However in studies where the EDTA technique was employed to collect phloem sap more GABA was formed in phloem (Layzell and RaRue 1982), indicating a possible toxic effect of EDTA on plant tissue.

(a-3) Short term pulse feeding and/or chase technique

The utilization and mobilization of organic nitrogenous compounds in the plant are quantitatively analyzed by 'feed' and 'chase' techniques. After the label is taken up, a 'chase' of unlabeled sap is admitted through the transport stream. The resulting information indicates the amounts and the extent of various solutes moving between different parts of the plant. On

the basis of this technique, a quantitative model for partitioning and utilization of organic nitrogen compounds in the plant can be made. In legumes the resulting information is classified as follows ; (i) direct incorporation of fixed nitrogen into the tissue of root nodules, (ii) primary distribution of fixed nitrogen from nodule to shoot in the xylem, (iii) direct xylem to phloem transfer in the shoot or leaf veins, (iv) indirect transport of nitrogen from xylem to phloem via leaf mesophyll cells, (v) transport of nitrogen from the shoot to the roots via the phloem (Pate 1983).

(b) Solutes in xylem and phloem

(b-1) Composition of xylem sap

Xylem sap is acidic (pH 5.2 to 6.5) and has a 1 to 20 mg/ml solid content (Pate 1975, Dickson 1979). Since essential mineral elements are taken up from the soil, the ionic composition of the xylem varies with the composition of the rooting medium and with the current ionic status of the root. Generally major cations of xylem sap are K^{+}, Ca^{+2}, Mg^{+2}, and Na^{+}. Major anions are PO_4^{-3}, Cl^{-}, and SO_4^{-2}.

Nitrogenous constituents are major solutes of xylem and are present at 0.1 to 0.5 mg/ml. The principal solute are amides (Asn, Gln), ureides (allantoin (ALN), allantoic acid (ALA)) and a wide variety of amino acids. The composition of nitrogenous solutes depends on the species. Thus plants are classified as amide-exporting plants *e.g. Lupinus, Pisum, Vicia*, and ureide-

exporting plants *e.g. Vigna, Phaseolus, Cajanus.* GABA was a minor component in xylem sap of pea (Pate *et al* 1974, Sharkey and Pate 1975, 1975), Lupin (Pate *et al.* 1981), Cowpea (Pate *et al.* 1984), and brocolli (Shelp 1987).

The organic nitrogen results from nitrate assimilation into products which are not retained in root storage pools but readily exported in xylem (Atkins and Pate 1983). Thus plants with active reduction of nitrate in their roots (*Lupinus, Pisum)* have high levels of organic nitrogen relative to free nitrate in the xylem. Species with little capacity to reduce nitrate in their roots such as *Vigna* have most of their nitrogen in the xylem as free nitrate (Wallace and Pate 1965, Oghoghorie and Pate 1972, Pate *et al.* 1975, Atkins and Pate 1983). In addition to nitrogen recently received from the rooting medium, the nitrogen component of xylem may also arise from protein turnover, discharge of storage pools of the root and cycling through the root of nitrogen from the shoot system (Atkins and Pate 1983).

Sugars are present in xylem sap of trees or woody plants. The xylem sap of herbaceous plants however tends to have less carbohydrate than the sap of woody species. Organic acids are also present resulting from export directly from the root or cycling of carbon through the root. Growth susbtances such as auxin, gibberellin, abscisin, or cytokinin have been found in xylem sap (Pate 1983).

(b-2) Composition of Phloem exudate

Phloem exudate is alkaline (pH 7.8 to 8.3) and has a 100 to 125 mg/ml dry matter. High sugar levels (80 to 210 mg/ml) and carbohydrate content (5 to 250 mg/ml) have been recorded in root of sugar beet, stem of *Ricinus*, legume fruit of *Spartium*, *Genesta*, *Lupinus*, and *Jacksonia* (Fife *et al.* 1962, Hall *et al.* 1971, Hall and Baker 1972, Pate *et al.* 1974).

In terms of composition of macroelements and microelements, K^{+} and Mg^{+2} are the major cations and Na^{+} and Ca^{+2} are present at a low level. The concentrations of $HPO_4^{-2}/H_2PO_4^{-}$, Cl^{-} are relatively high and the levels of $SO4^{-2}$ and HCO_3^{-} are low (Pate 1983, Hayashi and Chino 1986).

Protein occurs in phloem sap and ranges from 0.5 to 1.0 mg/ml. The concentration of nitrogenous solutes in phloem exudate is higher than in xylem sap of the same species and ranges from 8 to 28 mg/ml. The major nitrogenous solutes in phloem exudate is identical to and similar to those of xylem sap. The main components are amides (Asn, Gln), Glu, Ser, Thr, Val, and their relating amino acids. GABA has been found in *Nicotiana* (Hocking 1980), *Lupinus* (Pate *et al.* 1974, 1979), and wheat (Hayashi and Chino 1986), but was not detected in rice (Fukumorita and Chino 1982).

Large amounts of organic anions are present mainly as malate (Hall *et al.* 1971, Hall and Baker 1972). Phloem exudate also has auxin, gibberelline, and cytokinin and nucleotide *e.g.* ATP (0.4 to 0.6 mM) (Ziegler 1975).

2. Partitioning of organic nitrogen in the plant system

The basic transport system of the whole plant consists of the root, stem, mature leaf, and an apical sink region of the shoot (*e.g.* meristems, young vegetative organs, developing reproductive structure). Root and leaf are the sites where nutrients are loaded and unloaded whereas they are only unloaded at the apical regions. The transport relationships between the parts of a whole plant are discussed in this section. In particular (i) direct transfer of solute from root to mature leaf via the xylem, (ii) lateral transfer systems in roots and stems, and (iii) indirect transfer and/or later remobilization of protein from mature leaf into the phloem are discussed.

(a) Export of nitrogen from roots in the xylem

A number of reports on nitrogen metabolism indicate that organic nitrogen is exported from the root upwards to the shoot via xylem. Sources of nitrogen for export include atmospheric nitrogen, nitrate, amino acid pools and nitrogenous compounds received form the leaf via the phloem. A nonassimilatory source of nitrogen for xylem loading, other than recent assimilation, was shown in roots of *Pisum* seedlings grown without nitrogen and without nodules (Oghoghorie and Pate 1972). When a nitrogen source was present the compounds were Asn and Gln. However when a nitrogen source was absent the compounds in the xylem were Val, Leu and Asp. The roots of some species (*Lupinus, Pisum*) are active in nitrate reduction (Wallace and

Pate 1965, Oghoghorie and Pate 1972, Pate *et al.* 1975). Even when high levels of nitrate were provided to the roots, there was no transport of nitrate to the shoot in the xylem (Pate *et al.* 1975). In the case of *Glycine* and *Vigna*, the activity of the root in reducing nitrate is low, so both free nitrate and organic forms of nitrogen are present in the xylem. Consequently shoots can receive more nitrate-N than organic-N (McClure and Israel 1979, Dickson 1979). In older plants proteolysis in roots and the cycling of nitrogen through the root may contribute to the nitrogen solutes in the xylem.

Feeding studies have provided information on the particular form of nitrogenous compounds exported from roots in the xylem. $^{15}N_2$ and $^{15}NO_3$ were fed to the root system and leaves of pea (*Pisum*) (Oghoghorie and Pate 1972). ^{15}N labeled compounds were found to move preferentially upwards to the shoot through the xylem. In addition currently assimilated nitrogen from nodulated roots was cycled back to the root, indicating the presence of flow paths both up and down the plant.

(b) Lateral exchange of xylem solutes in stems

There is much evidence that the stem tissues of herbaceous as well as woody plants abstract organic nutrients from the ascending transpiration stream. In analyses of xylem sap collected at different heights of the shoot system of pea (Pate *et al.* 1964) and at different age of apple shoots (Cooper *et al.* 1972), it was found that the total solutes were diluted

with height up the stem. In addition these experiments showed that mainly Asn was selectively abstracted from the xylem of the stem (Pate *et al.* 1964). This selective abstraction is supported by experiments and autoradiography after feeding amino acids into the transpiration stream (Wooding and Northcote 1965, Pate and O'Brien 1968, Pate *et al.* 1970, McNeil *et al.* 1979). In shoots of *Pinus pines*, unusual wall thickening has been found on the innermost xylem tracheids of the stem. When tritiated Glu was fed to this stem tip at the cut base, autoradiography showed that the label was found in the starch of the xylem ray cells, phloem and the innermost tracheids (Wooding and Northcote 1965). These findings were extensively studied by Pate and O'Brien (1968). When major constitutents of the xylem sap, Gln, Asp, Asn, Glu, and Hser were fed singly to pea shoots via the transpiration stream, the label was found in xylem chlorenchyma, cambial initials, mesophyll cells of leaves, chlorenchyma of stem and petioles and elements of the phloem (Pate and O'Brien 1968). The distribution and time course of development of transfer cells in the hypocotyl of lettuce (*Lactuca*) and groundsel (*Senecio*) indicates a transport pathway from cotyledonary trace xylem element to xylem transfer cells to plumules. Analyses of xylem sap collected from above and below the zones of transfer cells in the hypocotyl showed that solutes could be removed from the xylem sap to transfer cells (Pate *et al.* 1970). These histoautoradiographic results clearly suggest that transfer cells function in the general nutrition of young tissues, the

abstraction of assimilates for local storage and interchange of assimilates between xylem and phloem (Pate *et al.* 1970).

The evidence for lateral abstraction of xylem solutes is clearly shown in experiments involving pulse feeding of major xylem compound over 10 to 20 minutes followed by a 10 to 220 minute chase in cut transpiring shoots of white lupin (McNeil *et al.* 1979). Autoradiography and radioassays of phloem sap, leaf and shoot parts harvested at intervals indicates the highly selective uptake of xylem stream solutes by the stem. In particular Arg was removed very effectively from vascular tissues of stem, petioles, and major leaflets. Shoots fed [^{14}C]-Asn, Gln, Val, Ser, and Arg showed intense labeling of leaflet veins and marked retention (35 to 78 %) of [^{14}C] by the stem and petioles. Shoots fed [^{14}C]-Asp and Glu showed heaviest [^{14}C] accumulation in nonvascular or interveinal mesophyll cells of mature leaves and low uptake of [^{14}C] by stem and petioles (McNeil *et al.* 1979, Vogelmann *et al.* 1985).

(c) Export of solutes from mature leaves in the phloem

Since the mature leaf is the major site of transpiration and export, an understanding of the transition of the leaf from an immature importing to a mature exporting organ provides information on the mechanism of vein loading and translocation. When the leaf has grown to approximately 20 to 45 % of its maximal size, a single leaf begins exporting assimilate before import has completely finished (Turgeon 1973,

Turgeon and Webb 1976). Therefore the direction of flow in the phloem reverses during leaf maturation. In pea, leaflets and stipules of leaf furnish 85 % of photosynthetically fixed carbon to the seeds (Flinn and Pate 1970). Generally simple sugars, sugar alcohols, and organic acids are the principal compounds exported from the leaves (Nelson 1962, Pate *et al.* 1974, Pate 1975, Zimmermann and Ziegler 1975).

Generally three major sources of nitrogen are available for phloem loading in the legume leaf (Pate and Atkins 1983) : (i) nitrogen arriving in the leaf via the xylem as organic nitrogen. (ii) nitrogen arriving as nitrate prior to reduction and incorporation into organic form, (iii) nitrogen released to the phloem after proteolysis of protein and/or discharge of storage pools of amino acid prior to and during leaf senecsence. The buildup of nitrogen in the phloem at leaf senescence is well documented for deciduous woody species in autumn when the nitrogen present in foliage is being withdrawn into the trunk (Ziegler 1975). Phloem loading studies of amino acids therefore can be conducted by feeding [^{14}C] or [^{15} N] labeled amino compounds to the leaf or shoot via the xylem and subsequent analysis of labeled metabolites in the phloem exudate. To avoid complications due to the reduction of nitrate, the species studied have been restricted to legumes which depend solely on the fixation of atmospheric nitrogen by nodules. In *Spartium* $^{14}CO_2$ feeding to source leaves coupled with analysis of phloem bleeding sap from cut distal tips of fruits showed that [^{14} C] was

located mainly in sucrose, but also fairly high specific activity was present in the organic acid fraction and in certain amino acids such as Ser, Ala, and Glu (Pate *et al.* 1974).

Autoradiograms of whole shoot of *Lupinus albus* fed with [^{14}C]-Arg, Asp, Asn, Val via the transpiration stream indicate that a large proportion of these amino acids is abstracted by stem tissue (McNeil 1979). Once these amino acids are abstracted from veins, they are readily loaded into the phloem. Asn, Gln, Val, Tyr, Ser were transferred rapidly and directly to the phloem without breakdown (*e.g.* Asn and Gln were recovered by 92 % and 77 % respectively). Asp and Glu were transferred less effectively so that only a small portion was retained in the stem vascular system. However 19 % and 8 % of Asp and Glu label respectively was recovered in mesophyll cells. Similar results with the acidic amino acids were obtained using *Populus deltoides* (Vogelmann *et al.* 1985).

This diversity of pattern of primary uptake and distribution of amino acids from the xylem may result from interactions with charges on the cell wall and/or the specificity of plasma membrane uptake process (McNeil 1979). Basic amino acids (*e.g.* Arg) are cationic at a xylem pH of 5.5 to 6.5 and may therefore be absorbed from the xylem due to negatively charged cell walls. The transport of neutral amino acids (*e.g.* Asn, Gln, Val) may depend on their metabolic fate and specific uptake at the plasma membrane. Acidic anionic amino acids (*e.g.* Asp, Glu) may be repelled by fixed negative charge on the surface of cell

wall so that lateral transfer does not occur and they are transferred to mature mesophyll cells according to the gradient of water potential imposed by water loss from mature leaves (Vogelmann *et al.* 1985).

GABA is usually present in the xylem as a minor component of the free amino acid pool in a large number of plant species such as pea (Pate *et al.* 1974, Sharkey and Pate 1975), lupin (Pate *et al.* 1981), cowpea (Pate *et al.* 1984), and broccoli (Shelp 1987). It is absent in rice (Fukumorita and Chino 1982) or found in the phloem of wheat at very low relative concentrations (Hayashi and Chino 1986). However the role of GABA in the transport of carbon and nitrogen within the plants is not understood and this question has rarely been raised.

MATERIALS AND METHODS

I. MATERIALS

1. Chemicals and suppliers

Acetone	BDH
Acetonitrile (HPLC grade)	Fisher
Aqueous Counting Scintillant (ACS)	Amersham
Γ-Amino butyric acid (GABA)	Sigma
Amino acid standard	Pierce
Borax	Fisher
n-Butyric acid	Sigma
Carbonyl cyanide *m*-chlorophenyl hydrazone (CCCP)	Sigma
Cacodylic acid	Fisher
Calcium hydroxide (AnalaR)	BDH
Calcium sulphate	BDH
Citric acid	Sigma
Dodecyl succinic anhydride	Fisher
Epon resin 812	Fisher
Formic acid	Fisher
Fumaric acid	Fisher
Glacial acetic acid	Fisher
Glutaraldehyde	BDH
L-Glutamic acid	Sigma
Hydrochloric acid	BDH
α-Ketoglutarate	Fisher
Lead acetate	BDH
Lead citrate (AnalaR)	BDH
Lead nitrate (AnalaR)	BDH
Maleic acid	Fisher
Malonic acid	Sigma
2-Mercaptoethanol	Kodak
2 [N-Morpholino] ethane sulfonic acid (MES)	Sigma
Methanol (HPLC grade)	BDH
Methylene blue	Fisher
Nadic methyl anhydride	Fisher
Ninhydrin spray	BDH
Oligomycin	Sigma
Oxaloacetic acid	Fisher
o-Pthalaldehyde (OPA)	Kodak
Phenol	Fisher
Phenylisothiocyanate	Fisher
Potassium chloride	Fisher
Potassium sulphate (AnalaR)	BDH
Propylene oxide	BDH
Pyruvic acid	Fisher

Silica gel G	Macherey Nagel
Silicone fluid AR 20 & AR 200	Wacker chemie
Sodium acetate	Fisher
Sodium azide	Sigma
Sodium borate	Fisher
Sodium hydroxide	BDH
Sodium phosphate	Sigma
Succinic acid	Sigma
Sulfuric acid (HPLC grade)	BDH
Tartaric acid	Sigma
Tetrahydrafuran (HPLC grade)	Fisher
Triethylamine (Sequanol grade)	Fisher
Uranyl acetate	BDH

2. Radiochemicals and suppliers

[U-^{14}C]L-Glutamic acid	; 250 mCi/mmol	NEN
	225 mCi/mmol	ICN
[1-^{14}C]L-Glutamic acid	; 59 mCi/mmol	Amersham
[U-^{14}C] -Amino butyric acid	; 238 mCi/mmol	NEN
^{14}C-n-Hexadecane	; 0.868 x 10^6 dpm/ml	Amersham

The radiochemical purity and the specific activity used :

[U-^{14}C]L-Glutamic acid ;
[U-^{14}C]L-Glutamic acid was supplied in aqueous solution containing 2 % ethanol in sterile borosilicate multidose vials. When stored in 0.01 N HCl at +3°C, it undergoes less than 1 % decomposition per month. Fifty mM 2,944 dpm/nmol, 2.5 mM 33,903 dpm/nmol, and 2 mM 49,955 dpm/nmol were prepared with non-labeled L-Glu.

[1-^{14}C]L-Glutamic acid ;
[1-^{14}C]L-Glutamic acid was supplied in aqueous solution containing 2 % ethanol in sterile, borosilicate multidose vials with additional screw caps. When stored at +2°C in its original solvent and its original concentration, decomposition does not usually exceed 2 % per year. 2.5 mM 32,560 dpm/nmol and 1.66 mM 38,784 dpm/nmol were prepared with non-labeled L-Glu.

[U-^{14}C]GABA ;
[U-^{14}C]GABA was supplied in aqueous solution containing 0.01 N HCl in sterile, borosilicate multidose vials with additional screw caps. When stored at +5°C in its original solvent and at its original concentration, the rate of decomposition is 1 % per year. Five mM 24,776 dpm/nmol, 46,835 dpm/nmol, and 266,826 dpm/nmol were prepared with non-labeled GABA.

3. Photographic supplies and suppliers

Fuji EM film	Fuji
Kodak Ektachrome 50 professional film	Kodak
Kodak GBX developer	Sigma
Kodak GBX fixer	Sigma
En^{3}hancer spray	Picker International
Ilford Ilfospeed 3.1 M paper	Ilford

4. Plant material

The mesophyll cells used in this study were isolated from greenhouse grown *Asparagus sprengeri* Regel plants. The plants were grown at 67°F in slightly acidic mixture of vermiculite pearlite and sphagnum peatmoss (40 : 60, v/v, pH 5 to 6.5) under natural sunlight. The plants were watered daily, fertilized weekly (N:P:K = 30:10:10) and the greenhouse was fumigated regularly.

II. METHODS

1. Isolation of mesophyll cells

Photosynthetically competent mesophyll cells were isolated from *Asparagus sprengeri* cladophylls according to the mechanical method of Colman *et al* (1979). Mature fronds possessing glossy, dark green cladophylls were harvested from the greenhouse. Five to 10 gm of 2 to 2.5 cm long cladophylls were collected in a Buchner funnel and washed with distilled water. The cladophylls were cut into pieces 0.5 cm long or less using a clean razor blade and were placed in a beaker containing approximately 50 ml of 1 mM $CaSO_4$. The medium was then vacuum infiltrated into the tissue in a vacuum desiccator for 20 minutes. Vacuum infiltrated cladophyll sections were gently ground in a mortar containing 5 to 10 ml of 1 mM $CaSO_4$. Mesophyll cells were squeezed out of the cladophyll epidermal envelope by this technique. The resulting cell suspension was then transferred into centrifuge tubes through 3 layers of muslin. The grinding and transfer processes were repeated several times until colorless epidermal sections were observed. The crude mesophyll suspension collected was centrifuged for 2 minutes in a clinical bench top centrifuge at setting 2 or 800 x *g*. The resulting supernatant fluid was discarded and the remaining pellet was immediately resuspended in the same medium and centrifuged again. The pellet obtained after the second centrifugation was resuspended in 30 to 40 ml of medium. Cells

were kept in an ice bucket in the dark. The cells were used within 6 hours of their isolation to minimize any effect of storage.

Cells with an intact plasma membrane retain their semi-permeable properties and therefore exclude Evans blue. Damaged cells become pigmented as the Evans blue dye penetrates (Gaff and Okong'O-Ogola 1971). Therefore, to test the integrity of the plasma membrane, a small amount of cell suspension was treated with a 20 % (w/v) Evans blue solution. The mixture was allowed to sit for 15 minutes before the cells were counted. Eighty to 90 % of the cells excluded the Evans blue dye.

The number of cells present per ml of cell suspension was determined using a Spencer Bright Line hemocytometer and a Wild light microscope. The number of cells per ml of cell suspension ranged from 2.5 to 3 x 10^6.

2. Proton flux measurements

The experiments measuring proton flux were performed in an open cylindrical glass reaction vessel (2.5 cm in diameter, 4 cm in depth). The reaction vessel was water-jacketed and connected to a circulating water bath regulated at 30°C. When cells were introduced into the reaction vessel, they were usually incubated for 5 minutes prior to starting the experiment. Aeration was accomplished by inserting the tip of Yale Luer-lok hypodermic needle into the cell suspension. This needle was connected to an air flow system that was regulated by a Brooks

E/C flow meter to a rate of 500 ml/min. The cell suspension was continuously stirred with a magnetic spinbar. The cells were illuminated or kept in darkness. When cells were illuminated, light was supplied by a Sylvania 200 W lamp with an irradiance at the surface of the vessel of 4.6×10^{-4} mol/m^2/sec (Alphametric model 1010 light meter). When cells were incubated in darkness, the reaction vessel was covered with a light tight black box. Light and dark experiments were performed consecutively in order to avoid any experimental variation from cell aging.

Six to 14×10^6 cells depending on the experiment were resuspended in 10 ml of 1 mM $CaSO_4$ and introduced into the reaction vessel. Recordings of pH changes with time were made using a Radiometer PHM 64 research pH meter equipment. A PHM 64 pH meter with a combination glass electrode (Radiometer GK 2321C) was connected to a REC 61 recorder through an REA 100 pH meter interface. Full scale deflection of the recorder was equivalent to a pH change of 0.7.

L-Glu or GABA at pH 6.0 .were added using a Hamilton microsyringe to give the concentrations indicated. Before and after each addition of L-Glu or GABA, the contents of the reaction vessel were titrated with 1 mM H_2SO_4 or 1 mM NaOH in order to determine the buffering capacity of the cell suspension medium before and after its addition.

The net rate of proton flux was calculated on the basis of three known values *i.e.* the rate of change of pH with time, the buffering capacity of the cell suspension and the number of

cells present in the reaction vessel. Thus, the rate of proton flux was calculated as follows :

$$\frac{\frac{\text{pH units}}{\text{min}} \times \frac{\text{nmol } H^+}{\text{pH unit}}}{\text{number of cells} \times 10^{-6}} = \text{nmol } H^+ / 10^6 \text{ cells / min}$$

Also the extent of proton flux was calculated as follows ;

$$\frac{\text{pH unit} \times \frac{\text{nmol } H^+}{\text{pH unit}}}{\text{number of cells} \times 10^{-6}} = \text{nmol } H^+ / 10^6 \text{ cells}$$

3. Measurement of uptake rates of labeled compounds

Experiments were performed in an open water jacketed glass reaction vessel maintained at 30°C. The cell suspension was stirred, not aerated and exposed to light supplied with a sylvania 200 W lamp with an irradiance at the surface of the vessel of 4.6×10^{-4} mol/m^2/sec or kept in darkness with a light tight black box. When the rate of uptake of [U-^{14}C]L-Glu was measured, the number of cells in the cell suspension medium was 6.6×10^6 cells in 2.2 ml of 5 mM MES/1mM $CaSO_4$ adjusted to pH 6.0 with $Ca(OH)_2$. When the rate of uptake of [U-^{14}C]GABA was measured, 4.4×10^6 cells were present in 1.1 ml of the same medium.

An aliquot (0.2 ml for L-Glu, 0.1 ml for GABA) of cell suspension was removed and collected on a Millipore filter (HA type 0.45 um). This was called the blank. To the remaining 2.0

or 1.0 ml of cell suspension, 20 ul of 50 mM [U-^{14}C]L-Glu (specific activity 2,944 dpm/nmol) was added to give a final concentration of 0.5 mM L-Glu or 25 ul of 5 mM GABA (specific activity 24,776 dpm/min) was added to give a final concentration of 0.125 mM GABA. Aliquots were then removed from the cell suspension at 0 minute and 2 minute intervals for 10 minutes. Cells were collected on Millipore filters and washed with 1 x 5 ml, 2 x 10 ml of cold medium. After washing the filters with cells were transferred directly to a scintillation vial containing 1 ml of 100 % methanol to disrupt cell structure. After 5 minutes 14 ml of aqueous counting scintillant (ACS, Amersham) was added to each vial, shaken vigorously, and then counted in a Beckman LS 1800 scintillation counting system.

Uptake rates of labeled compounds were calculated using the increase in cpm with time, the counting efficiency, the specific activity, and the number of cells. Rates of uptake are expressed as nmol/min/10^6 cells or dpm/min/10^6 cells.

4. GABA efflux measurements

(a) Net efflux of GABA

Efflux was measured as the loss of radioactivity from cells which had accumulated an equilibrium level of [^{14}C]GABA label. This efflux is net efflux, which is the result of uptake and export.

The cell suspension was stirred, not aerated, and exposed to the light. Experiments were started by suspending 4.4

x 10^6 cells in 1.1 ml of 5 mM MES/1 mM $CaSO_4$ adjusted to pH 6.0 with $Ca(OH)_2$. Upon the addition of 25 ul of 5 mM [U-^{14}C]GABA (specific activity 24,776 dpm/nmol, final concentration of GABA 0.125 mM), an aliquot (0.1 ml) of cell suspension was removed every 2 minutes for 6 minutes and collected on Millipore filter (HA type 0.45 um) as described in section 3. At 6 minutes, 20 ul of 50 mM L-Glu (1 mM), 20 ul of 500 mM K_2SO_4 (10 mM), 10 ul of 1 mM CCCP (10 uM), 10 ul of oligomycin (10 ug/ml), or 20 ul of 250 mM butyric acid (5 mM) was added to determine their influence on the net efflux of GABA. Aliquots were removed and collected every 2 minutes for a further 12 minutes.

(b) Unidirectional efflux of GABA

To measure the unidirectional efflux of GABA label, the procedure was the same as in section 4 (a) upto 6 minutes. At this point the cells were washed with 2 x 10 ml of fresh medium to remove radioactivity. The washing procedures took 6 minutes. At the 12 minute mark, 0.8 ml of incubation medium was added to cell pellets and measurements of efflux were initiated. Upon starting incubation at 12 minutes, an aliquot (0.1 ml) of cell suspension was removed and 16 ul of 50 mM L-Glu (1 mM), 16 ul of 500 mM K_2SO_4 (10 mM), 8 ul of CCCP (10 uM), 8 ul of oligomycin (10 ug/ml), or 16 ul of 250 mM butyric acid (5 mM) was added to the cell suspension. Aliquots were removed and cells were collected on Millipore filters every 2 minutes for a further 12 minutes.

5. Scintillation Counting

To measure radioactivity, Millipore filters with collected cells were placed in vials containing 1 ml of 100 % methanol. After 5 minutes, 14 ml of ACS was added and then vials were kept in the counting system for 1 hour to eliminate delayed fluorescence from the scintillation fluid. The vials were counted for 20 minutes using a Beckman LS 1800 Scintillation counting System.

The efficiency of this counting system was determined using both an automated external standard system and an internal standard, ^{14}C-n-hexadecane, which was added directly to vials. In order to determine the counting efficiency, with increased quenching the number of cells was increased from 0.02 to 2 x 10^6 cells. Cells were placed in vials containing 1 ml of methanol for 5 minutes to disrupt the cells. Fourteen ml of ACS and 10 ul of ^{14}C-n-hexadecane (8,640 dpm) were then added and counted. The counting efficiency was obtained by dividing cpm values obtained by the dpm value of the internal standard. The % efficiency decreased with an increasing number of cells. The H # which is automatically obtained from this counter is an index of counting efficiency and increased with an increasing number of cells. The standard curves for both % efficiency and H # were obtained as a function of the number of cells (Fig 1). These standard curves were used to produce a plot of % efficiency as a function of H # (Fig 2).

Fig. 1 : Counting efficiency and H # as a function of number of cells

- Increasing numbers cells were placed in scintillation vials containing 1 ml of methanol for 5 minutes.
- Fourteen ml of ACS and 10 ul of ^{14}c-n-hexadecane (8,680 dpm) were added to vials and counted in the scintillation counting system (Beckman LS 1800).
- The counting efficiency was obtained by dividing cpm values of samples by the known dpm value of ^{14}C-n-hexadecane.
- The H # was automatically obtained from the output of the counting system and increased with the number of cells.

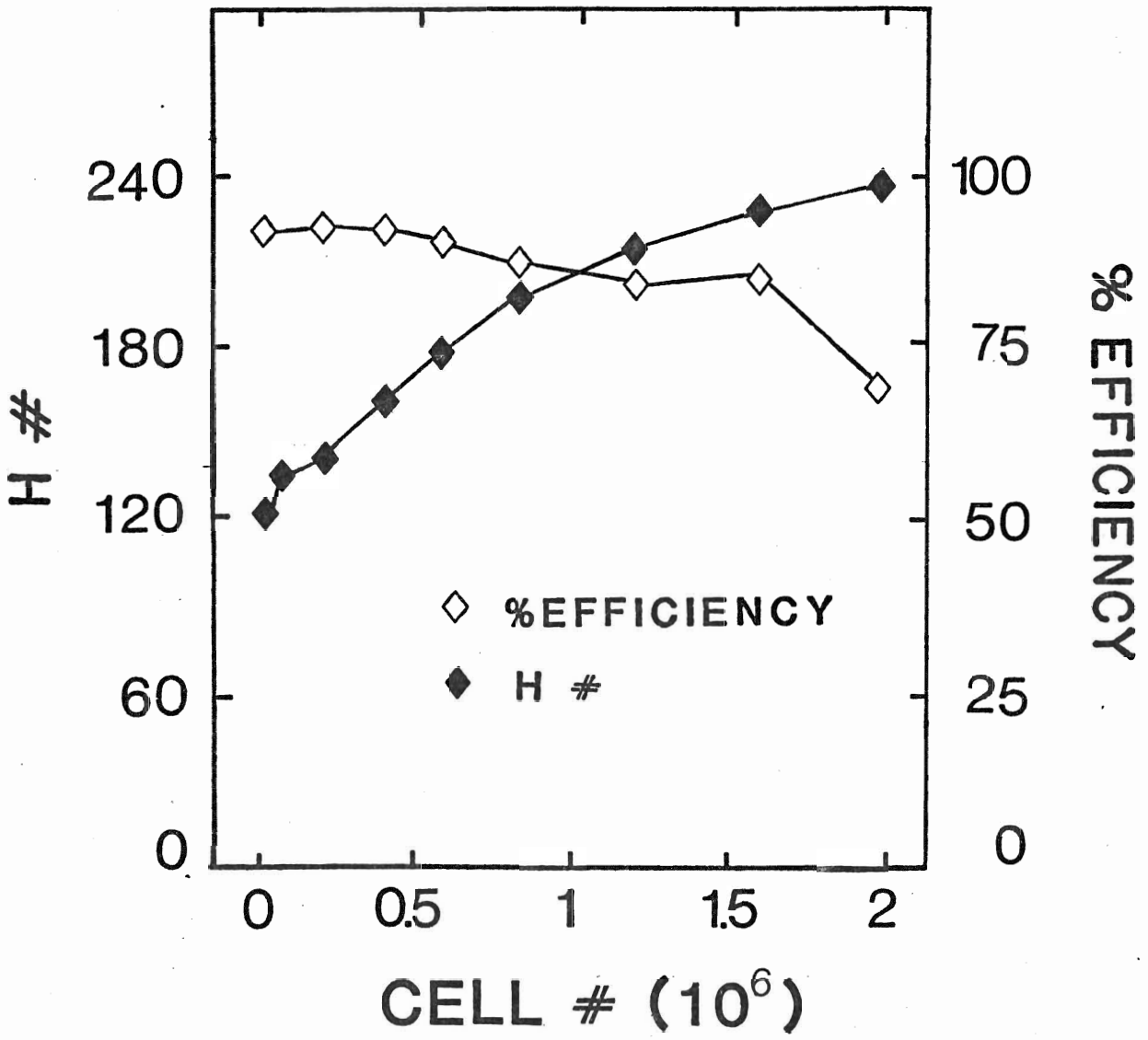
240
180
120
60
0
H #
100
75
50
25
0
% EFFICIENCY
0
0.5
1
1.5
2
CELL # (10^6)
%EFFICIENCY
H #

Fig 2 : Counting efficiency as a function of H #

- Conditions are same as Fig 1.
- The counting efficiency obtained with an increasing the number of cells was plotted as a function of the corresponding H #.

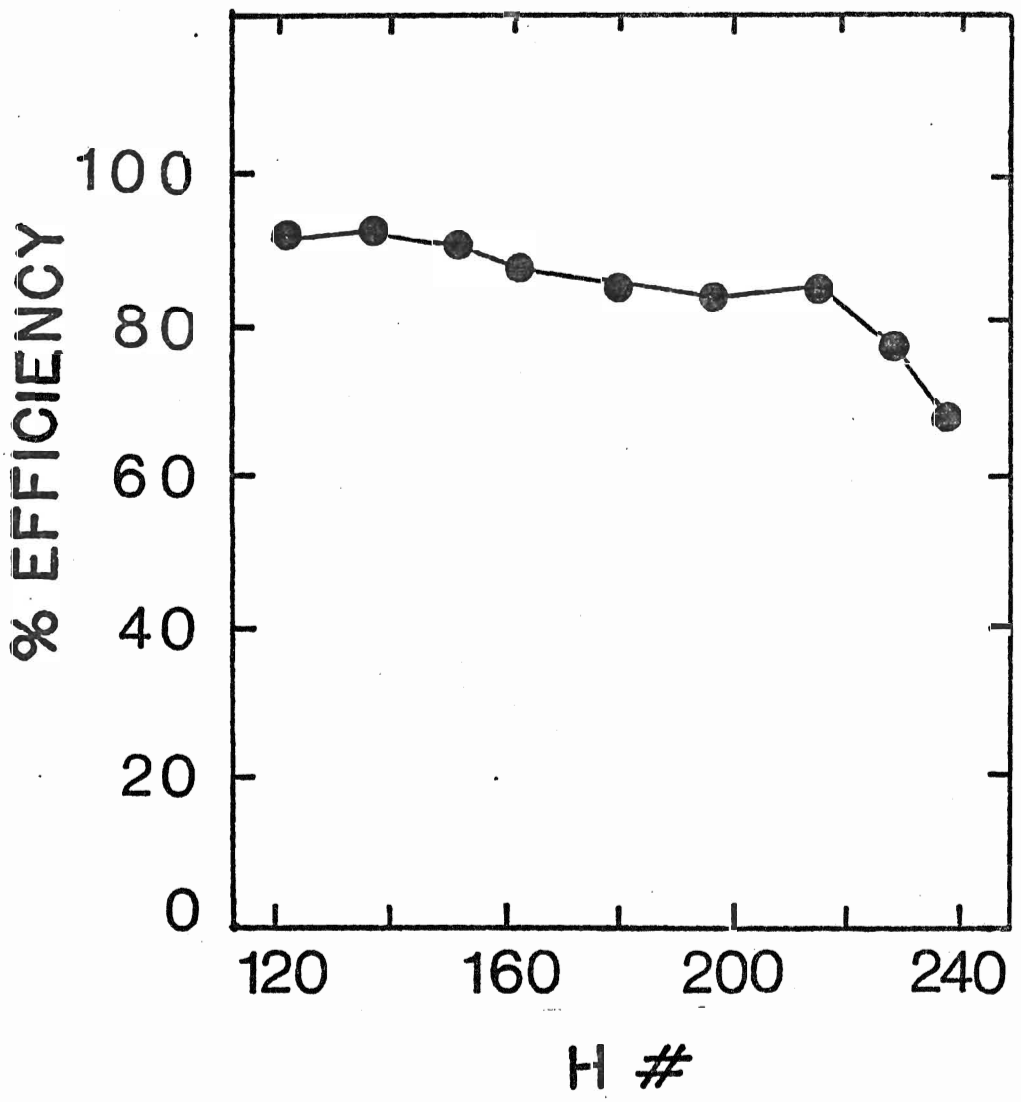
% EFFICIENCY
100
80
60
40
20
0
120
160
200
240
H #

6. Metabolism of [^{14}C]L-Glu and [^{14}C]GABA

(a) Feeding

Twenty million cells were incubated in the reaction vessel containing 4.7 to 4.8 ml of 5 mM MES/1 mM $CaSO_4$ adjusted to pH 6.0 with $Ca(OH)_2$ in the light and dark. After a few minutes 200 ul of 2.5 mM [U-^{14}C]L-Glu (specific activity 49,955 dpm/nmol, final concentration of L-Glu 0.1 mM), 250 ul of 2 mM [U-^{14}C]L-Glu (specific activity 33,903 dpm/nmol, final concentration of L-Glu 0.1 mM), 200 ul of 2.5 mM [1-^{14}C]L-Glu (specific activity 32,560 dpm/nmol, final concentration of L-Glu 0.1 mM), or 300 ul of 1.67 mM [1-^{14}C]L-Glu (specific activity 38,784 dpm/nmol, final concentration of L-Glu 0.1 mM) was added to the cell suspension and cells were incubated for 10 minutes. After a 10 minute incubation the medium was separated by centrifugation at setting 6 or 2,350 x *g* for 2 minutes and this medium was called the medium fraction. The cell pellet was then washed in 1 x 15 ml of cold medium and prepared as a cellular fraction.

After [U-^{14}C]L-Glu had been taken up into the cells for 10 minutes, chases with unlabeled L-Glu were performed. Twenty million cells were incubated in the dark for 10 minutes in the reaction medium containing 4.75 to 4.8 ml of 5 mM MES/1 mM $CaSO_4$ adjusted to pH 6.0 with $Ca(OH)_2$ and 200 ul of 2.5 mM [U-^{14}C]L-Glu (specific activity 33,903 dpm/nmol, final concentration of L-Glu 0.1 mM) or 250 ul of 2 mM [U-^{14}C]L-Glu (specific activity 49,955 dpm/nmol, final concentration of L-Glu 0.1 mM). After the 10

minute incubation period, cells were separated from the medium by centrifugation at setting 6 in a clinical bench top centrifuge. The cells were resuspended in 5 ml of 5 mM MES/1 mM $CaSO_4$ adjusted to pH 6.0 with $Ca(OH)_2$ plus 125 ul of 4 mM unlabeled L-Glu (final concentration of L-Glu 0.1 mM). The cells were then incubated for 10 or 60 minutes in the dark. After the desired incubation period, cells were separated from the resuspension medium and fractionated.

(b) Cell fractionation

After the desired incubation period, the cell suspension was taken and centrifuged at setting 6 for 2 minutes. The supernatant fluid was separated from cells and called the medium fraction. The cell pellet was quickly washed in 1 x 15 ml of cold 5 mM MES/1 mM $CaSO_4$ adjusted to pH 6.0 with $Ca(OH)_2$ to remove exogenous radioactivity and centrifuged at setting 6 for 2 minutes. The supernatant fluid was discarded and the resulting cell pellet was taken and the fractionation was initiated by adding 2.5 ml of 100 % methanol. Five ml of chloroform was then added, mixed and allowed to sit for 30 minutes. After which 2.5 ml of distilled water was added and mixed intermittently for 30 minutes. The resulting thick milky green mixture was separated into 3 phases by centrifugation at setting 7 or 2,900 x *g* for 10 minutes. The top transparent yellowish aqueous phase was removed and called the cell fraction. Both the medium fraction and the cell fractions were dried in 40°C water bath in a filtered air

stream. Once the fraction were dried, analyses for amino acids, organic acids and associated radioactivites were performed using thin layer chromatography (TLC) and high performance liquid chromatography (HPLC).

(c). Chromatographic methods

(c-1) Thin layer chromatography (TLC)

Chromatographic plates were cleaned with 95 % ethanol and prepared for TLC. Thirty gm of powdered $CaSO_4$ binder Silica gel G were vigorously slurried with 30 ml of distilled water. This homogenous slurry was spread at a thickness of 0.25 mm on 20 cm x 20 cm glass plates. They were dried in a horizontal position with a blow drier for 10 minutes, placed in a drying rack and activated in the oven by heating for 1.5 hours at 55°C. Plates were prepared daily and used immediately to keep a consistent water content. The dried medium and aqueous cell fractions were dissolved in 200 ul of 0.1 N HCl. Twenty ul was then applied 1.0 cm from the bottom edge using 20 ul microcapillaries. The starting point was equally sized and the diameter did not exceed 5 mm to ensure clear separation.

The solvent used to develop the chromatograms was phenol : distilled water in a ratio of 75 : 25 (w/w) with 20 mg of NaN_3 as an antioxidant. The solvent was added to a glass developing chamber (21 cm x 21 cm x 9 cm) to depth of about 0.5 cm for ascending development. The lid of the chamber was tightly sealed with petroleum grease and the chamber was saturated to

avoid edge effect before developing. Two plates were placed in the chamber. Separation was carried out at room temperature for 3.5 hours. The chamber was covered with a black cloth. The developed chromatograms were removed from the chamber and dried in the fume hood overnight. For visualization of the chromatograms ninhydrin was evenly sprayed on the chromatograms in a fume hood. Color was developed after heating for 10 minutes at 60°C in the horizontal position. Amino acids, if present, appeared as pinkish purple zones.

To remove amino acids, the chromatographic spots were marked and scraped off using a razor blade and spatula onto a sheet of waxed paper. They were then extracted in 1 ml of distilled water and separated by centrifugation at setting 7 for 5 minutes. The clear supernatant fluid was introduced into a glass scintillation vial containing 14 ml of ACS solution and counted in a Beckman LS 1800 liquid scintillation counting system.

For autoradiography of thin layer chromatograms, the chromatograms were sprayed with En^{3}hancer spray and dried in a fume hood. The chromatograms were then exposed to a Kodak 20 cm x 25 cm X-ray film, wrapped in a Kodak 20 cm x 25 cm exposure cassette and kept for 36 to 48 hours at -70°C depending on the radioactivity of the chromatograms. The film was developed under safelight illumination and fixed for 30 minutes and then rinsed for 1 hour in running tap water.

(c-2) High performance liquid chromatography (HPLC)

(c-2-1) HPLC amino acid separation of PTC derivatives

Dried medium and aqueous cell fractions were dissolved in 500 ul of filtered water and passed through 0.45 um filters and then 300 ul was used for HPLC amino acid analyses. The standard contained 12.5 ul of 2.5 mM Pierce amino acid calibration standard containing aspartate (Asp), glutamate (Glu), serine (Ser), threonine (Thr), alanine (Ala), arginine (Arg), proline (Pro), tyrosine (Tyr), valine (Val), methionine (Met), isoleucine (Ile), leucine (Leu), phenylalanine (Phe) and lysine (Lys), plus 25 ul of 2.5 mM Γ-amino butyric acid (GABA), 25 ul of 2.5 mM citrulline (Citl), 12.5 ul of 5 mM tryptophan (Trp), 12.5 ul of 5 mM asparagine (Asn), 12.5 ul of 5 mM homoserine (Hser), 25 ul of 2.5 mM argininosuccinate (ArgS), 25 ul of 2.5 mM glutamine (Gln), and 12.5 ul of 5 mM ornithine (Orn) together with 0.5 uCi [^{14}C]L-Glu, 0.5 uCi [^{14}C]GABA, 0.5 uCi [^{14}C]Gln, and 0.5 uCi [^{14}C]Pro. This standard and samples were vacuum dried using a vacuum concentrator (Savant Speed Vac). They were then resuspended in 50 ul of methanol (HPLC grade)/water/triethylamine (Sequanol grade) (2/2/1 by volume) and allowed to redry in vacuum. Fifty ul of derivatization solution containing methanol/triethylamine/water/phenylisothiocyanate (7/1/1/1 by volume) was added to each sample, which was then allowed to sit for 35 minutes. Then the samples were vacuum dried and resuspended in 600 ul of diluent before being injected. The diluent was prepared by adding 710 mg Na_2HPO_4 to 1 l of water

adjusting to pH 7.4 with 10 % H_3PO_4 and then adding acetonitrile (HPLC grade) to a final volume of 5 % (v/v). Ten or 50 ul of the solution containing the mixture of standard amino acids plus ^{14}C labeled amino acids and 100 or 200 ul of samples was injected into the HPLC apparatus using a Hamilton microsyringe. Deionized water purified by a Millipore Milli-Q™ water system was used for all amino acid analyses of PTC-derivatives.

The HPLC hardware included two Waters M-45 pumps, Waters 440 fixed Wavelength Absorbance Detector set at 254 nm, a Waters Temperature Control Module set at 46°C, a Waters 710B WISP™ Sample Processor and a Ramona Radiochromatography System. A software Package for data analysis operated in conjunction with an IBM PC. The column was a Waters Pico-Tag™ column (3.9 mm x 300 mm).

The eluting buffer system consisted of buffer A and buffer B. The composition of buffer A was 70 mM NaAcetate (pH 6.55)/Acetonitrile (97.5/2.5 by volume). The composition of buffer B was Acetonitrile/methanol/water (45/15/40 by volume). The methods described have been published (Micallef *et al.* 1989). The gradient and separation profile are shown in Fig 3.

Fig 3 : HPLC amino acid separation of PTC-derivatives and gradient employed

- The sample contained a Pierce amino acid calibration standard (2,600 pmol Asp, Glu, Ser, Gly, Thr, Arg, Ala, Pro, Tyr, Val, Met, Ile, Leu, Phe, Lys, and 1,300 pmol Cys), 5,000 pmol of ArgS, Asn, Gln, Hser, GABA, Citl, and Orn.
- The composition of buffer A was 70 mM NaAcetate (pH 6.55) / acetonitrile (97.5/2.5, by volume). The composition of buffer B was acetonitrile/methanol/water (45/15/40 by volume).
- A Waters Pico-Tag™ column (3.9 mm x 300 mm) was used.

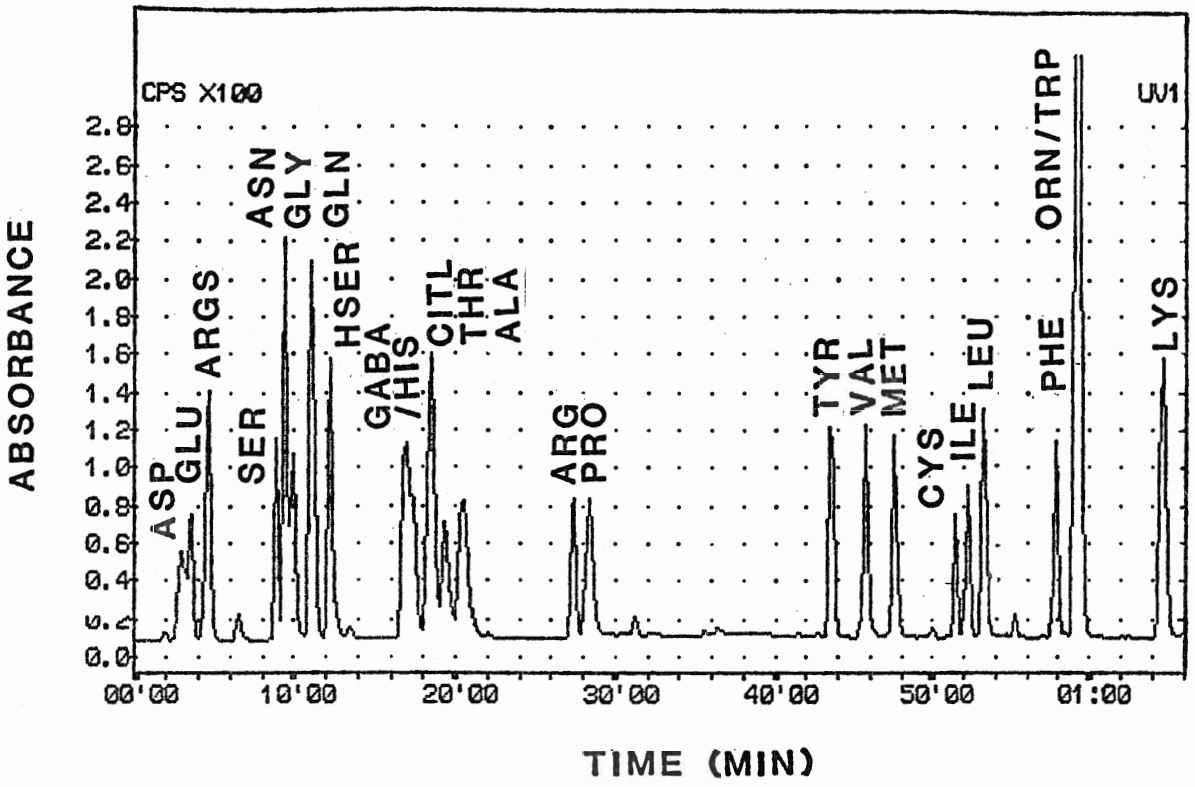

GRADIENT

Time (min)	Flow (ml/min)	% A	% B	Curve
Initial	1.00	100	0	*
13.50	1.00	99	1	11
24.00	1.00	95	5	8
30.00	1.00	91	9	5
50.00	1.00	66	34	6
62.00	1.00	66	34	6
65.00	1.00	0	100	6
75.00	1.00	0	100	6
76.00	1.00	100	0	6
82.00	1.00	100	0	6

(c-2-2) HPLC amino acid separation of OPA derivatives

Dried medium and aqueous cell fractions were dissolved in 300 ul of filtered water. Samples and 10 ul of Pierce amino acid calibration standard plus 10 ul of a 2.5 mM Gln, 10 ul of a 5 mM GABA, 10 ul of 2.5 mM Citl and 4 ul of 12.5 mM ArgS were vacuum dried in a vacuum concentrator.

Fifty ul of standard or samples was added to 262 ul of daily prepared *o*-pthalaldehyde (OPA) reagent consisting of 1.1 mg OPA and 40 ul of 2-mercaptoethanol (2-ME) in 10 ml of 0.4 M NaBorate (pH 10.4)/methanol solution (9/1 by volume). This sample was allowed to react for 2 min and then 10 ul of the standard amino acids or samples was injected into the HPLC apparatus using a Hamilton microsyringe. Deionized water purified by a Millipore Milli-Q™ water system was used for all HPLC amino acid analyses of OPA derivatives.

The HPLC hardware included two Waters M-45 pumps, a Waters 420 Fluorescence Detector set at 360 nm excitation and 455 nm emission, a Waters Temperature Control Module set at 44°C, a Waters U6K Universal Liquid Chromatography Injector, a Waters Resolve™ C_{18} guard-Pack Precolumn Insert and a Waters C_{18} Resolve™ column (3.9 mm x 150 mm).

The eluting buffers consisted of buffer A and buffer B. The composition of buffer A was 50 mM NaAcetate and 50 mM Na_2HPO_4 adjusted to pH 7.0 with glacial acetic acid/methanol/ tetrahydrafuran (96/2/2 by volume). The composition of buffer B was methanol/water (62/38 by volume). The methods described have

been published (McCutcheon *et al.* 1988). The gradient and separation profiles are shown in Fig 4.

Fig 4 : HPLC amino acid separation of OPA-derivatives and gradient system employed

- The sample contained a Pierce amino acid calibration standard (520 pmol Asp, Glu, Thr, Arg, Ala, Pro, Tyr, Met, Val, Phe, Ile, Leu, Lys, and 260 pmol Cys), 1,000 pmol Asn, Gln, Hser, GABA, and Orn.
- The composition of buffer A is 50 mM NaAcetate and Na_2HPO_4 (pH 7.0)/methanol/tetrahydrafuran (96/2/2/ by volume). The composition of buffer B was methanol/water (62/38, by volume).
- A Waters Resolve™ C_{18} column (13.9 mm x 150 mm) was used.

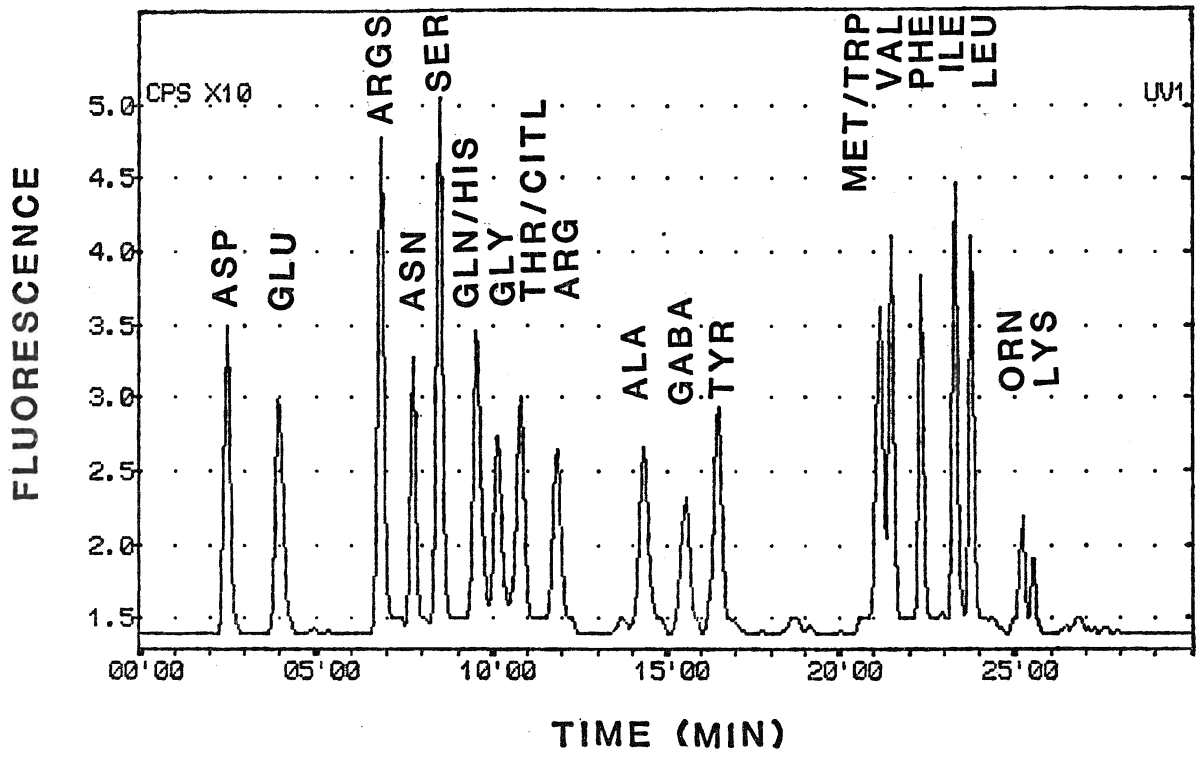

GRADIENT

Time (min)	Flow (ml/min)	% A	% B	Curve
Initial	0.10	90	10	*
0.50	1.50	90	10	6
5.50	1.50	65	35	7
20.00	1.50	20	80	7
24.00	1.50	0	100	6
27.00	1.50	90	10	11
34.00	0.10	90	10	11

(c-2-3) HPLC organic acid separation

The dried medium and aqueous cell fractions were dissolved in 500 ul of filtered water and passed through 0.45 um filters and then 200 ul was used for HPLC organic acid analyses. Twenty ul of the organic acid standard mixture containing oxaloacetate, citrate, α-KG, tartaric acid, malate, malonate, succinate, formate, acetate and fumarate and 150 to 200 ul of samples were injected into a HPLC apparatus using a Hamilton syringe. Deionized water purified by a Millipore Milli-Q™ water system was used for all HPLC organic acid analyses.

The hardware included one Waters M-45 pump, a Waters 440 Fixed Wavelength absorbance Detector set at 210 nm, a Waters 710B WISP™ Sample Processor, a Waters U6K Universal Liquid Chromatography Injector and a Ramona Radiochromatography System. A software Package in conjunction with an IBM PC was employed for data analysis. The columns were a Bio-Rad ion exclusion organic acid HPX-87H Aminex and a Bio-Rad H^+ cation microguard column (7.8 mm x 300 mm). The methods described have been published (McCutcheon *et al.* 1988). A separation profile is shown in Fig 5.

Fig 5 : HPLC organic acid separation

- The sample contained 9.5 nmol oxaloacetate, 24 nmol citrate (Cit), 15 nmol α-KG, 40 nmol malate, 184 nmol malonate (Malon), 184 nmol succinate, 636 nmol formate, 629 nmol acetate, and 3 nmol fumarate.
- The eluting solution was 0.008 N H_2SO_4.
- A Bio-Rad ion exclusion organic acid HPX-87H Aminex and a Bio-Rad H^+ cation column (7.8 mm x 300 mm) were used.

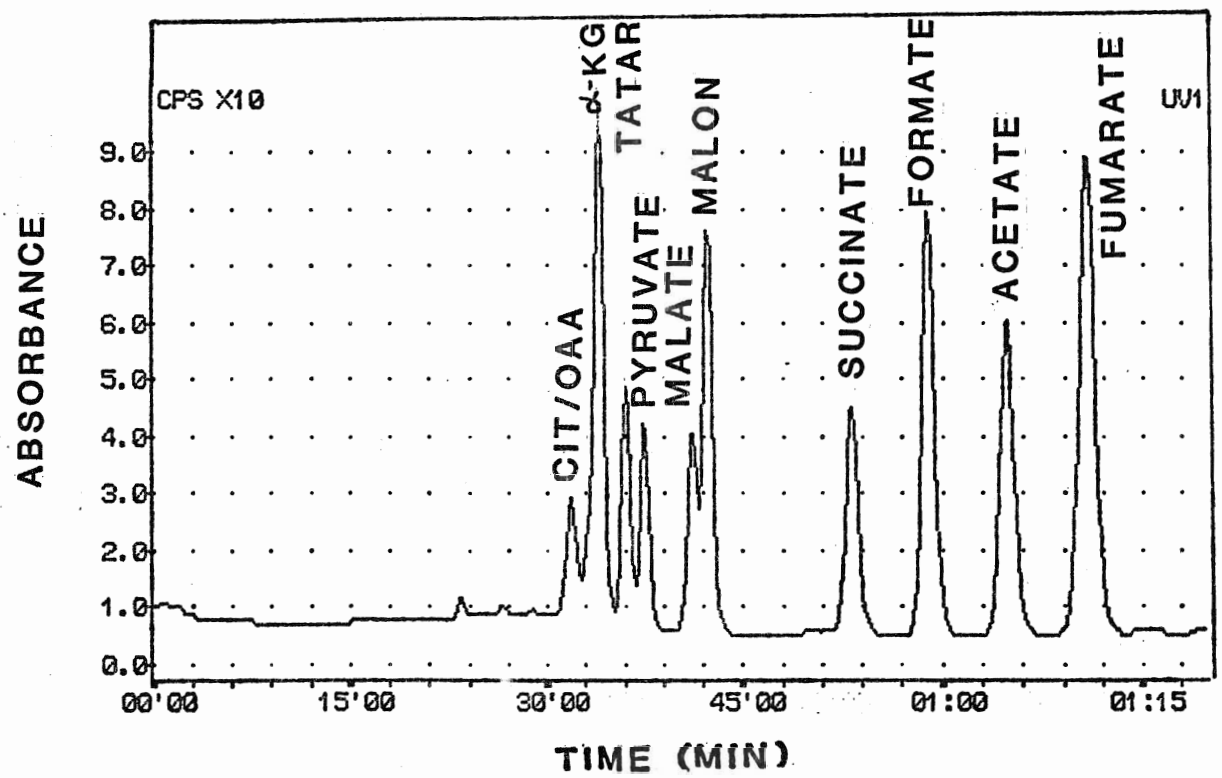
CPS X10
UV1
ABSORBANCE
9.0
8.0
7.0
6.0
5.0
4.0
3.0
2.0
1.0
0.0
CIT/OAA
α-KG
TATAR
PYRUVATE
MALATE
MALON
SUCCINATE
FORMATE
ACETATE
FUMARATE
00'00
15'00
30'00
45'00
01:00
01:15
TIME (MIN)

(c-2-4) HPLC radioactivity determination

The ^{14}C radioactivity was determined by passing the eluate into the solid yttrium silicate cell (500 ul) of a Ramona -D (Raytest Instrument) flow through isotope detector. Peaks were integrated manually and radioactivity was quantified using the relationship Q = Zv/EV, where Q is the dpm/peak, Z is the integrated counts, v is the flow rate (ml/min), E is the static efficiency of detector for ^{14}C (56 %) and V is the cell size (ml) (Micallef *et al.* 1989).

7. Collection of xylem sap for HPLC amino acid analysis

Plants were watered 2 hours before the xylem sap was collected. Collection was performed at 11 AM for 1 to 1.5 hours. Sixty cm long stems were usually taken and the first incision was made 20 cm from the top. The exudate was collected from the attached stem into a tube (20 mm in diameter, 35 mm in depth) using a low vacuum device (Nalgene, MitVac). The second incision was made 20 cm nearer the base and the sap was collected. The last incision was made near the base and the sap was collected. Collection of xylem sap from every incision was completed within 10 minutes and the sap from 4 or 5 incisions was pooled. The sap was kept in ice during the collection period. This procedure was employed on 3 separate days to give a total of 9 samples.

The collected xylem sap was dried in a vacuum concentrator and dissolved in 100 to 200 ul of filtered water. An aliquot from the dissolved volume was taken and derivatized

with 2-ME/OPA. Then 10 ul from the diluted sample was injected into the HPLC apparatus (Method section 6 (c-2-2)).

8. Sample preparation of intact tissue, cell debris and isolated cells for HPLC amino acid analysis

Approximately 250 to 300 cladophylls corresponding to the left and right sides of the stems were collected. The cladophylls of one group were put directly into 20 to 25 ml of boiling 100 % methanol for 30 minutes. After boiling, the cladophylls were ground in 4 ml of 5 mM MES/1 mM $CaSO_4$ adjusted to pH 6.0 with $Ca(OH)_2$. This tissue slurry was mixed with 30 ml of chloroform and 15 ml of water and agitated for 1 hour. Then the aqueous fraction was separated from the chloroform fraction after centrifugation and dried in a stream of air at 40°C (Method section 6 (b)). This was called the intact tissue.

Mesophyll cells were isolated from the cladophyll of the other group. Twenty million cells were incubated in 5 ml of 5 mM MES/1 mM $CaSO_4$ adjusted to pH 6.0 with $Ca(OH)_2$ for 10 minutes in the light. After incubation, the cells were separated from the external medium by centrifugation. The cell pellet was solubilized with 2.5 ml of 100 % methanol for 30 minutes, 5 ml of chloroform for 30 minutes and 25 ml of distilled water for 30 minutes. The aqueous fraction was separated from the chloroform fraction by centrifugation, and dried. This was called the isolated cells.

The tissue debris remaining after cell isolation was

solubilized with 6 ml of 100 % methanol for 1 hour, 12 ml of chloroform for 1 hour and 6 ml of distilled water for a subsequent 1 hour. The aqueous fraction was also separated and dried. This was called the cell debris.

The dried aqueous fractions from intact cladophylls, isolated cells and cell debris were dissolved in 300 ul of filtered water. An aliquot was then taken, derivatized with 2-ME/OPA and 10 ul from the derivatized sample was injected into the HPLC apparatus (Method section 6 (c-2-2)).

9. Measurement of cell volume

(a) Dimensional estimation

Measurement of the size of isolated cells was carried out using an ocular eyepiece calibrated within a um scale and a Leitz light microscope at 400 x. The cell volume was then estimated by measuring the radius half way along the length and the length of the cells and assuming that the cell shape is cylindrical. Thus cell volume was calculated using $V = \pi r^2 h$, where V is the cell volume, r is the radius, and h is the length of the cell.

(b) Measurement via cross sectional areas

Epon-embedded serial sections of intact cladophylls (1 um thickness) were made using an ultramicrotome (LKB Bromma Ultratonme System 2128). The sections were heat-fixed on glass slides, and stained with toluidine blue solution for a few

seconds. The sections were then placed under an Olympus light microscope at 400 x and the areas were determined using the microcomputer imaging device (MCID) software package (Imaging Research Inc.) in conjunction with an IBM PC. Each section was converted to volume using V = Sh, where S is the cross sectional area and h is the section thickness. All sections from 1 cell were measured and then the cell reconstructed to produce the total cell volume.

10. Measurement of buffering capacity

(a) Measurement of the external buffering capacity

Experiments were performed in an open water jacketed glass reaction vessel maintained at 30°C. Twenty million cells suspended in 10 ml of 1 mM $CaSO_4$ were stirred without aeration in the ambient light. The external buffering capacity was determined by adding aliquots of 400 to 500 nmol H^+ to the pH 7.2 cell suspension and recording pH changes of the suspension changing the pH from 7.2 to 5.0. The external buffering capacity was obtained in units of nmol Eq. H^+/ml cell suspension/pH unit (Guern *et al.* 1986, Komor *et al.* 1989).

(b) Measurement of the internal buffering capacity

Two million cells per 1 ml of 1 mM $CaSO_4$ were disrupted by passing through a french press (Aminco) at 1200 psi. The resulting cell homogenate was observed under a light microscope to contain very few intact cells. The internal buffering

capacity of cell homogenates was determined by adding aliquots of 400 to 500 nmoles of H^+ or OH^- to the 10 ml of pH 6.1 cell homogenate and recording the pH changes of the cell homogenate from 6.1 to 5 and 6.1 to 7.0. The internal buffering capacity was calculated by subtracting the external buffering capacity from the buffering capacity of cell homogenate. The buffering capacity of 10 ml of cell homogenate was then converted to that of cells by employing the cell volume (4.68 ul/10^6 cells, Table 2). The units of buffering capacity were obtained as umol H^+/ml cytoplasm/pH unit over the pH range 5 to 7 (Guern *et al.* 1986, Komor *et al.* 1989).

11. Light and electron microscopy

The detached *Asparagus* cladophylls were immersed in 2.5 % glutaraldehyde-paraformaldehyde/0.1 mM cacodylate buffer (pH 7.2) for 20 minutes to harden. The tissues were then cut into small pieces (not less than 1 mm^3) and immersed again in the same aldehyde solution overnight at 4°C. The samples were then washed with 0.1 M cacodylate buffer (pH 7.2) for 3 x 20 minutes at 4°C. After washing, the tissues were postfixed for 2 hours in 1.33 % osmium tetroxide (OsO_4)/0.1 M cacodylate buffer (pH 7.2) at room temperature. The samples were then washed with 0.1 M cacodylate buffer for 3 x 20 minutes. The graded dehydration series consisted of 15 minutes changes in 50 %, 60 %, 70 %, 80 %, 90 %, 95 %, and 2 x 100 % ethanol. Samples were placed in propylene oxide for 20 minutes and then a mixture of propylene oxide and

Epon (50/50, v/v) overnight. The final Epon resin for embedding was prepared mixing in a 3 to 7 ratio for mixture A (epon/dodecyl succinic anhydride, 62/100, v/v) and with mixture B (epon/nadic methyl anhydride, 100/89, v/v). Tissues were embedded within capsules (Beem) and polymerized for 6 hours at 35°C, 12 hours at 45°C, and overnight at 60°C (Glauert 1981).

Semi-thin sections of epon (250 nm thickness) were cut using glass knives on an ultramicrotome (LKB Bromma Ultratome System 2128). Semi-thin sections were heat-fixed on glass slides and were stained with toluidine blue solution for a few seconds. The semi-thin sections were examined under a Leitz light microscope and light micrographs were taken with 1 second exposure on Ektachrome 50 professional slide film.

Ultrathin sections of epon (50 nm thickness) were cut using glass knives for electron microscopy. The sections were picked up on 300 mesh copper grids. The grid-mounted sections were stained with saturated uranyl acetate for 10 minutes at 45°C and lead citrate for 5 minutes by floating the grids in these solutions (Milloning 1961, Reynold 1963). Sections were examined and the electron micrographs were taken using an Hitachi H-500 transmission electron microscope at 75 KV for 4 seconds on Fuji 4 x 5 inches plate films. Plate films were developed and fixed. Prints were produced using a Durst Laborator 138S enlarger and processed using a Kodak Royalprint Processor.

RESULTS

I. ANATOMY OF THE *Asparagus sprengeri* CLADOPHYLL

An investigation was made to obtain information on the tissue structure of *Asparagus sprengeri* cladophylls. The principal objectives of this structural study were (i) to determine the location of isolated mesophyll cells within the intact cladophyll, (ii) to determine the symplastic and the apoplastic connection between these cells and the vascular bundle, and (iii) to determine the size and volume of isolated mesophyll cells so that calculations concerned with cytoplasmic buffering and solute concentrations could be made.

1. Light microscope studies

Light microscopic observations of epon embedded sections of a mature cladophyll showed that the cladophyll was covered on both sides by an epidermis one cell thick. Epidermal cells were rectangular and possessed a thickened cuticle but lacked chloroplasts. Guard cells occurred in pairs with a stomatal pore and were surrounded by epidermal cells called subsidiary cells (Fig. 6A and 6B).

The layers below the epidermis is mesophyll tissue. The mesophyll tissue was differentiated into palisade and spongy mesophyll cells. The palisade mesophyll cells were attached to the epidermis and are densely packed throughout their lengths. Nuclei and large vacuoles were visible and chloroplasts lined the

walls. Compared to the palisade mesophyll cells, spongy mesophyll cells were much less numerous, elongated, bigger and the chloroplasts were scattered throughout their cytoplasm. A few small border mesophyll cells were also attached to the vascular bundle. Very few symplastic connections between palisade mesophyll cells and the vascular bundle through spongy mesophyll cells were observed. In fact one of the noticeable features of the structure is that there is a very large intercellular air space between the palisade mesophyll cells and the vascular bundle with very few connections via the spongy mesophyll cells (Fig. 7A and 7B).

A section of mechanically isolated mesophyll cells showed that isolated cells were not mixed with other types of cells. Chloroplasts lined the cell walls and large central vacuoles occupied a major part of the cell volume (Fig. 8). Both dimensional estimation (Table 1) and the comparison of chloroplast position and central vacuole indicate that the isolated cells were subepidermal palisade mesophyll cells, not spongy mesophyll cells.

Fig. 6A : Light micrograph of the transverse section of an *Asparagus* cladophyll

- The light micrograph indicates the arrangement of tissues. The epidermal layer surrounds all other tissues and large intercellular air spaces are shown between the mesophyll cells and the vascular bundle.
- Note : Ep, epidermis ; IS, intercellular space ; VB, vascular bundle
- A cladophyll was fixed in buffered glutaraldehyde and OsO_4 and embedded in epon.
- Toluidine blue, x 40

Fig. 6B : Light micrograph of the transverse section of an *Asparagus* cladophyll

- Guard cells of stomata are shown in the epidermis. Palisade mesophyll cells are tightly arranged adjacent to the epidermal layer with their long axes parallel. Spongy mesophyll cells are composed of bigger elongated cells and connect the palisade mesophyll cells and vascular bundle. A large intercellular air space exists between the vascular bundle and the palisade mesophyll cells. The vascular system contains xylem, phloem, and a few mesophyll ce4lls at the periphery at the vascular bundle.
- Note : Ep, epidermis ; IS, intercellular space ; Ph, phloem ; Pm, palisade mesophyll ; Sm, spongy mesophyll ; X, xylem
- A cladophyll was fixed in buffered glutaraldehyde and OsO_4 and embedded in epon.
- Toluidine blue, x 100

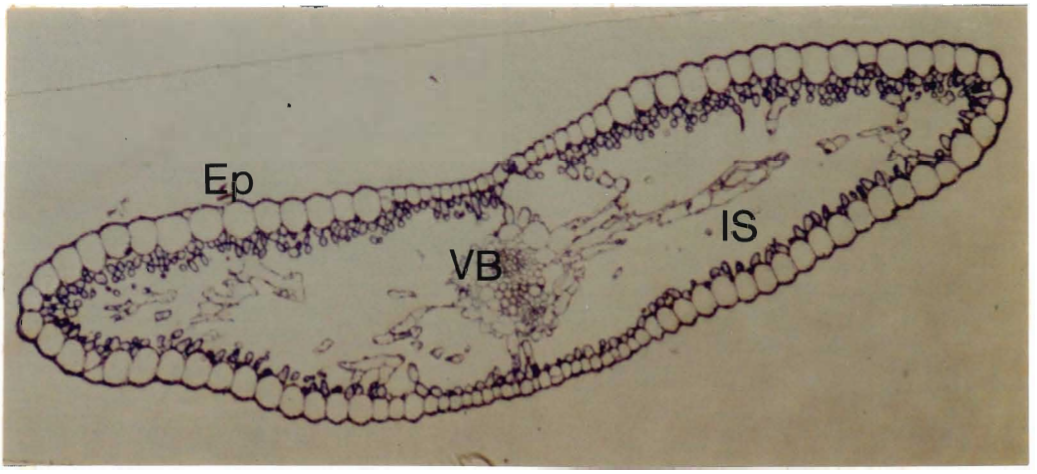
Ep
VB
IS

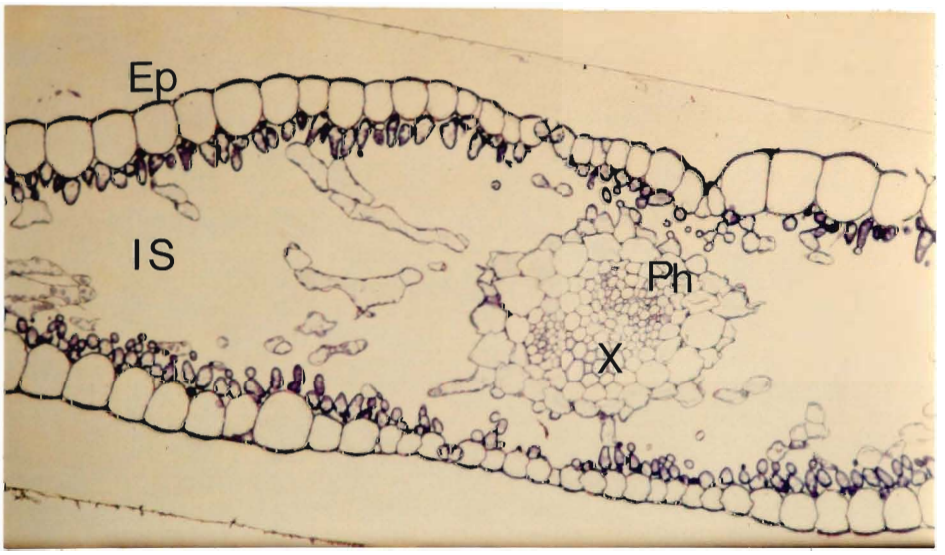
Ep
IS
Ph
X

Fig. 7A : Highly magnified light micrograph of the transverse section of an *Asparagus* cladophyll

- A mature cladophyll consists of two or three layers of palisade mesophyll cells, underlying a single celled epidermal layer.
- Note : Ep, epidermis ; IS, intercellular space ; Pm, palisade mesophyll ; Sm, spongy mesophyll
- A cladophyll was fixed in buffered glutaraldehyde and OsO_4 and embedded in epon.
- Toluidine blue, x 400

Fig. 7B : Highly magnified light micrograph of the transverse section of an *Asparagus* cladophyll

- The highly magnified light micrograph indicates the spatial connection between the mesophyll cells and the vascular bundle.
- Note : Ep, epidermis ; IS, intercellular space ; P, Phloem ; Pm, palisade mesophyll ; Sm, spongy mesophyll ; X, xylem
- A cladophyll was fixed in buffered glutaraldehyde and OsO_4 and embedded in epon.
- Toluidine blue, x 400

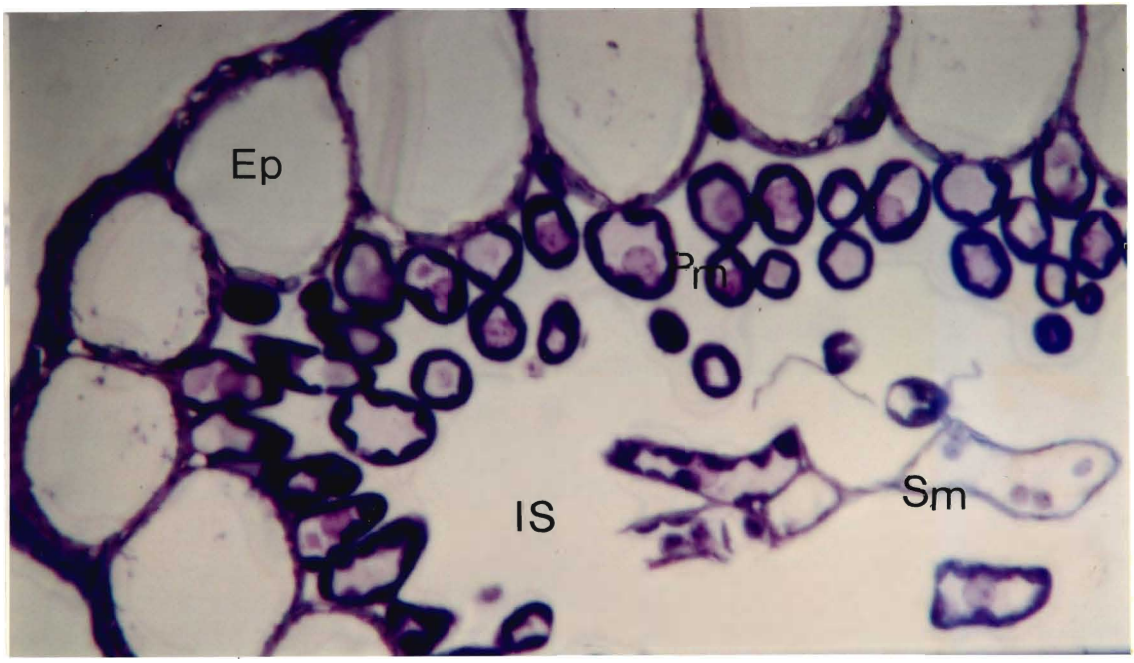
Ep
Pm
IS
Sm

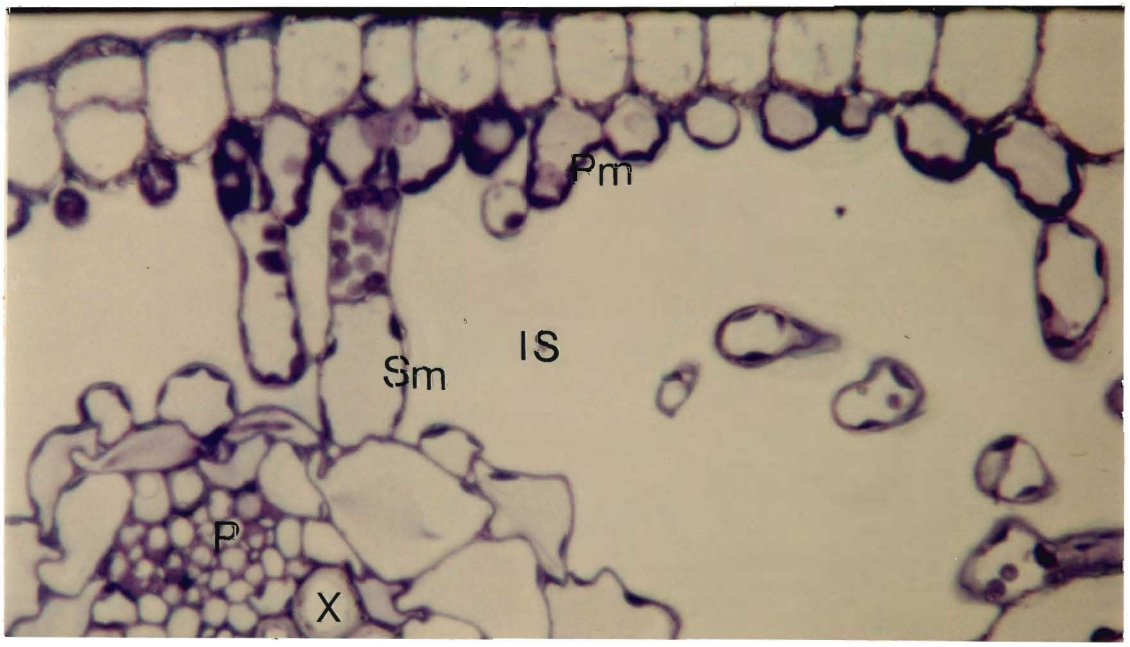
Pm
IS
Sm
P
X

Fig. 8 : Light micrograph of isolated *Asparagus* cells

- The light micrograph was obtained from a section of mechanically isolated embedded cells. Nuclei are visible and the cells contain large vacuoles and chloroplasts line the cell walls.
- Isolated cells were fixed in buffered glutaraldehyde and OsO_4 and embedded in epon.
- Toluidine blue, x 400

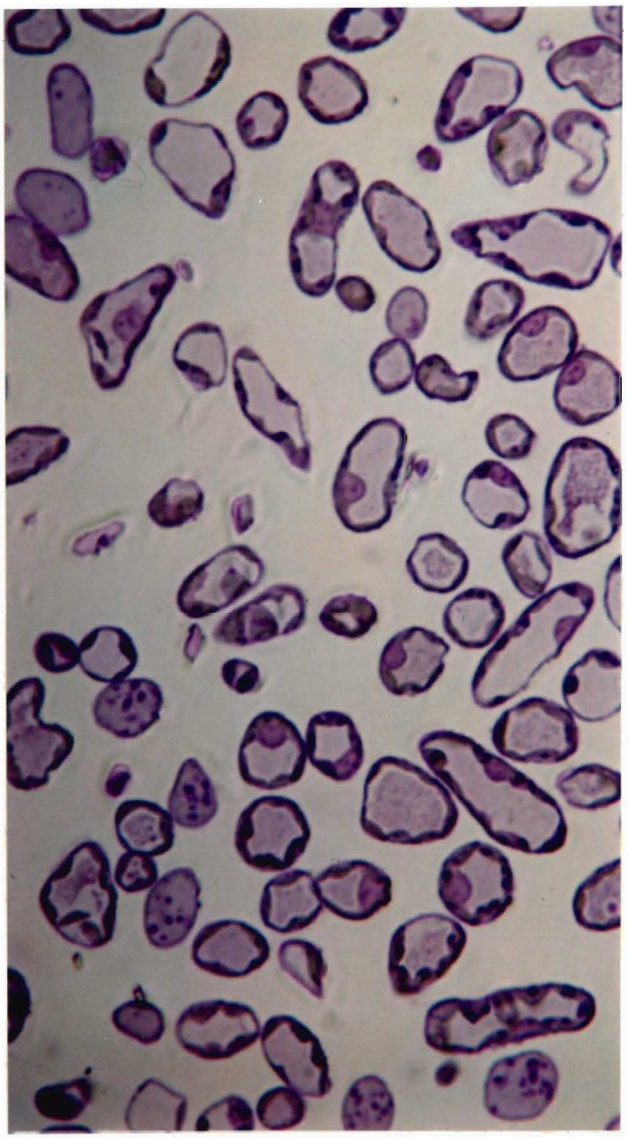

2. Electron microscope studies

Palisade mesophyll cells attached to epidermal cells were thin-walled (0.3 to 0.5 um) and 10 to 30 um in length depending on the plane of the section. Cells were highly vacuolated and contained a large number of mitochondria and chloroplasts. Nuclei were spherical or irregular. Chloroplasts were positioned under the plasma membrane and usually contained several large starch grains and well developed grana and stroma lamellae, indicating a higher level of photosynthetic activity (Fig. 9A, 9B, 12A, and 12B). Plasmodesmata were observed between palisade mesophyll cells, between palisade and spongy mesophyll cells, and betwen border mesophyll cells surrounding the vascular bundle and the bundle itself (Fig. 9C, 9D, 10, and 11). Although difficult to quantify there appeared to be many plasmodesmata between the vascular bundle and the border mesophyll cells. In contrast there appeared to be few plasmodesmata between palisade mesophyll cells and these cells and spongy mesophyll cells. The lack of plasmodesmatal connections between the subepidermal palisade mesophyll cells and the vascular bundle suggests the importance of apoplastic transport of solutes between these two tissues.

Fig. 9A : Transmission electron micrograph of an *Asparagus* cladophyll

- The electron micrograph indicates the arrangement of palisade mesophyll cells. The palisade mesophyll cells are attached to epidermal cells. Chloroplasts lie adjacent to the PM and large central vacuoles are distinct. Huge intercelluar air spaces are noticeable.
- Note : Ch, cloroplast ; Ep, epidermal cell ; IS, intercelluar space ; V, vacuole
- The cladophyll was fixed in buffered glutaraldehyde and OsO_4 and embedded in epon.
- Uranyl acetate and lead citrate, bar = 1 um

Fig. 9B : Transmission electron micrograph of an *Asparagus* cladophyll

- The electron micrograph indicates that palisade mesophyll cells are densely packed. Irregular shaped nuclei, mitochondria, large vacuoles, and chloroplasts containing starch grains are observed.
- Note : Ch, cloroplast ; Ep, epidermal cell ; IS, intercelluar space ; M, mitochodria ; N, nucleus ; Sg, starch grain ; V, vacuole
- A cladophyll fixed in buffered glutaraldehyde and OsO_4 and embedded in epon.
- Uranyl acetate and lead citrate, bar = 1 um


Ep
V
IS
1µm


IS
Ch
Ep
N
N
V
Ep
1µm

Fig. 9C : Transmission electron micrograph of an *Asparagus* cladophyll

- The electron micrograph indicates plasmodesmatal connections between palisade mesophyll cells and a spongy mesophyll cell. The palisade mesophyll cells are thin-walled and chloroplasts are adjacent to the PM. The spongy mesophyll cells contain thicker cell walls and chloroplasts are scattered throughout the cytoplasm. Plasmodesmata (insets) between the palisade mesophyll cells and between the palisade and the spongy mesophyll cells are shown.
- Note : Ch, chloroplast ; IS, intercellular space ; N, nucleus ; V, vacuole ; pd, plasmodesmata ; Pm, palisade mesophyll cell ; Sm, spongy mesophyll cell
- A cladophyll fixed in buffered glutaraldehyde and OsO_4 and embedded in epon.
- Uranyl acetate and lead citrate, bar = 1 um

Fig. 9D : Transmission electron micrograph of an *Asparagus* cladophyll

- The electron micrograph indicates the arrangement of the palisade and spongy mesophyll cells. Plasmodesmata between the palisade and the spongy mesophyll cells are shown.
- Note : Ch, chloroplast ; IS, intercellular space ; N, nucleus ; V, vacuole ; pd, plasmodesmata ; Pm, palisade mesophyll cell, Sm, spongy mesophyll cell
- A cladophyll fixed in buffered glutaraldehyde and OsO_4 and embedded in epon. bar = 1 um

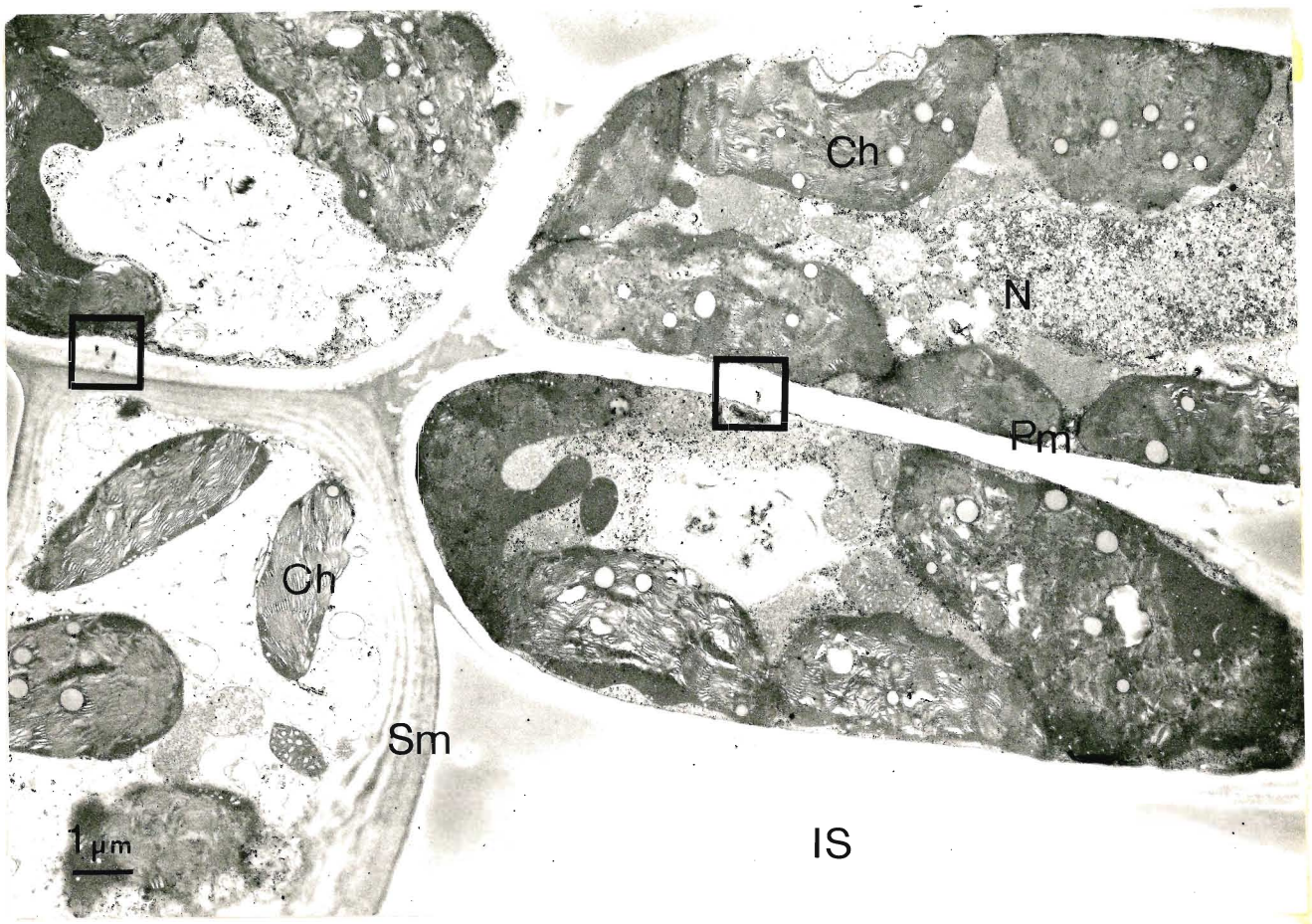
Ch
N
Pm'
Ch
Sm
1μm
IS

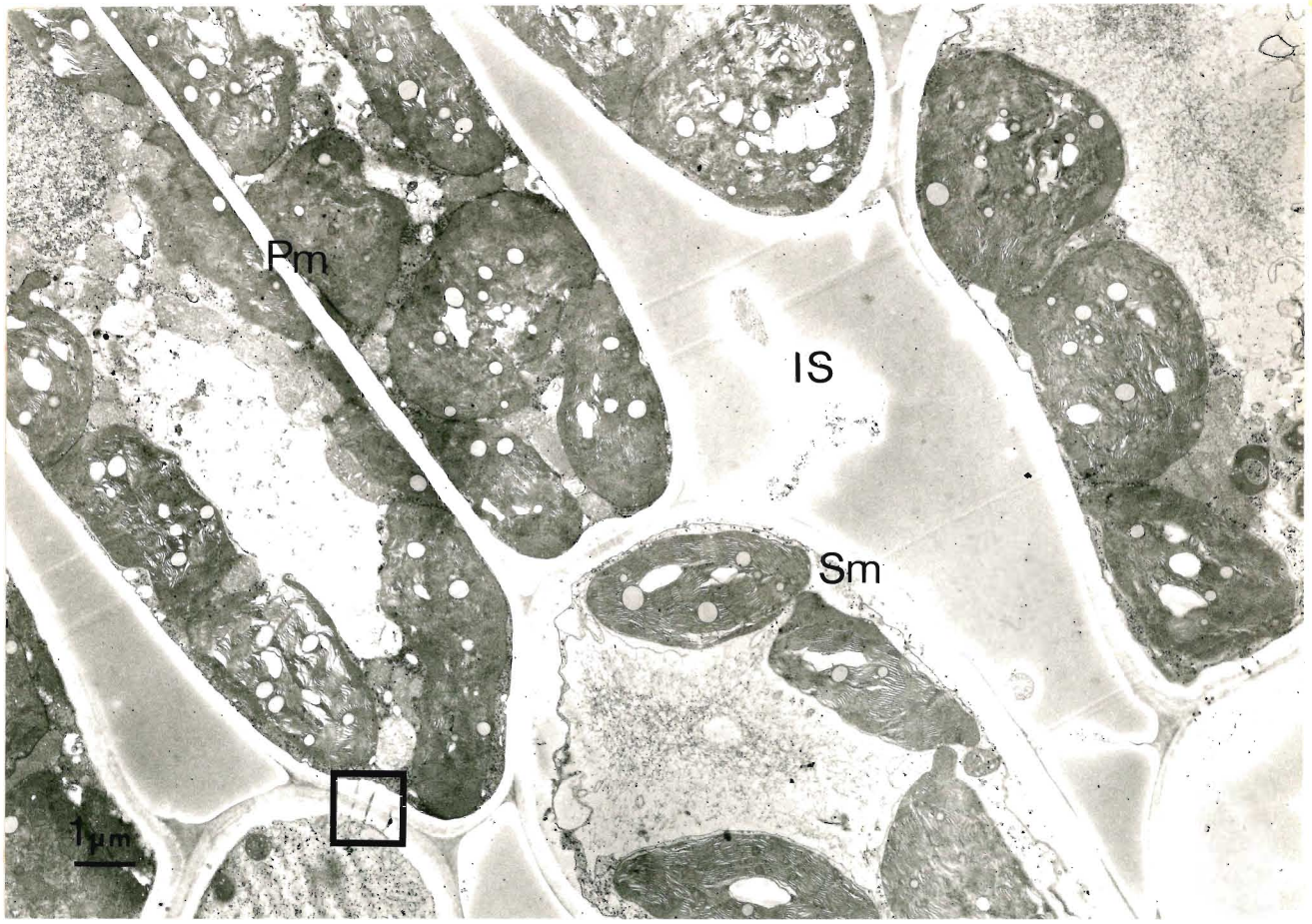
Pm
IS
Sm
1μm

Fig. 10 : Transmission electron micrograph of an *Asparagus* cladophyll

- The electron micrograph indicates a mesophyll parenchyma cell adjacent to a vascular bundle. A large number of plasmodesmata (inset) is present between the mesophyll parenchyma cell and the vascular bundle sheath.
- Note : Ch, chloroplast ; CW, cell wall ; IS, intercellular space ; V, vacuole ; VB, vascular bundle ; Bm, border mesophyll cell ; pd, plasmodesmata
- A cladophyll fixed in buffered glutaraldehyde and OsO_4 and embedded in epon.
- Uranyl acetate and lead citrate, bar = 1 um

Fig. 11 : Highly magnified electron micrograph of plasmodesmata

- The electron micrograph indicates the highly magnified plasmodesmata of Fig. 9D. Cytoplasmic connections between palisade and spongy mesophyll cells are visible. Chloroplasts containing developed grana and stroma lamellae are enclosed by the chloroplast membrane.
- Note : pd, plasmodesmata, Pm, palisade mesophyll cell ; Sm, spongy mesophyll cells
- A cladophyll fixed in buffered glutaraldehyde and OsO_4 and embedded in epon.
- Uranyl acetate and lead citrate, bar = 1 um

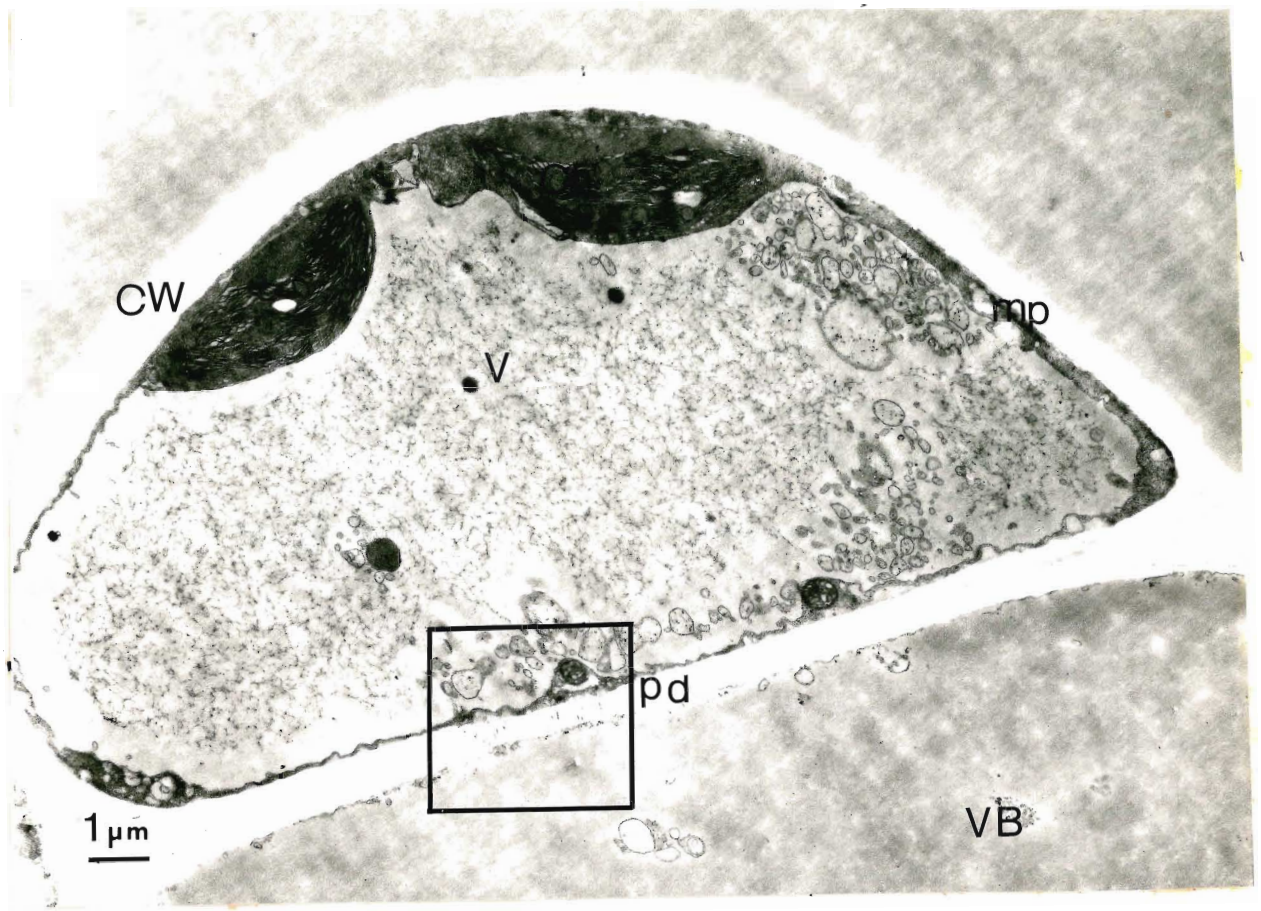
CW
V
mp
pd
1 µm
VB

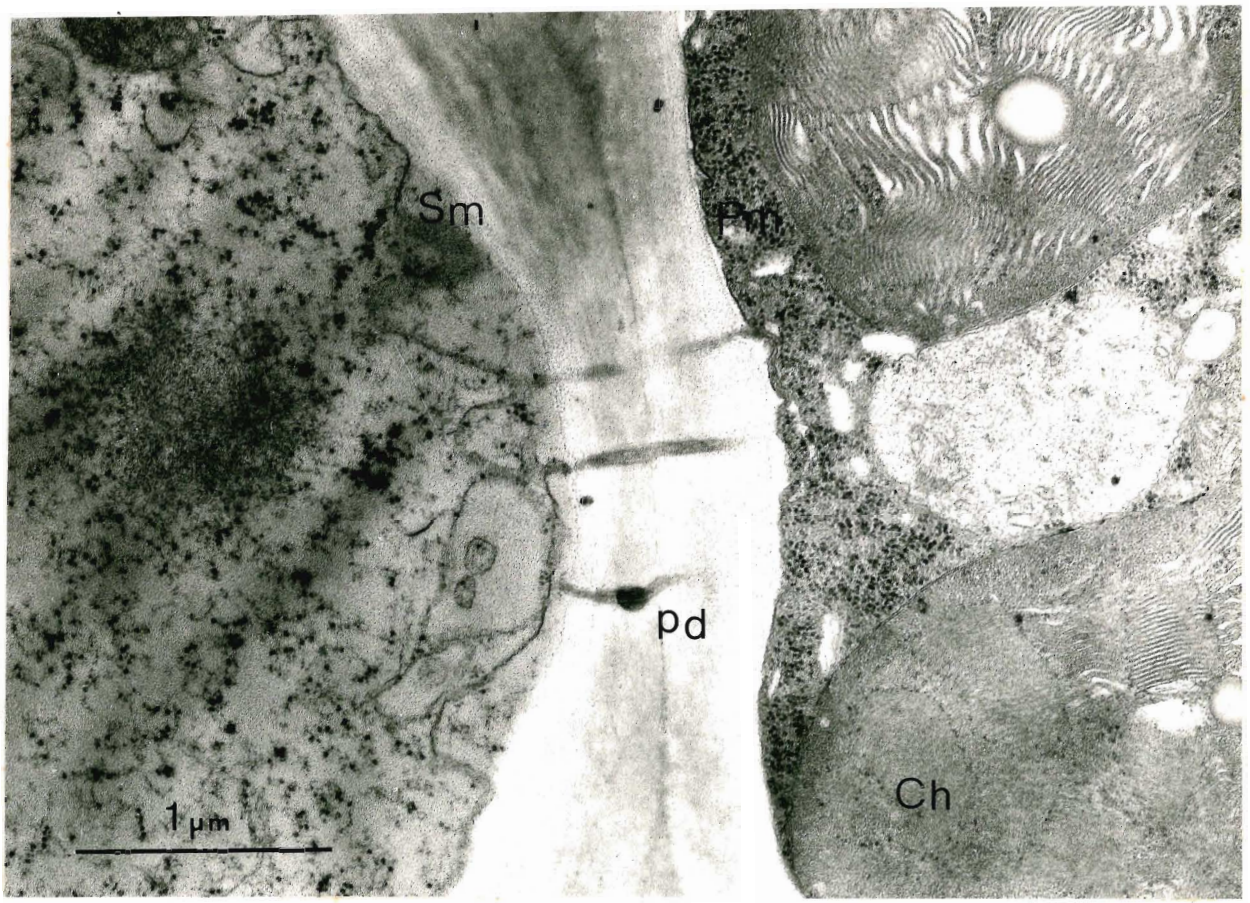
Sm
Pm
pd
1 µm
Ch

Fig 12A and 12B : Transmission electron micrograph of isolated mesophyll cells

- The electron micrograph indicates two shapes of isolated mesophyll cells. Sperical nuclei and large central vacuoles are distinct. Chloroplasts containing starch grains are abundant and enclosed by chloroplast membrane.
- Note : Ch, chloroplast ; M, mitochondria ; N, nucleus ; PM, plasma membrane ; SG, starch grain ; V, vacuole ; Vm, vacuolar membrane
- A cladophyll fixed in buffered glutaraldehyde and OsO_4 and embedded in epon.
- Uranyl acetate and lead citrate, bar = 1 um

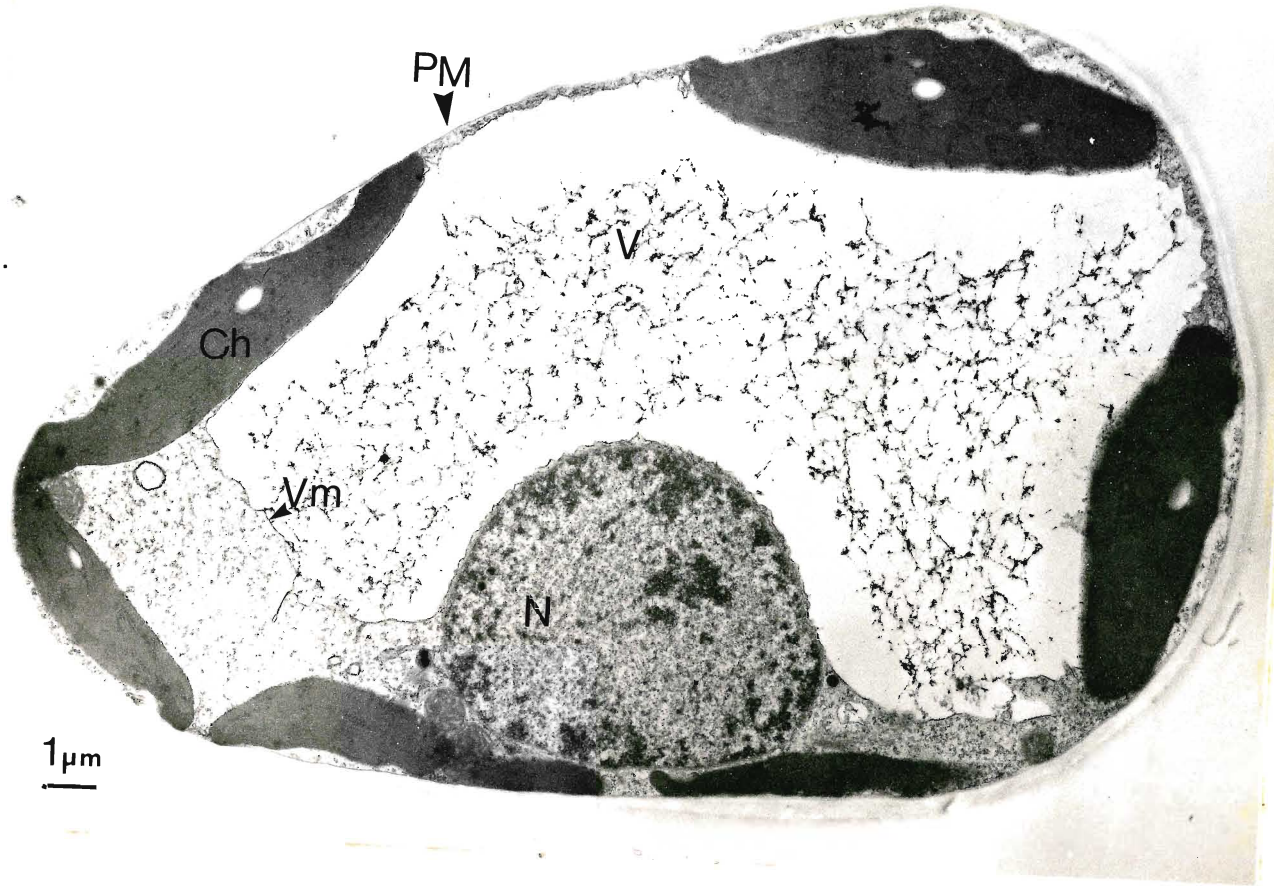
PM
V
Ch
Vm
N
1µm

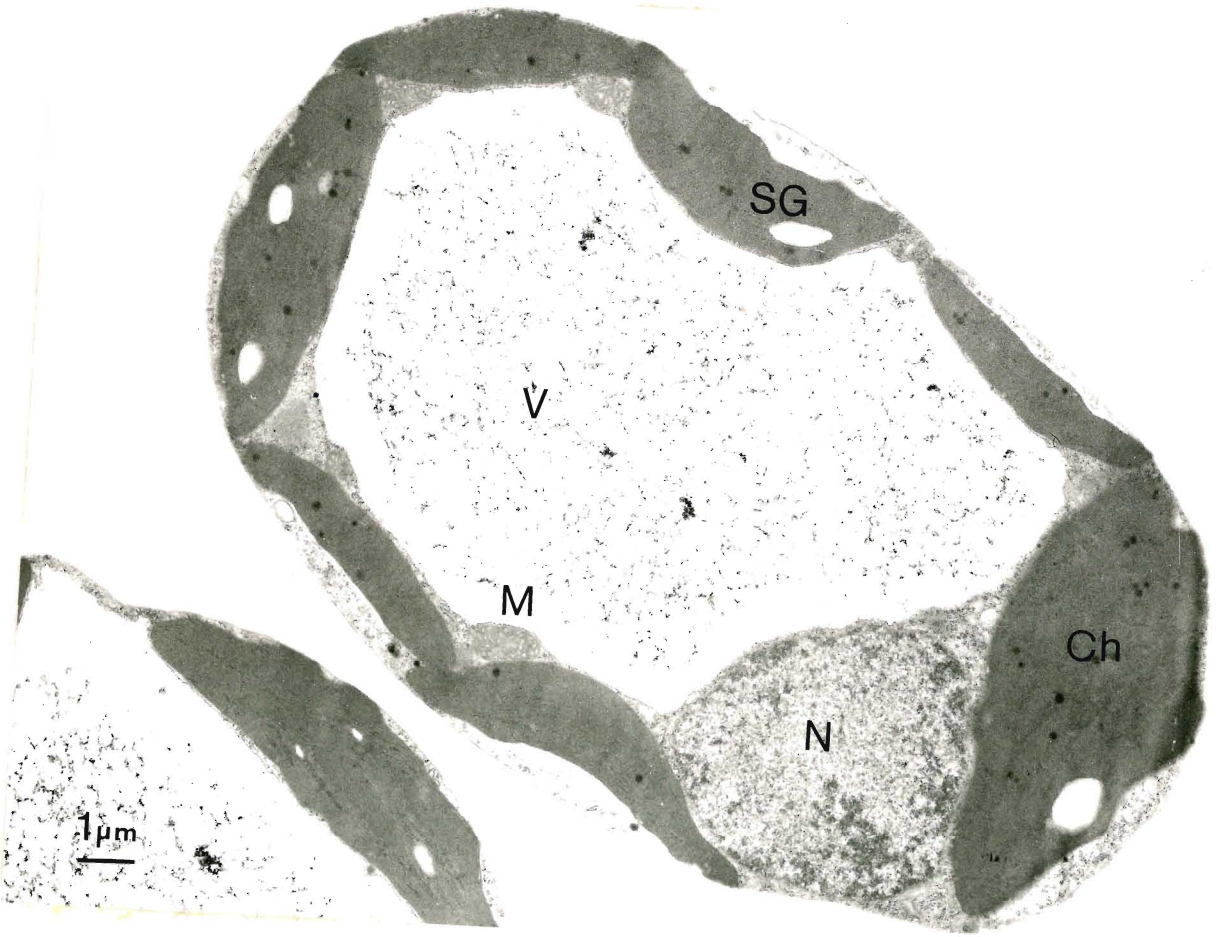
SG
V
M
Ch
N
1µm

3. Cell volume

Cell volume was determined by two different methods, a measurement of length and width and a measurement of areas of serial sections. When the cell volume was estimated by measuring the length and diameter half way along the length and assuming that the cell is a cylindrial shape, the cell volume was 5.8×10^{-6} ul per cell (Table 1). Measurement of areas of epon embedded serial sections and their subsequent reconstruction resulted in 4.68×10^{-6} ul per cell (Table 2). Thus values of cell volume estimated by both methods were in agreement. Since both methods included the cell wall volume, the cytoplasmic volume was slightly overestimated.

Table 1 : Cell volume determination through determination of length and width

Experiment No.	Cell Volume (S.D.) (ul x 10^{-6})
1	5.9 (1.7)
2	6.9 (2.0)
3	4.9 (1.3)
4	6.2 (1.9)
5	5.0 (1.3)
Mean	5.8

- The cell volume was estimated by measuring the length and diameter half way along the length using a light microscope at 400 x magnification. The cell volume was then obtained by assuming that the cell is cylindrical.
- Each experiment involved measurements on more than 50 cells.
- Cell volumes are expressed in terms of ul per cell.

Table 2 : Cell volume determination through analysis of serial sections

Cell No.	Cell volume (ul x 10^{-6})
1	5.66
2	3.58
3	5.33
4	5.18
5	5.53
6	4.27
7	3.03
8	3.79
9	5.12
10	5.01
Mean (S.D.)	4.68 (0.85)

- Serial epon-embedded sections of intact cladophylls (1 um thickness) were made and cell areas were determined under the light microscope at 400 x magnification in conjunction with an IBM PC. Each section was converted to volume and then the cell reconstructed to produce the total cell volume.
- 10 cells were measured and cell volumes are expressed in terms of ul per cell. The mean and S.D. are indicated.

II. AMINO ACID COMPOSITION STUDIES

1. Amino acid pool sizes

Pool sizes of amino acids in isolated *Asparagus* mesophyll cells were determined after incubating cells for 10 and 60 minutes in the presence and absence of 1 mM L-Glu with and without illumination. In illuminated and nonilluminated cells incubated in the absence of L-Glu, Ala was the most abundant free amino acid and stayed at a relatively constant level during the incubation periods. GABA and L-Glu were the second and third most abundant amino acids after a 10 minute incubation but the third and second after a 60 minute incubation. L-Glu tended to increase with a longer incubation period by 30 % or more, but GABA levels decreased by 23 % and 10 % in the light and dark, respectively. The decline in GABA levels is consistent with observations of GABA efflux (Table 3 and 4).

When cells were incubated for 10 and 60 minutes in the presence of 1 mM L-Glu, Ala was again the most abundant free amino acid followed by L-Glu and GABA both in the light and dark. Over a 60 minute period L-Glu increased by 24 % and 46 % in the light and dark, respectively. However, the level of GABA was constant with incubation. The pool sizes of L-Glu and GABA after 10 and 60 minute incubation periods were compared to the levels of those in 1 mM L-Glu treated cells. L-Glu levels increased by 45 % and 20 % in the light, and exhibited a 22 % increase after 60 minutes in the dark. After a 10 and a 60 minute incubation the level of GABA increased by 11 % and 40 % in the light, and

decreased slightly in the dark (Table 3 and 4).

Amino acids in the cell suspension medium were also analysed after 10 and 60 minute incubations with and without illumination in the presence and absence of L-Glu. GABA constituted the largest amino acid pool in the medium after 10 and 60 minute incubations except for the exogenously added L-Glu. In the absence of L-Glu GABA in the illuminated medium was 1.3 and 2.5 fold times greater than Lys, which was the second largest amino acid, and was 3.5 and 2.7 fold times greater than the L-Glu pool. In the dark GABA levels were 1.6 and 3.4 fold times greater than L-Glu levels after 10 and 60 minute incubation. The loss of GABA from the cells and the appearance in the medium indicate efflux of GABA from the cell (Table 5 and 6).

When cells were incubated in exogenous 1 mM L-Glu, L-Glu in the medium decreased by 33 % and 34 % in the light and dark, respectively, indicating that L-Glu had been utilized. Compared to the level of GABA in the medium containing no L-Glu, GABA in the medium in the presence of 1 mM L-Glu increased after 10 and 60 minute incubation by 2,743 % and 2,842 %, respectively in the light, and 2,241 % and 4,423 %, respectively in the dark. This rapid and large GABA efflux indicated the presence of a specific efflux process for GABA, since Ala which is a larger internal pool was not a large pool in the medium. In addition, the huge increase of GABA and the concomitant decrease of L-Glu in the medium indicate that most of the utilized L-Glu was converted to produce GABA and released to the medium (Table 5 and 6).

Fig. 13 : TLC indicating GABA production in the medium in the presence and absence of L-Glu with and without illumination

- Twenty million cells were suspended in 5 ml of 1 mM $CaSO_4$ and stirred.
- The cell suspension was incubated for 10 minutes in the presence (+) and absence (-) of 1 mM L-Glu with (L) and without (D) illumination.
- The dried medium was solubilized in 200 ul of 0.1 N HCl and 20 ul was loaded with standard at origin indicated.
- The solvent system was phenol/water (75/25, w/w).
- Note : ST - a mixture of known L-Glu and GABA
  1 - solvent front
  2 - GABA
  3 - L-Glu
  4 - origin

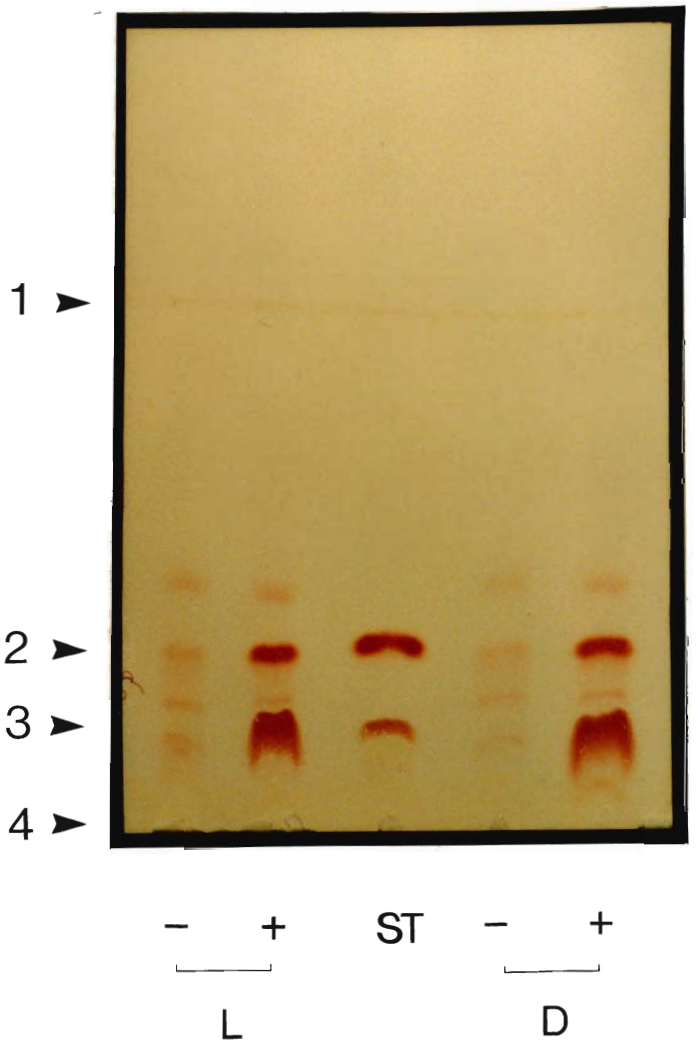
1
2
3
4
−
+
ST
−
+
L
D

Table 3, 4, 5, and 6 : Amino acid composition of the medium and cells after incubation with and without illumination in the presence and absence 1 mM L-Glu

- The number of cells was 30 x 10^6 or 40 x 10^6.
- Cells were suspended in 5 ml of 5 mM MES/1 mM $CaSO_4$ (pH 6.0) and stirred.
- The cell suspension was incubated for 10 min or 60 min in the presence or absence of 1 mM L-Glu (pH 6.0) with and without illumination.
- The dried medium and aqueous cell fractions were derivatized with 2-ME/OPA and analysed by the HPLC apparatus.
- Each value is the mean of 2 analyses of 2 different samples.

Table 3 :Amino acid composition of the cells after illuminating cells in the presence and absence of L-Glu

Amino acid	(−) L-Glu		(+) L-Glu	
	10 min	60 min	10 min	60 min
	(nmol/million cells)			
Asp	0.32	0.38	0.45	0.31
Glu	5.10	7.59	7.42	9.09
Asn	1.26	1.67	1.81	2.20
Ser	1.40	1.20	1.62	1.20
Gln/His	1.93	3.85	1.90	3.89
Gly	1.96	3.08	1.71	2.81
Thr	1.24	1.57	1.61	1.92
Arg	0.71	0.78	0.40	0.95
Ala	13.10	12.83	19.89	19.94
GABA	5.73	4.40	6.37	6.10
Tyr	1.47	2.07	1.77	2.15
Met	0.12	0.26	0.03	0.34
Val/Trp	1.26	1.72	1.41	2.31
Phe	0.67	0.98	1.90	1.15
Ile	0.55	0.72	1.66	0.89
Leu	0.81	1.30	0.93	1.54
Lys	1.82	2.77	1.93	2.86

Table 4 :Amino acid composition of the cells after incubating cells without illumination in the presence and absence of L-Glu

Amino acid	(-) L-Glu		(+) L-Glu	
	10 min	60 min	10 min	60 min
	(nmol/million cells)			
Asp	0.39	0.58	0.39	0.96
Glu	6.13	7.94	5.56	8.09
Asn	4.79	2.36	4.71	1.80
Ser	2.18	1.50	1.78	0.97
Gln/His	3.39	1.23	3.17	1.19
Gly	2.88	2.42	1.81	1.20
Thr	1.66	1.49	1.45	1.49
Arg	0.66	0.70	0.55	0.61
Ala	18.14	19.39	17.10	19.95
GABA	5.49	4.96	4.51	4.50
Tyr	0.99	2.10	1.09	1.50
Met	0.00	0.20	0.00	0.03
Val/Trp	0.92	1.36	1.09	1.37
Phe	0.30	0.79	0.43	0.90
Ile	0.34	0.55	0.33	0.70
Leu	0.34	0.87	0.40	1.15
Lys	1.09	2.28	1.07	2.32

Table 5 : Amino acid composition of the medium after illuminating cells in the presence and absence of L-Glu

Amino acid	(−) L-Glu		(+) L-Glu	
	10 min	60 min	10 min	60 min
	(nmol/million cells)			
Asp	0.02	0.15	0.12	0.39
Glu	0.10	0.47	53.15	34.84
Asn	0.03	0.19	0.06	0.30
Ser	0.01	0.07	0.00	0.29
Gln/His	0.05	0.36	0.06	0.69
Gly	0.03	0.21	0.11	0.43
Thr	0.02	0.12	0.00	0.19
Arg	0.03	0.22	0.00	0.24
Ala	0.13	0.25	0.38	0.56
GABA	0.35	1.25	9.60	35.52
Tyr	0.04	0.05	0.03	0.42
Met	0.00	0.05	0.00	0.01
Val/Trp	0.04	0.16	0.04	0.16
Phe	0.02	0.12	0.03	0.20
Ile	0.01	0.06	0.04	0.12
Leu	0.04	0.37	0.00	0.27
Lys	0.14	0.98	0.03	0.89

Table 6 :Amino acid composition of the medium after incubating cells without illumination in the presence and absence of L-Glu

Amino acid	(-) L-Glu		(+) L-Glu	
	10 min	60 min	10 min	60 min
	(nmol/million cells)			
Asp	0.05	0.10	0.47	0.40
Glu	0.28	0.23	59.47	40.13
Asn	0.24	0.00	0.23	0.27
Ser	0.08	0.01	0.06	0.11
Gln/His	0.18	0.02	0.16	0.18
Gly	0.13	0.02	0.20	0.27
Thr	0.08	0.02	0.06	0.17
Arg	0.08	0.06	0.05	0.25
Ala	0.54	0.08	0.51	0.97
GABA	0.46	0.79	10.31	34.94
Tyr	0.08	0.12	0.07	0.36
Met	0.00	0.00	0.00	0.00
Val/Trp	0.05	0.02	0.07	0.13
Phe	0.04	0.05	0.04	0.18
Ile	0.03	0.01	0.03	0.10
Leu	0.07	0.05	0.08	0.28
Lys	0.19	0.33	0.08	0.82

2. Amino acid concentrations

The amino acid concentrations both in cells and medium in the presence and absence of 1 mM L-Glu were determined using the pool sizes of amino acids (Table 3, 4, 5, and 6) and the volume of cells (Table 2) and medium. The concentrations of L-Glu and GABA in the cells and medium are shown in Table 7, 8, 9, and 10. In illuminated cells, the concentrations of L-Glu and GABA were 1.090 mM and 1.225 mM after a 10 minute incubation and 1.622 mM and 0.941 mM after a 60 minute incubation. When cells were incubated with exogenous L-Glu, the concentrations of L-Glu and GABA were 1.586 mM and 1.362 mM after a 10 minute incubation and 1.943 mM and 1.304 mM after a 60 minute incubation. Although the cells were incubated in the presence of 1 mM L-Glu, there was a slight increase in the cellular concentration of L-Glu but a constant or slight decrease in concentration of GABA (Table 7 and 8).

In the absence of exogenous L-Glu the concentrations of L-Glu and GABA in the illuminated medium were 0.001 mM and 0.002 mM after a 10 minute incubation and 0.003 mM and 0.007 mM after a 60 minute incubation. Because the volume of the medium was much larger than that of cells, the concentration of GABA in the medium was much lower even when much more GABA was present in the medium than in the cells. In the presence of exogenous 1 mM L-Glu, the concentrations of L-Glu and GABA in the medium were 0.318 mM and 0.057 mM after a 10 minute incubation and 0.209 mM and 0.213 mM after a 60 minute incubation. Thus exogenous L-Glu

increased the concentration of GABA by a factor or 30 (Table 9 and 10).

The size of the concentration gradient of GABA across the plasma membrane was calculated after incubation with 1 mM L-Glu. The concentration gradients in the illuminated cells after 10 and 60 minutes were 24 fold and 6 fold. In the nonilluminated cells the gradients of GABA were 16 fold and 5 fold after 10 and 60 minute incubations. Thus the concentration gradient favors GABA efflux. This suggests that an active mechanism for GABA efflux is not required.

Table 7, 8, 9, and 10: Amino acid concentrations in the medium and cells after incubation with and without illumination in the presence and absence of 1 mM L-Glu

- Concentrations of amino acids were derived from amino acid composition data (Table 3, 4, 5, and 6) and cell volume data (Table 2)
- Conditions were the same as in Table 3, 4, 5, and 6.
- Concentrations in cells were calculated by dividing the amounts of amino acids by the cytoplasmic volume (4.68 ul / 10^6 cells).
- Concentrations in the medium were calculated by dividing the amount of amino acids by the volume of the surrounding medium (167 ul / 10^6 cells).
- Each value is the mean of 2 trials.

Table 7 :Amino acid concentrations in cells after illuminating cells in the presence and absence of L-Glu

Amino acid	(-) L-Glu		(+) L-Glu	
	10 min	60 min	10 min	60 min
	(mM)		(mM)	
Asp	0.068	0.081	0.096	0.066
Glu	1.090	1.622	1.586	1.943
Asn	0.269	0.357	0.387	0.470
Ser	0.299	0.257	0.346	0.257
Gln/His	0.413	0.823	0.406	0.832
Gly	0.419	0.658	0.366	0.601
Thr	0.265	0.336	0.344	0.410
Arg	0.152	0.167	0.086	0.203
Ala	2.800	2.743	4.252	4.263
GABA	1.225	0.941	1.362	1.304
Tyr	0.314	0.442	0.378	0.460
Met	0.026	0.056	0.006	0.073
Val/Trp	0.269	0.368	0.301	0.494
Phe	0.143	0.209	0.406	0.246
Ile	0.118	0.154	0.355	0.190
Leu	0.173	0.278	0.199	0.329
Lys	0.389	0.592	0.413	0.611

Table 8: Amino acid concentrations in cells after incubating cells without illumination in the presence and absence of L-Glu

Amino acid	(−) L-Glu		(+) L-Glu	
	10 min	60 min	10 min	60 min
	(mM)		(mM)	
Asp	0.083	0.124	0.083	0.205
Glu	1.310	1.697	1.189	1.729
Asn	1.024	0.504	1.007	0.385
Ser	0.466	0.321	0.381	0.207
Gln/His	0.725	0.263	0.678	0.254
Gly	0.616	0.517	0.387	0.257
Thr	0.355	0.319	0.310	0.319
Arg	0.141	0.150	0.118	0.130
Ala	3.878	4.145	3.655	4.265
GABA	1.174	1.060	0.964	0.962
Tyr	0.212	0.449	0.233	0.321
Met	0.000	0.043	0.000	0.006
Val/Trp	0.197	0.291	0.233	0.293
Phe	0.064	0.169	0.092	0.192
Ile	0.073	0.118	0.071	0.150
Leu	0.073	0.186	0.086	0.246
Lys	0.233	0.487	0.229	0.496

Table 9 :Amino acid concentrations in medium after illuminating cells in the presence and absence of L-Glu

Amino acid	(-) L-Glu		(+) L-Glu	
	10 min	60 min	10 min	60 min
	(mM)		(mM)	
Asp	0.000	0.001	0.001	0.002
Glu	0.001	0.003	0.318	0.209
Asn	0.000	0.001	0.000	0.002
Ser	0.000	0.000	0.000	0.002
Gln/His	0.000	0.002	0.000	0.004
Gly	0.000	0.001	0.001	0.003
Thr	0.000	0.001	0.000	0.001
Arg	0.000	0.001	0.000	0.001
Ala	0.001	0.001	0.002	0.003
GABA	0.002	0.007	0.057	0.213
Tyr	0.000	0.000	0.000	0.003
Met	0.000	0.000	0.000	0.000
Val/Trp	0.000	0.001	0.000	0.001
Phe	0.000	0.001	0.000	0.001
Ile	0.000	0.000	0.000	0.001
Leu	0.000	0.002	0.000	0.002
Lys	0.001	0.006	0.000	0.005

Table 10 : Amino acid concentrations in medium after incubating cells without illumination in the presence and absence of L-Glu

Amino Acid	(-) L-Glu		(+) L-Glu	
	10 min	60 min	10 min	60 min
	(mM)		(mM)	
Asp	0.000	0.001	0.003	0.002
Glu	0.002	0.001	0.356	0.240
Asn	0.001	0.000	0.001	0.002
Ser	0.000	0.000	0.000	0.001
Gln/His	0.001	0.000	0.001	0.001
Gly	0.001	0.000	0.001	0.002
Thr	0.000	0.000	0.000	0.001
Arg	0.000	0.000	0.000	0.001
Ala	0.003	0.000	0.003	0.006
GABA	0.003	0.005	0.062	0.209
Tyr	0.000	0.001	0.000	0.002
Met	0.000	0.000	0.000	0.000
Val/Trp	0.000	0.000	0.000	0.001
Phe	0.000	0.000	0.000	0.001
Ile	0.000	0.000	0.000	0.001
Leu	0.000	0.000	0.000	0.002
Lys	0.001	0.002	0.000	0.005

3. Amino acids in intact tissue, tissue debris, and isolated cells

Since GABA constituted one of the largest free amino pools in isolated mesophyll cells and the largest in the medium, experiments were performed to determine whether the large GABA pool was generated by the stress of the cell isolation procedure. Therefore profiles of amino acid pools from the intact tissue, tissue debris and isolated cells were determined (Table 11).

In isolated cells, GABA was the third largest amino acid pool representing 6.35 % of the total. In intact tissue GABA was the second largest amino acid at 18.78 %, and in tissue debris GABA was the largest amino acid with 25.39 %. Thus the level of GABA in isolated cells was actually much lower than that in intact tissue and debris, suggesting GABA efflux from the cells. Therefore the profile of amino acids in intact tissue and isolated cells clearly suggests that the large GABA pool was not generated by the mechanical cell isolation procedure but GABA was already present in large concentration before cell isolation. Some of this GABA leaves the cells during the cell isolation procedure.

Table 11 : Amino acid composition of intact tissue, tissue debris and isolated cells

- Dried aqueous fraction from intact tissue, tissue debris, and isolated cells was dissolved in 300 ul of filtered water. An aliquot from the 300 ul of dissolved volume was taken and diluted 3 or 5 times. Then 10 ul from the diluted sample was derivatized with 2-ME/OPA and then injected into the HPLC apparatus.
- Using standard amino acid concentrations and corresponding integration values, amino acid values for each analysis was converted into pmol units. When pmol values were converted to % pmole values, the unknown amino acid peaks were ignored.
- The mean and standard deviation (S.D.) of three separate samples are shown in % pmole values.

Table 11 : Amino acid composition of intact tissue, tissue debris and isolated cells

Amino Acid	Intact tissue	Tissue Debris	Isolated Cell
	% pmole (S.D.)	% pmole(S.D)	% pmole(S.D.)
Asp	13.59 (4.62)	4.01 (0.93)	2.70 (1.09)
Glu	19.72 (3.69)	9.76 (3.49)	29.18 (7.64)
Asn	3.91 (1.85)	4.58 (3.53)	4.81 (2.05)
Ser	7.95 (2.08)	7.17 (0.60)	2.38 (0.17)
Gln/His	3.36 (0.90)	2.35 (0.22)	4.07 (0.37)
Gly	2.44 (0.25)	7.07 (0.78)	4.35 (0.51)
Thr/Cit	1.46 (0.21)	1.60 (0.25)	1.71 (0.26)
Arg	1.18 (0.80)	2.21 (0.59)	3.24 (1.25)
Ala	12.97 (2.79)	16.50 (1.88)	22.68 (7.44)
Gaba	18.78 (4.15)	25.39 (3.28)	6.35 (1.05)
Tyr	1.18 (0.25)	1.37 (0.27)	2.35 (0.42)
Met/Trp	0.38 (0.23)	0.53 (0.28)	0.32 (0.19)
Val	2.53 (0.69)	2.79 (0.65)	3.35 (0.67)
Phe	1.34 (0.34)	1.80 (0.36)	2.38 (0.62)
Ile	3.21 (1.54)	2.16 (0.68)	2.03 (0.26)
Leu	1.19 (0.37)	2.53 (0.56)	3.79 (0.67)
Lys	4.80 (2.72)	8.19 (2.64)	4.31 (1.80)
Sum	100.00	100.00	100.00

4. Amino acids in xylem sap

The objective of the analysis of xylem sap was to determine the contributions of L-Glu and GABA to the amino acid pool of the xylem sap (Table 12).

At the top, middle, and base sections of stems, Asn was the main amino acid of the xylem sap constituting over 50 % of the pool. GABA was the second largest component of the sap and there was no proportional difference in its contribution to sap from the top, middle, and base of the stems since it represented 11 %, 10 %, and 11 % of the total pool, respectively. In contrast, L-Glu was one of the smallest amino acids representing less than 1 % of the pool throughout the stems. These results suggest that GABA may play an important role in C and N transport and metabolism. In addition, considering that L-Glu is the second biggest component in the isolated cells, it is quite noticeable that L-Glu is one of the smallest components of the xylem sap.

Table 12 : Amino acid compositon of xylem sap extracted from the top, mid-section, and base of the *Asparagus* stem

- Dried xylem sap was dissolved into 100 or 200 ul of filtered water. An aliquot from the 100 or 200 ul of dissolved volume was taken, diluted 5 or 10 times, and derivatized with 2-ME/OPA. Then 10 ul was injected into the HPLC apparatus.
- Using standard amino acid concentrations and corresponding integration values, xylem amino acid values (pmol) were converted into % pmol units.
- The mean and standard deviation (S.D.) of three separate samples are shown in % pmole values.

Table 12 : Amino acid composition of xylem sap extracted from the top, mid-section, and base of the *Asparagus* stem

Amino Acids	Top	Middle	Base
	% pmole(S.D.)	% pmole(S.D.)	% pmole(S.D.)
Asp	1.90 (0.21)	1.67 (0.51)	1.14 (0.25)
Glu	0.65 (0.20)	0.40 (0.29)	1.12 (1.16)
Asn	53.88 (14.92)	66.34 (4.46)	67.60 (7.30)
Ser	2.76 (0.83)	3.00 (0.65)	2.92 (0.05)
Gln/His	6.26 (1.20)	6.41 (0.58)	6.13 (0.76)
Gly	1.64 (0.62)	1.52 (0.29)	0.98 (0.70)
Thr/Cit	0.71 (0.11)	0.84 (0.20)	0.49 (0.28)
Arg	9.15 (5.04)	3.34 (1.12)	1.88 (1.25)
Ala	2.29 (1.01)	1.91 (0.25)	1.93 (0.57)
Gaba	10.72 (4.38)	9.63 (2.84)	11.36 (3.53)
Tyr	0.36 (0.26)	0.35 (0.08)	0.30 (0.23)
Met/Trp	0.36 (0.25)	0.21 (0.13)	0.25 (0.19)
Val	1.97 (1.05)	1.47 (0.42)	1.30 (0.95)
Phe	0.81 (0.43)	0.62 (0.14)	0.49 (0.37)
Ile	1.35 (0.20)	0.53 (0.14)	0.50 (0.38)
Leu	3.89 (1.55)	1.39 (0.37)	1.31 (1.00)
Lys	1.30 (1.83)	0.45 (0.64)	0.29 (0.41)
Sum	100.00	100.09	100.00

III. L-GLUTAMATE AND GABA TRANSPORT STUDIES

1. GABA and medium alkalinization

GABA is a major metabolite of L-Glu in isolated *Asparagus* cells and is found in the medium after feeding L-Glu (Table 9 and 10, Fig. 13). If L-Glu is decarboxylated to GABA outside the cells by an extracellular located enzyme, L-Glu dependent medium alkalinization may result from metabolism not H^+/L-Glu symport. In addition GABA itself may alkalinize the medium through a H^+/GABA symport process. Experiments were conducted to determine whether or not L-Glu dependent medium alkalinization is caused by metabolism and/or a H^+/GABA symport process.

When 5 mM L-Glu was added to the cell suspension, L-Glu caused an immediate and large medium alkalinization. The initial rate of medium alkalinization was 3.35 nmol $H^+/10^6$cells/minute in the light and 2.98 nmol $H^+/10^6$ cells/minute in the dark. Addition of 5 mM GABA, however, did not cause medium alkalinization in the light or dark. In fact it appeared to inhibit H^+ efflux (Fig. 15). Thus it is clear that the medium alkalinization is not caused by a H^+/GABA symport process. Other results demonstrated that alkalinization is not due to extracellular GABA production (Fig. 29,30, 31A, and 31B).

2. The influence of GABA on L-Glu dependent medium alkalinization

In order to determine whether GABA influences the rate of L-Glu dependent medium alkalinization, the initial rate of L-Glu dependent medium alkalinization was measured in the presence and absence of 5 mM GABA. Rates of 5 mM L-Glu dependent medium alkalinization were 3.35 nmol $H^+/10^6$ cells/minute in the light and 2.98 nmol $H^+/10^6$ cells/minute in the dark (Fig. 14 and Table 13). Preincubation with GABA for 20 minutes inhibited the 5 mM L-Glu dependent medium alkalinization rate by 30 % in the light and 20 % in the dark. When 5 mM GABA was added simultaneously with 1 mM L-Glu, the medium alkalinization was stimulated by 50 % and 61 % in the light and dark, respectively (Table 14).

Five mM GABA was added 10 minutes after the initiation of alkalinization with 5 mM and 0.5 mM L-Glu. GABA inhibited the 5 mM L-Glu dependent medium alkalinization by 50 % in the light and by 56 % in the dark. However GABA stimulated 0.5 mM L-Glu dependent medium alkalinization by 48 % in the light (Table 16, Fig. 16).

Five mM GABA inhibited both the initial rate of 5 mM L-Glu dependent medium alkalinization and the medium alkalinization rate after the incubation with 5 mM L-Glu for 10 minutes by 20 % to 50 %. However the same concentration of GABA stimulated the 0.5 mM and 1 mM L-Glu dependent medium alkalinization rates by 48 % and more than 50 %, respectively.

Fig 14 : 5 mM L-Glu dependent medium alkalinization

- 7.7 million cells were suspended in 10 ml of 1 mM $CaSO_4$ and introduced into a reaction vessel maintained at 30° C.
- The cell suspension was aerated, stirred and exposed to the light.
- L-Glu was added where indicated and the medium alkalinization was measured.
- After the addition of L-Glu, the contents of the reaction vessel were titrated with 100 nmol H^+ or 100 nmol OH^- in order to determine the buffering capacity.
- The initial rate of medium alkalinization was calculated from the change in pH, the buffering capacity of the cell suspension medium, and the number of cells, and expressed in nmol $H^+/10^6$ cells/minute.

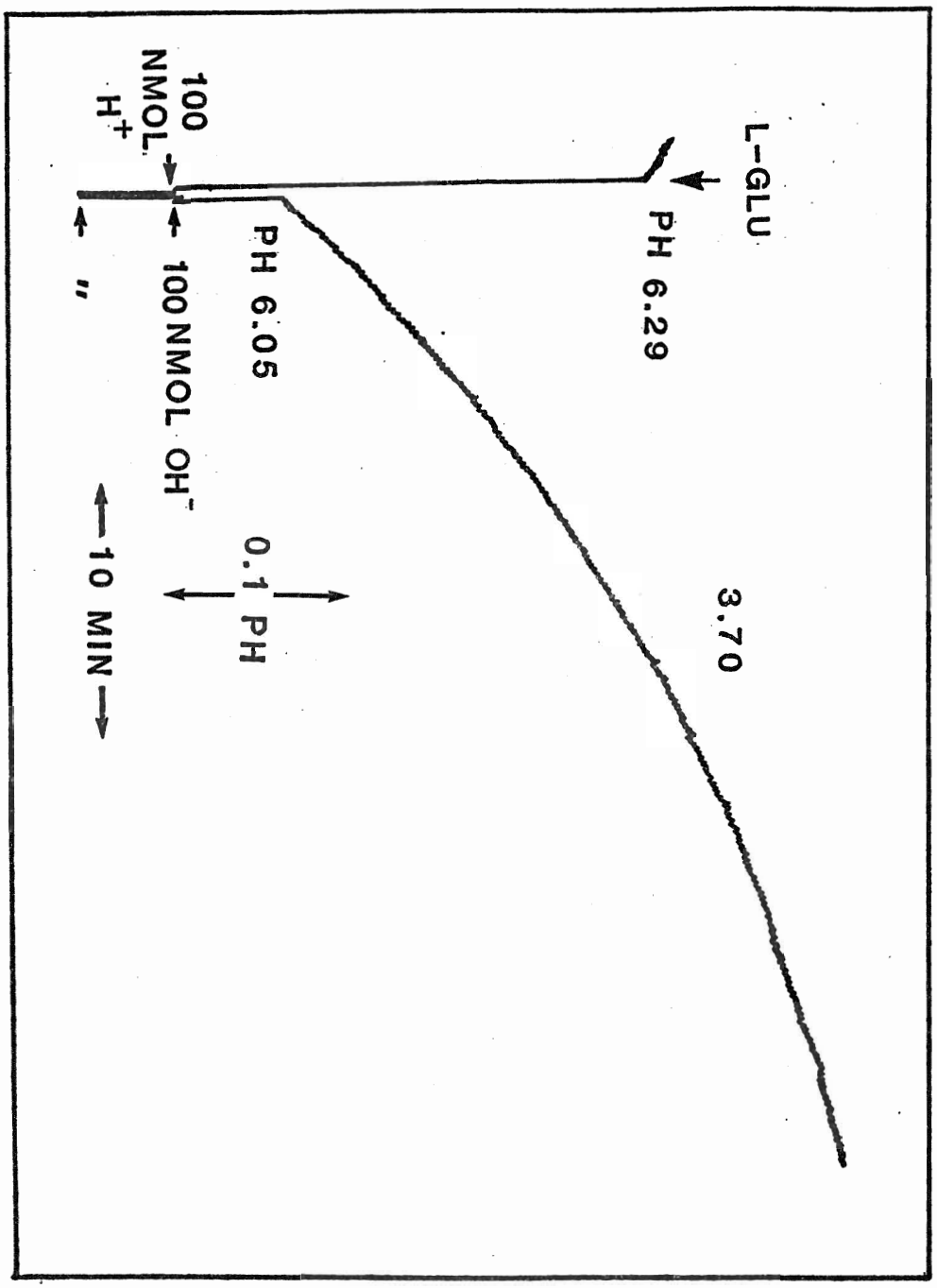
L-GLU
PH 6.29
3.70
100 NMOL H+
"
100 NMOL OH-
PH 6.05
0.1 PH
10 MIN

Fig 15 : 5 mM L-Glu dependent medium alkalinization as influenced by 5 mM GABA

- 7.7 million cells were suspended in 10 ml of 1 mM $CaSO_4$ and introduced into a reaction vessel maintained at 30° C.
- The cell suspension was aerated, stirred and preincubated for 18 minutes in the presence of 5 mM GABA with illumination.
- L-Glu was added where indicated and the medium alkalinization was measured.
- After the addition of GABA and L-Glu, the contents of the reaction vessel were titrated with 100 nmol H^+ or 100 nmol OH^- in order to determine the buffering capacity.
- The initial rate of medium alkalinization was calculated from the change in pH, the buffering capacity of the cell suspension medium, and the number of cells, and expressed as nmol $H^+/10^6$ cells/minute.

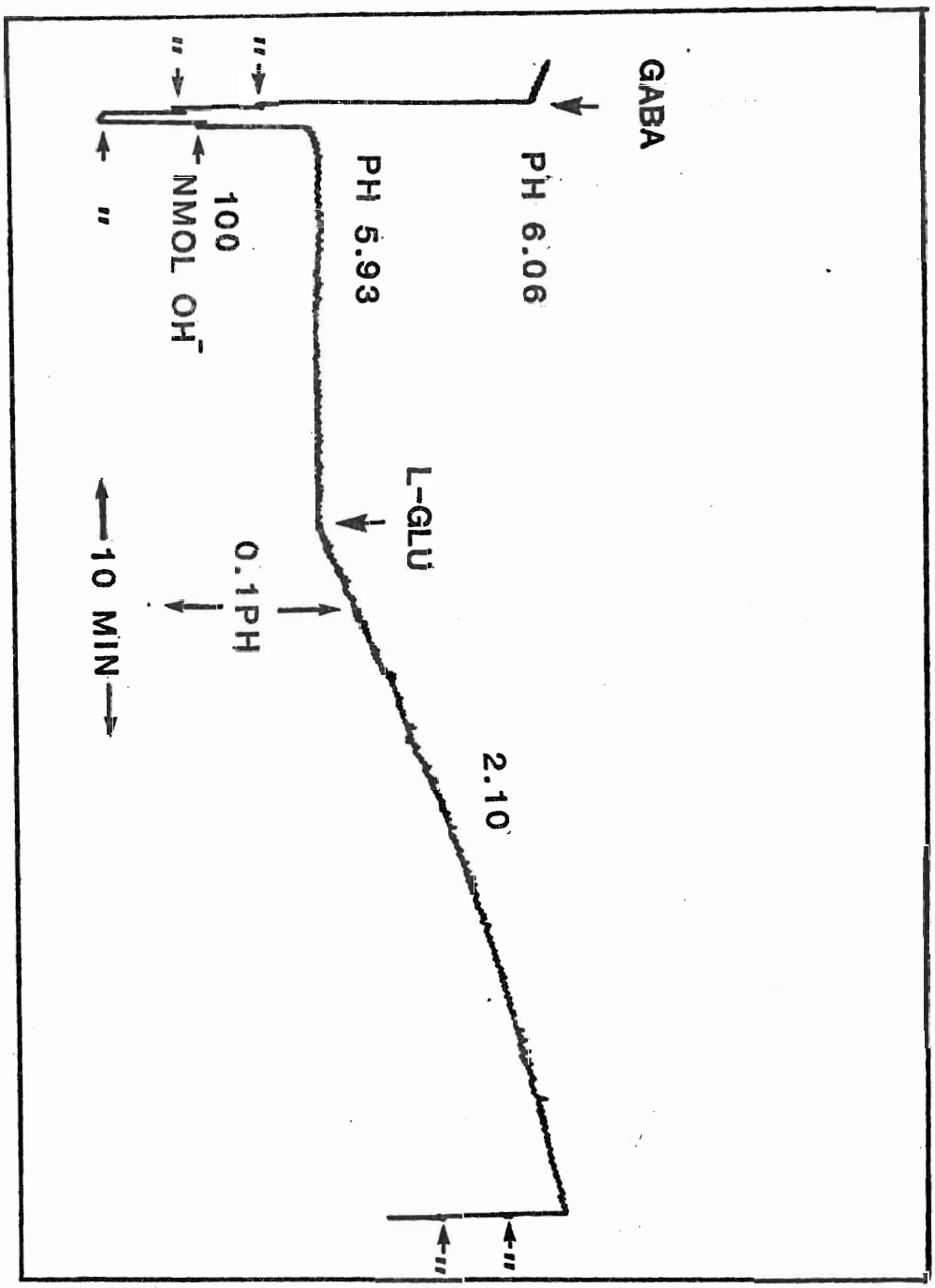
GABA
PH 6.06
PH 5.93
L-GLU
2.10
0.1PH
100
NMOL OH⁻
10 MIN

Table 13 : The initial rate of alkalinization when 5 mM L-Glu was added to cells in the presence and absence of 5 mM GABA

L			D		
(-)GABA	(+)GABA	% Control	(-)GABA	(+)GABA	% Control
4.21	2.33	55	4.86	2.20	45
4.54	2.41	53	2.06	2.28	111
-	-	-	2.18	1.81	83
-	-	-	2.80	2.20	79
2.29	2.21	97	-	-	-
1.98	1.72	87	-	-	-
3.75	2.12	57	-	-	-
3.35(1.03)	2.16(0.24)	70	2.97(1.12)	2.13(0.18)	80

- Five to 10 x 10^6 cells were suspended in 10 ml of 1 mM $CaSO_4$ and introduced into a reaction vessel maintained at 30°C.
- The cell suspension was aerated, stirred and exposed to the light (L) or dark (D) in the presence (+) and absence (-) of 5 mM GABA for approximately 20 minutes.
- L-Glu was added to give 5 mM after 20 minutes.
- After the addition of GABA and L-Glu, the contents of the reaction vessel were titrated with 100 nmol H^+ or 100 nmol OH^- in order to determine the buffering capacity.
- Each experimental value indicates the net rate of proton uptake expressed as nmol $H^+/10^6$ cells/minute.Rates were expressed as a % of control.
- The mean and S.D. of 4 to 5 trials are indicated.

Table 14 : The initial rate of alkalinization when 1 mM L-Glu and 5 mM GABA were simultaneously added to cells

L			D		
(-)GABA	(+)GABA	% Control	(-)GABA	(+)GABA	% Control
2.24	2.78	124	-	-	-
1.56	1.79	115	-	-	-
1.19	1.80	151	-	-	-
0.97	1.67	173	-	-	-
2.71	2.98	110	-	-	-
0.65	0.89	136	0.33	0.61	187
0.67	1.61	241	0.49	0.67	135
1.43(0.73)	1.95(0.67)	150	0.41	0.64	161

- Five to 10 x 10^6 cells were suspended in 10 ml of 1 mM $CaSO_4$ and introduced into a reaction vessel maintained at 30°C.
- The cell suspension was aerated, stirred and exposed to the light (L) or dark (D) in the presence (+) and absence (-) of 5 mM GABA.
- L-Glu was added to give 1 mM.
- After the addition of L-Glu ± GABA, the contents of the reaction vessel were titrated with 100 nmol H^+ or 100 nmol OH^- in order to determine the buffering capacity.
- Each experimental value indicates the net rate of proton uptake expressed as nmol $H^+/10^6$ cells/minute. Rates were expressed as a % of control.
- The mean and S.D. of 2 to 7 trials are indicated.

Fig 16 : Rate of 5 mM L-Glu dependent medium alkalinization as influenced by subsequent addition of 5 mM GABA

- 5.6 million cells were suspended in 10 ml of 1 mM $CaSO_4$ and introduced into a reaction vessel maintained at 30°C.
- The cell suspension was aerated, stirred and incubated for 10 minutes with L-Glu as indicated.
- GABA was added to give 5 mM where indicated and the subsequent rate was measured.
- After the addition of L-Glu and GABA, the contents of the reaction vessel were titrated with 100 nmol H^+ or 100 nmol OH^- in order to determine the buffering capacity.
- The subsequent rate of medium alkalinization was calculated from the change in pH, the buffering capacity of the cell suspension medium, and the number of cells, and expressed as nmol $H^+/10^6$ cells/minute.

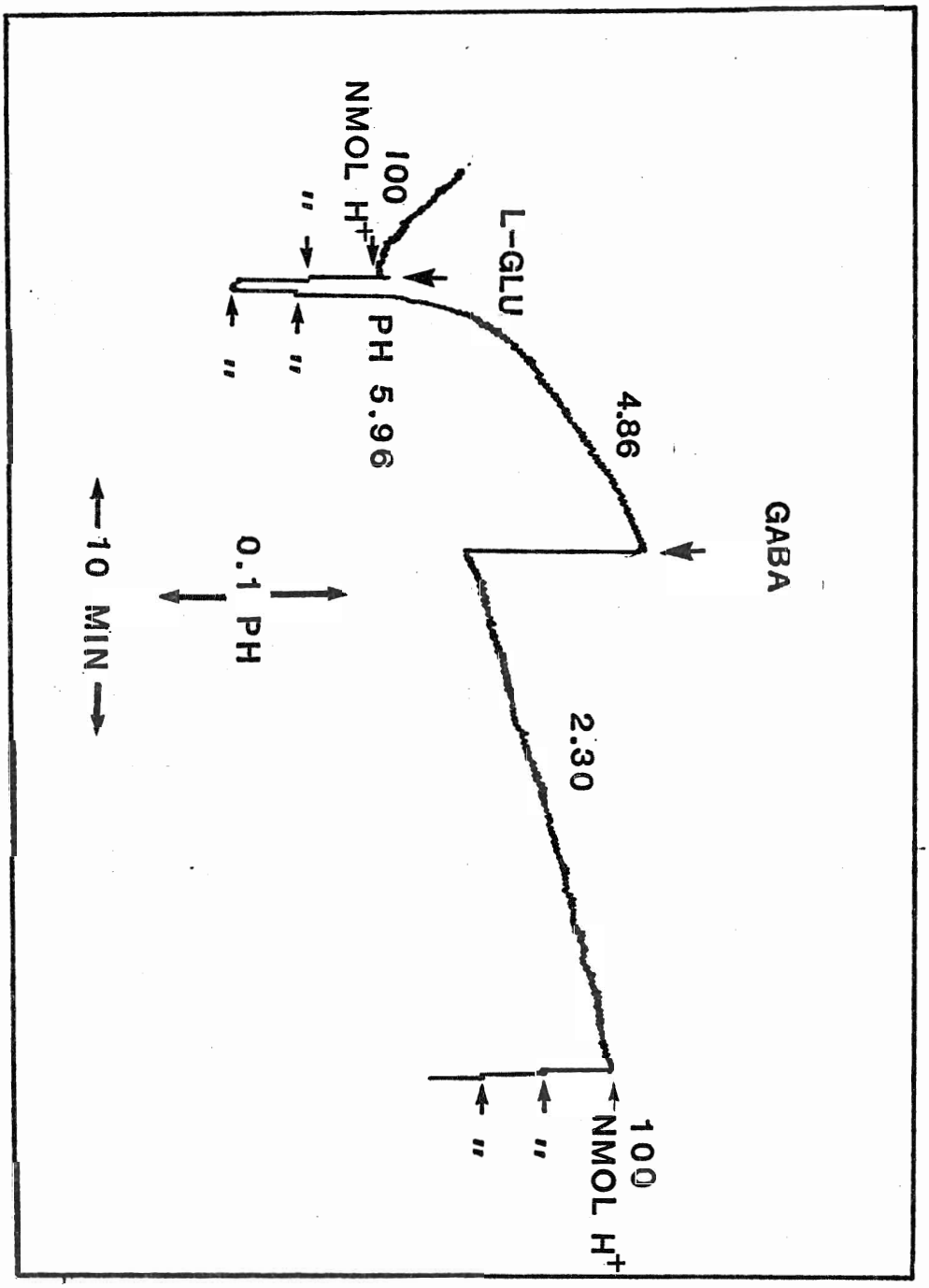
GABA
4.86
2.30
L-GLU
100 NMOL H+
"
"
"
PH 5.96
"
"
100 NMOL H+
0.1 PH
10 MIN

Table 15 : Rates of 5 mM L-Glu dependent medium alkalinization as influenced by subsequent addition of 5 mM GABA

L			D		
(-)GABA	(+)GABA	% Control	(-)GABA	(+)GABA	% Control
4.17	2.20	53	2.80	1.56	45
4.86	2.30	47	-	-	-
2.29	1.14	50	-	-	-
3.77(1.09)	1.88(0.52)	50	2.80	1.56	56

- Five to 10 x 10^6 cells were suspended in 10 ml of 1 mM $CaSO_4$ and introduced into a reaction vessel maintained at 30°C.
- The cell suspension was aerated, stirred and exposed to the light (L) and incubated for 10 minutes with 5 mM L-Glu.
- GABA was added to give 5 mM and the subsequent rate was measured.
- After the addition of L-Glu and GABA, the contents of the reaction vessel were titrated with 100 nmol H^+ or 100 nmol OH^- in order to determine the buffering capacity.
- Each experimental value indicates the net rate of proton uptake expressed as nmol $H^+/10^6$ cells/minute. Rates were expressed as a % of control.
- The mean and S.D. of 3 trials are indicated.

Table 16 : Rates of 0.5 mM L-Glu dependent medium alkalinization as influenced by subsequent addition of 5 mM GABA

L			D		
(-)GABA	(+)GABA	% Control	(-)GABA	(+)GABA	% Control
0.79	1.47	187	-	-	-
0.93	1.27	136	-	-	-
0.89	1.33	150	-	-	-
0.88	1.07	121	-	-	-
0.87(0.05)	1.29(0.14)	148	-	-	-

- Five to 10 x 10^6 cells were suspended in 10 ml of 1 mM $CaSO_4$ and introduced into a reaction vessel maintained at 30°C.
- The cell suspension was aerated, stirred and exposed to the light (L) and incubated for 10 minutes with 0.5 mM L-Glu.
- GABA was added to give 5 mM and the subsequent rate was measured.
- After the addition of L-Glu and GABA, the contents of the reaction vessel were titrated with 100 nmol H^+ or 100 nmol OH^- in order to determine the buffering capacity.
- Each experimental value indicates the net rate of proton uptake expressed as nmol $H^+/10^6$ cells/minute. Rates were expressed as a % of control.
- The mean and S.D. of 4 trials are indicated.

3. Protoplasmic buffering capacity

Buffering capacities of cell suspensions and cell homogenates were measured in ambient light. The objective of measuring the buffering capacity of the protoplasm was to calculate the theoretical pH change of cytoplasm after addition of L-Glu. This can be calculated from the protoplasmic buffering capacity, the rate of H^+ influx following L-Glu addition and cytoplasmic volume (Table 2). The buffering capacity of the cell suspension medium plus intact cells between pH 5.8 and 7.2 was 70 nmol Eq. $H^+/2x10^6$ cells in 1 ml cell suspension/pH unit. The buffering capacity of the cell homogenate between pH 6.5 and 7.3 was 209 nmol Eq. $H^+/2x10^6$ cells in 1 ml cell homogenate/pH unit. The buffering capacity of protoplasm was then obtained by subtracting the buffering capacity of the cell suspension plus cells from the cell homogenate buffering capacity (139 nmol/$2x10^6$ cells in 1 ml cell homogenate/pH unit). Consequently, using the cell volume, the buffering capacity of 1 ml of protoplasm was found to be 15 µmol Eq. H^+/ml protoplasm/pH unit (Table 17).

Therefore it is possible to obtain a theoretical cytoplasmic pH change by measuring the flux of H^+ into the cell on addition of L-Glu (Table 13). The value is theoretical because it assumes the absence of active mechanisms regulating intracellular pH. The calculation of the theoretical intracellular pH change on addition of 5 mM L-Glu is as follows : The rate of 5 mM L-Glu dependent medium alkalinization is 3.35 nmol $H^+/10^6$ cells/minute in the light (Table 13) ------ (1)

2.97 nmol $H^+/10^6$ cells/minute in the dark (Table 13) ------ (2)

The cell volume is 4.68 µl/10^6 cells (Table 2) ---------- (3)

The protoplasmic buffering capacity is 15 µmol Eq. H^+/ml protoplasm/pH unit (Table 17) ---------- (4)

Given the four values,

The theoretical H^+ uptake for 1 hour is

3.35 x 60 or 201 nmol $H^+/10^6$ cells/hour in the light ---- (1-1)

2.97 x 60 or 178 nmol $H^+/10^6$ cells/hour in the dark ---- (2-1)

On the cell volume basis (3), the protoplasmic buffering capacity of 15 µmol Eq. H^+/ml protoplasm/pH unit is equal to 70 nmol Eq. $H^+/10^6$ cells/pH unit ---------- (4-1)

Therefore the theoretical intracellular pH change is obtained by dividing the rate of H^+ uptake of 10^6 cells (1-1 and 2-1) by the protoplasmic buffering capacity of 10^6 cells (4-1). Thus, the intracellular pH change for 1 hour on addition of 5 mM L-Glu is 2.87 and 2.53 in the light and dark, respectively.

Table 17 : Measurement of extracellular and intracellular buffering capacity

1. The buffering capacity of the cell suspension medium plus intact cells betwen pH 5.8 and 7.2

   = 70 (± 8) nmol Eq. $H^+/2x10^6$ cells in 1 ml cell suspension/pH unit

2. The buffering capacity of the cell homogenate between pH 6.5 and 7.3

   = 209 (± 39) nmol Eq. $H^+/2x10^6$ cells in 1 ml cell homogenate/pH unit

3. The buffering capacity of protoplasm between pH 6.5 and 7.3

   = 139 nmol Eq. $H^+/2x10^6$ cells in 1 ml cell homogenate/pH unit

   = 139 nmol Eq. $H^+/2x4.68$ ul cytoplasm/pH unit

   = 14.9 µmol Eq. H^+/ml protoplasm/pH unit

- Experiments were performed in an open water jacketed glass reaction vessel maintained at 30°C.
- Twenty million cells were suspended in 10 ml of 1 mM $CaSO_4$. The cell suspension and cell homogenate (french press) were stirred, but not aerated in the ambient light.
- The buffering capacities of cell suspension and cell homogenate were measured in the pH range 7.3 to 5.8.
- The protoplasmic buffering capacity was obtained by subtracting the external buffering capacity from the cell homogenate buffering capacity.
- The cell volume used was 4.678 µl/10^6 cells (Table 2).
- Values were obtained from 4 measurements using 2 different batches of cells (N = 8).

4. Uptake of [U-^{14}C]L-Glu

The objective was to determine whether GABA affects the uptake of [U-^{14}C]L-Glu. Cells were suspended in 5 mM MES/1 mM $CaSO_4$ (pH 6.0) with illumination and the uptake of L-Glu was measured. The uptake was linear for 10 minutes and linear regression analysis gave a correlation coefficient of 0.998. The rate of uptake of 0.5 mM L-Glu was 0.17 nmol L-Glu/10^6 cells/minute. Five mM GABA inhibited this uptake by 19 % (Fig. 17A).

When the suspension medium was non-buffered 1 mM $CaSO_4$, the uptake of L-Glu again showed a linear increase for 10 minutes. The uptake of L-Glu was stimulated by 69 % in the presence of simultaneously added 5 mM GABA (Fig. 17B).

Thus 5 mM GABA stimulated the uptake of 0.5 mM L-Glu and 0.5 mM L-Glu dependent medium alkalinization by 69 % and 49 %, respectively, when cells were suspended in nonbuffered 1 mM $CaSO_4$ (Fig. 17B, Table 16). It should be noted however that when 0.5 mM L-Glu was added to cells suspended in $CaSO_4$ the rate of alkalinization was 0.8 nmol $H^+/10^6$ cells/minute (Table 16) where the apparent rate of uptake was 0.13 nmol L-Glu/10^6 cells/minute (Fig. 17B).

Fig 17A : Effect of GABA on the uptake of L-Glu

- Six million cells were suspended in 2 ml of 5 mM MES/1 mM $CaSO_4$ (pH 6.0).
- The cell suspension was stirred and the uptake was measured by removing a 200 ul aliquot every 2 minutes for 10 minutes in the light.
- The concentration and specific activity of L-Glu were 0.5 mM and 2,920 dpm/nmol, respectively.
- The concentration of GABA was 5 mM.
- Each value was expressed as a % of control and the mean and S.D. of 3 trials are indicated.
- Each graph was produced from linear regression and the correlation coefficient was 0.998.

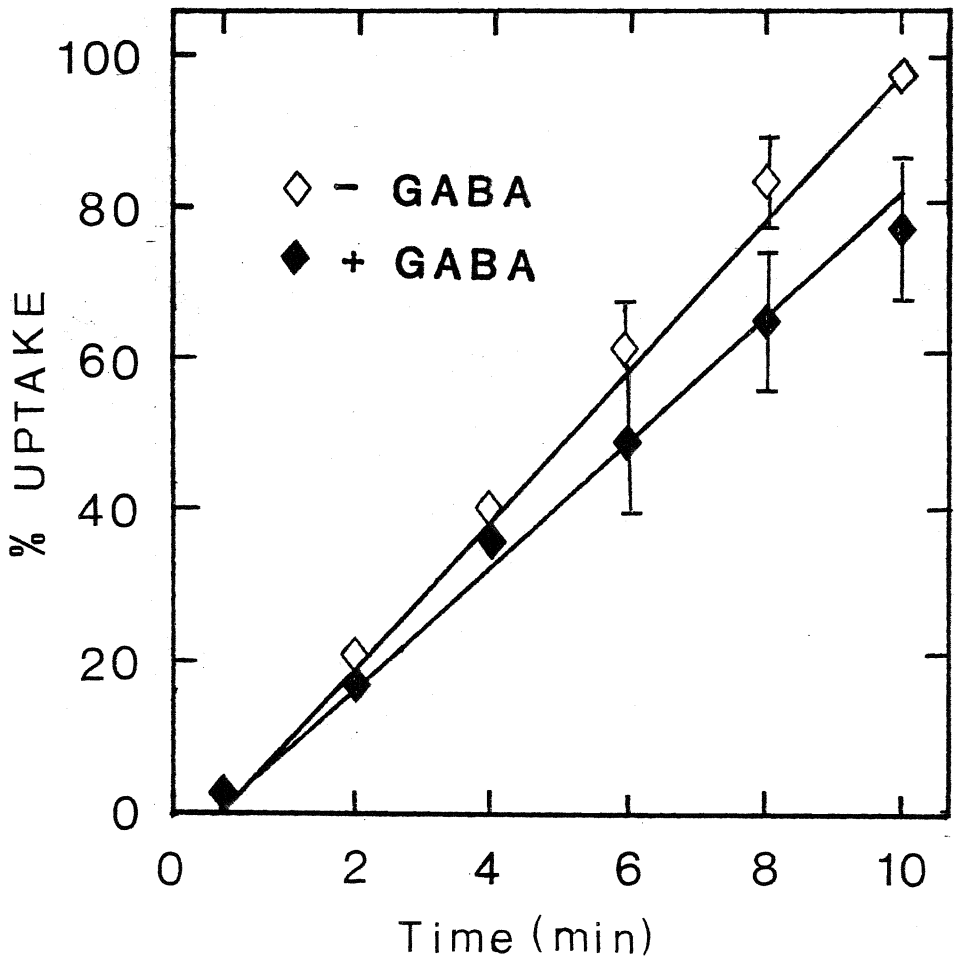
100
80
60
40
20
0
% UPTAKE
◇ - GABA
◆ + GABA
0
2
4
6
8
10
Time (min)

Fig 17B : Effect of GABA on the uptake of L-Glu

- Six million cells were suspended in 2 ml of 1 mM $CaSO_4$.
- The cell suspension was stirred and the uptake was measured by removing a 200 ul aliquot every 2 minutes for 10 minutes in the light.
- The concentration and specific activity of L-Glu were 0.5 mM and 2,920 dpm/nmol, respectively.
- The concentration of GABA was 5 mM.
- Each value was expressed as a % of control and the mean and S.D. of 3 trials are indicated.
- Each graph was produced from linear regression and the correlation coefficient was 0.998.

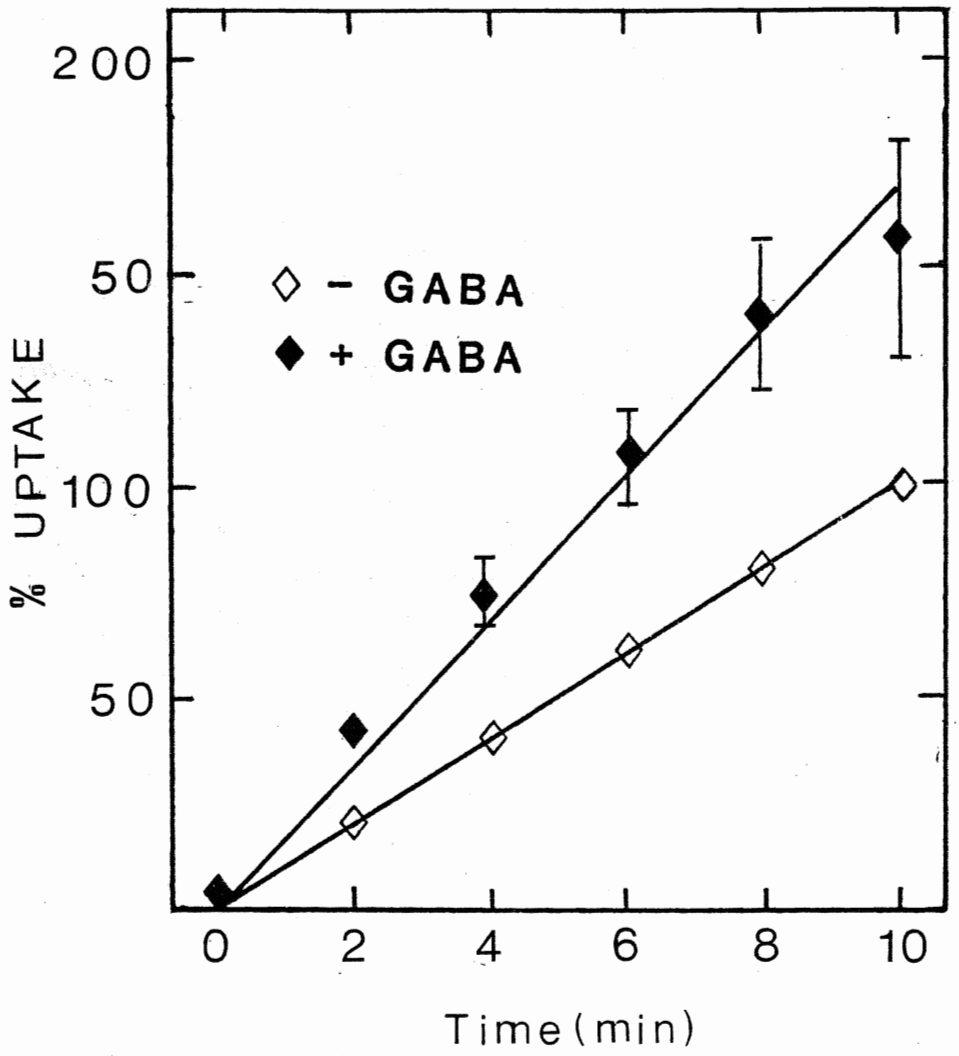
200
50
100
50
% UPTAKE
◇ - GABA
◆ + GABA
0
2
4
6
8
10
Time (min)

5. The effect of K_2SO_4 and CCCP on the rate of uptake of L-Glu

The primary objective was to determine whether GABA is produced inside or outside the cells. Experiments were conducted by employing agents which inhibit membrane transport. If GABA is produced inside the cells, then inhibitors of transport should inhibit the GABA production. However, if GABA is produced outside the cells, these inhibitors should not affect the GABA production. Cells were suspended in 5 mM MES/1 mM $CaSO_4$ (pH 6.0) and the rate of uptake of [U-^{14}C]L-Glu was measured with illumination. The rate of uptake of L-Glu was 0.12 nmol L-Glu/10^6 cells/minute. Twenty mM K^+ and 10 uM CCCP inhibited the uptake of L-Glu label by 17 % and 95 %, respectively, and inhibited the corresponding GABA production by 17 % and 50 %, respectively (Fig. 18, Table 18). These results indicate that GABA was not produced outside the cells but was produced inside the cells and released to the medium.

Fig 18 : The effect of K_2SO_4 and CCCP on the uptake of [U-^{14}C]L-Glu

- Twenty million cells were suspended in 5 ml of 5 mM MES/1 mM $CaSO_4$ (pH 6.0).
- The cell suspension was stirred and preincubated for 10 minutes in the medium with 10 mM K_2SO_4 , or 10 uM CCCP in the light.
- The concentration and the specific activity of [^{14}C-U]L-Glu were 0.5 mM and 3151 dpm/nmol, respectively.
- Each value was expressed as a % of control and the mean and S.D. of 3 trials are indicated.
- Each graph was produced from linear regression and the correlation coefficient was 0.998.

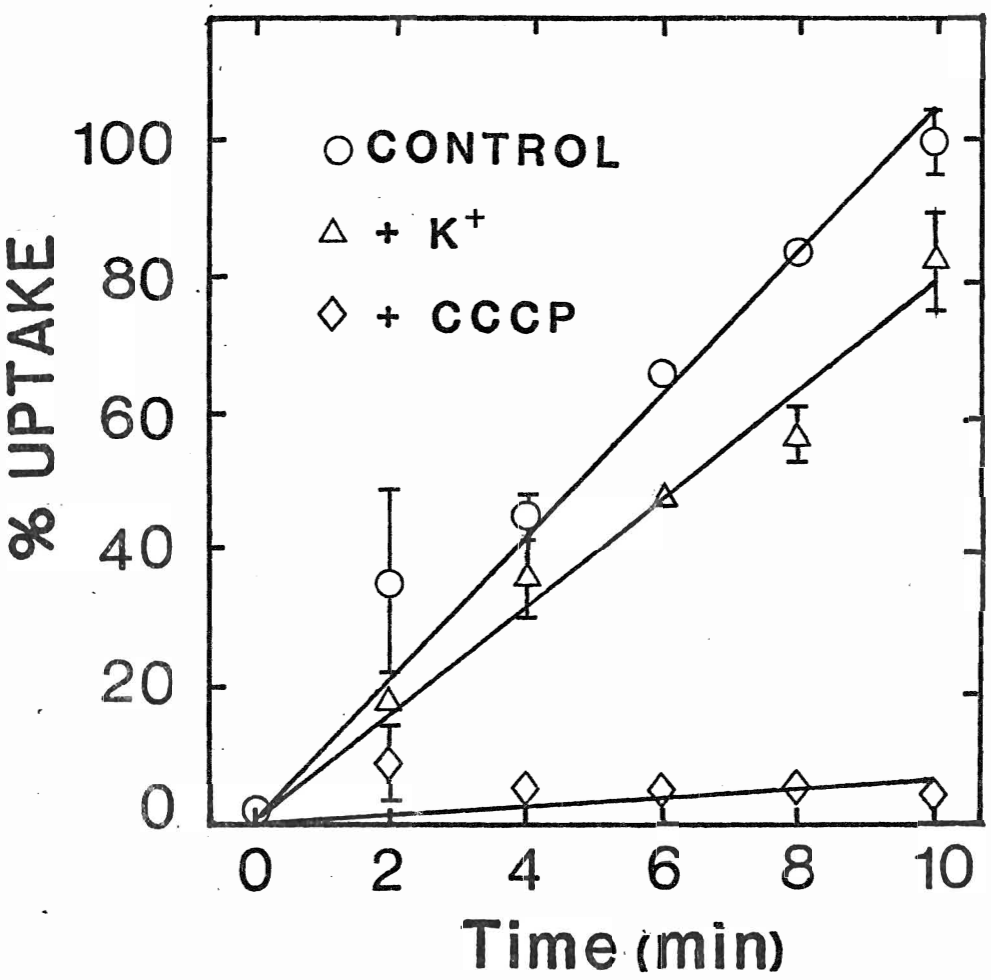
% UPTAKE
100
80
60
40
20
0
CONTROL
+ K+
+ CCCP
0
2
4
6
8
10
Time (min)

Table 18 : The effect of K_2SO_4 and CCCP on GABA production

	Uptake of [U-^{14}C]L-Glu		labeled GABA in medium	
Condition	Mean (S.D.)	% Control	Mean (S.D.)	% Control
	DPM	%	DPM	%
Control	3,683 (947)	100	22,894 (2,053)	100
K_2SO_4	3,074 (918)	83	18,194 (1,891)	83
CCCP	183 (50)	5	11,503 (634)	50

- The number of cells was 20 x 10^6.
- The cells were suspended in 5 ml of 5 mM MES/1 mM $CaSO_4$ (pH 6.0).
- The cell suspension was stirred and preincubated for 10 minutes in the medium with 10 mM K_2SO_4 , or 10 uM CCCP in the light.
- The concentration and the specific activity of [U-^{14}C]L-Glu were 0.5 mM and 3,151 dpm/nmol, respectively.
- The mean values represent the dpm/10^6 cells/10 minutes.
- Effects of K_2SO_4 and CCCP on the uptake of [^{14}C-U]L-Glu and the GABA production were converted to % control.
- Each value is the mean and S.D. of 3 trials.

Fig 19 : TLC of the medium and subsequent autoradiography after feeding [U-^{14}C]L-Glu to cell suspensions

- This is a photograph of the autoradiograph produced from the TLC.
- Twenty million cells were suspended in 5 ml of 5 mM MES/1 mM $CaSO_4$ (pH 6.0).
- The cell suspension was stirred and preincubated for 10 min in 10 mM K_2SO_4 , or 10 uM CCCP in the light.
- The concentration and the specific activity of [^{14}C-U]L-Glu were 0.5 mM and 3151 dpm/nmol, respectively.
- Immediately after measurement of uptake, the remaining cell suspension (14 x 10^6 cells in 3.6 ml) was fractionated.
- The dried medium was solubilized in 200 ul of 0.1 N HCl and 20 ul was applied at origin indicated
- The solvent system was phenol/water (75/25, w/w).
- Autoradiograph was exposed at -70°C for 36 hours.

-Note : (1) control (2) + K^+ (3) + CCCP

(A) GABA (B) L-Glu (C) origin

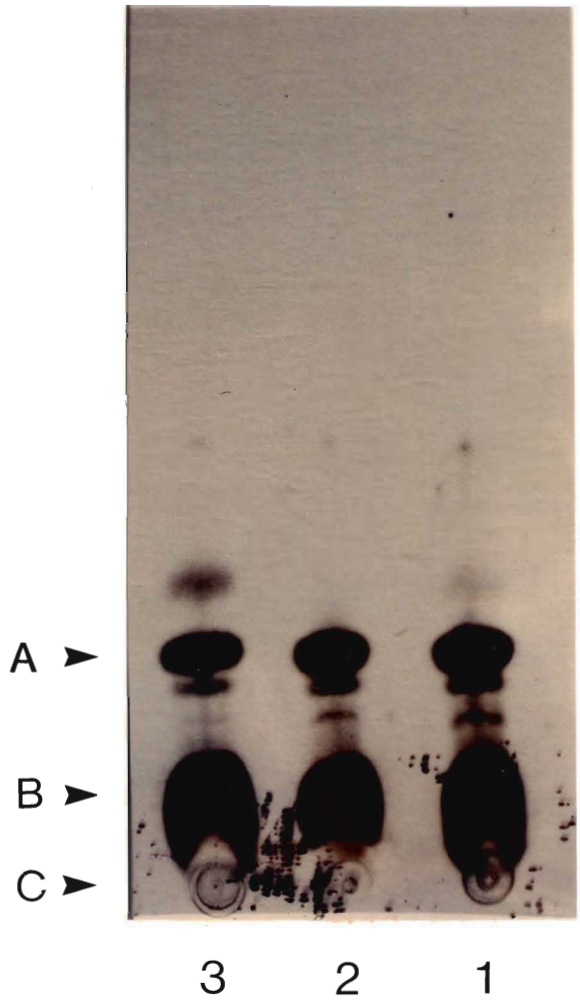
A
B
C
3
2
1

6. Influx of GABA

The objective was to measure GABA uptake to characterize GABA transport at the plasma membrane of *Asparagus* mesophyll cells. In addition the possibility of an antiport process involving the opposite flux of L-Glu and GABA was also investigated. Measurements of GABA uptake were performed in the light or dark using cells suspended in 5 mM MES/1 mM $CaSO_4$ (pH 6.0). The pattern of GABA uptake was different in the light and dark. In the light, the uptake of labeled GABA equilbrated to a constant level at 4 minutes. The rate was 0.325 nmol GABA/10^6 cells/minute during this period. In the dark, the rate of uptake was much slower, was not linear and did not reach equilibrium within 18 minutes (Fig. 19). The effect of a 10 minute preincubation with L-Glu, CCCP, oligomycin, and butyric acid on GABA uptake was determined (Fig. 21 and 22). One mM L-Glu slightly inhibited GABA uptake in the light but had no effect in the dark. Ten uM CCCP inhibited GABA uptake by 58 % and 29 % in the light and dark, respectively. Five mM butyric acid and 1 mg/ml oligomycin did not show any effect on the GABA uptake (Fig. 23). These results indicate that the GABA uptake process was not significantly influenced by L-Glu. In addition the acidification of the cytoplasm by butyric acid (McCutcheon *et al.* 1988) and inhibition of ATP production by oligomycin (Bown and Nicholls 1985) did not affect the GABA uptake process. However the dissipation of the proton electrochemical gradient by CCCP inhibited GABA uptake, indicating that GABA uptake is dependent on $\Delta\psi$ or ΔpH (Bown 1982).

Fig 20 : Uptake of GABA in the light and dark

- Four million cells were suspended in 1 ml of 5 mM MES/1 mM $CaSO_4$ (pH 6.0).
- The cell suspension was stirred and the uptake was measured by removing a 100 ul aliquot every 2 min in the light and dark.
- Concentration and specific activity of GABA were 0.125 mM and 24,776 dpm/nmol, respectively.
- Each value was expressed as a % of control and the mean and S.D. of 3 trials are indicated.

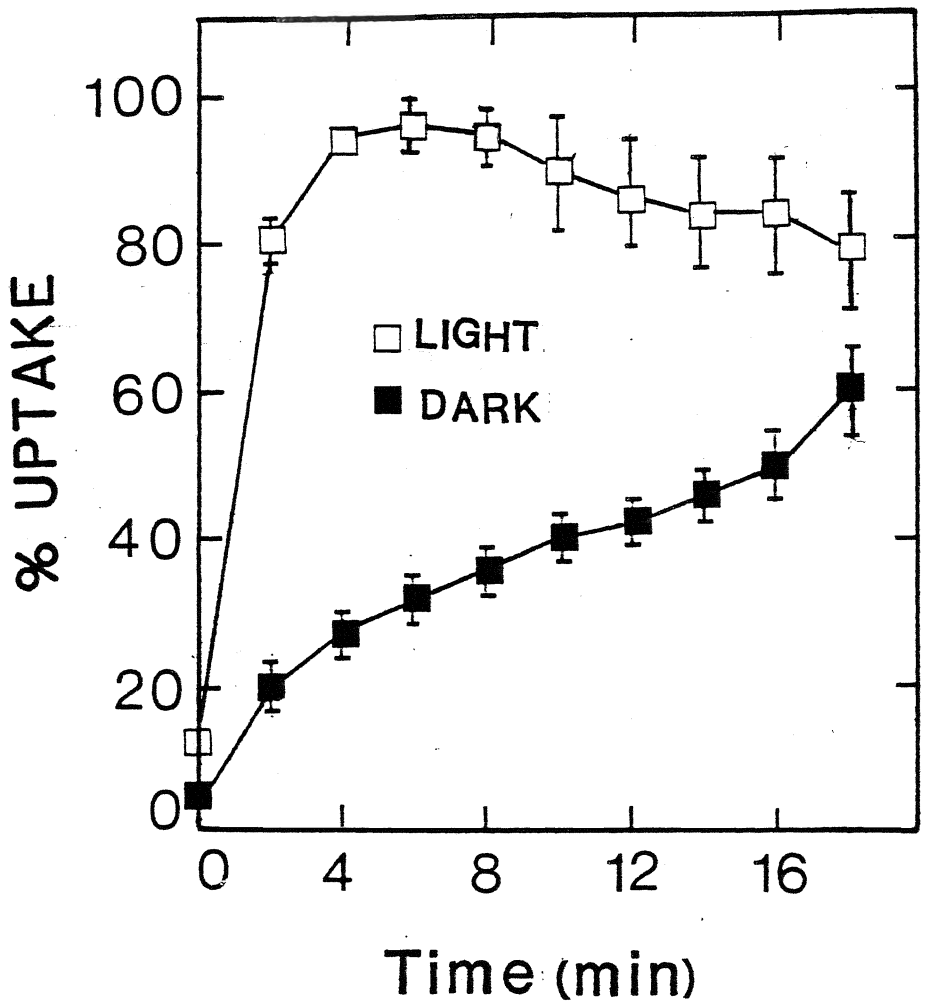
100
80
60
40
20
0
% UPTAKE
LIGHT
DARK
0
4
8
12
16
Time (min)

Fig 21 : Effect of L-Glu and CCCP on the uptake of GABA in the light

- Four million cells were suspended in 1 ml of 5 mM MES/1 mM $CaSO_4$ (pH 6.0).
- The cell suspension was stirred and the uptake was measured by removing a 100 ul aliquot every 4 min in the light.
- Concentration and specific activity of GABA were 0.125 mM and 24,776 dpm/nmol, respectively.
- Concentration of L-Glu was 1.0 mM.
  Concentration of CCCP was 10 uM.
- Each value was expressed as a % of control and the mean and S.D. of 3 trials are indicated.

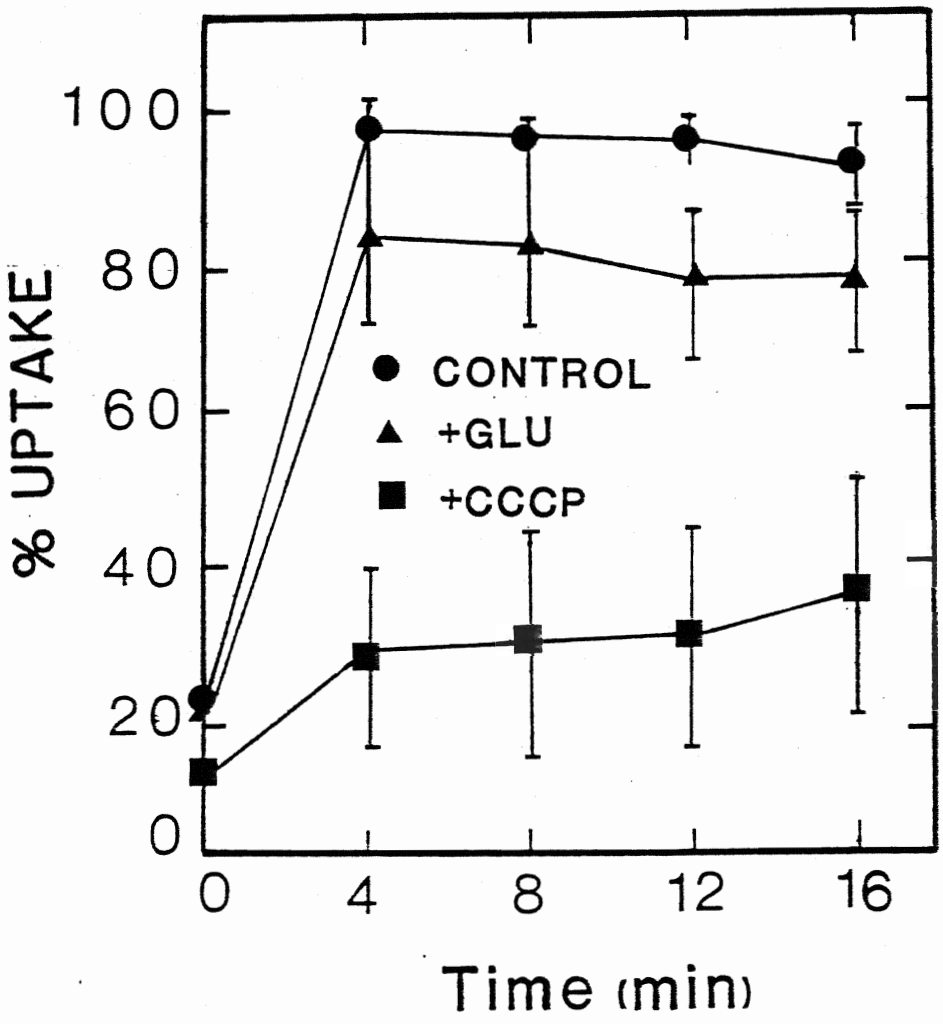
100
80
60
40
20
0
% UPTAKE
CONTROL
+GLU
+CCCP
0
4
8
12
16
Time (min)

Fig 22 : Effect of L-Glu and CCCP on the uptake of GABA in the dark

- Four million cells were suspended in 1 ml of 5 mM MES/1 mM $CaSO_4$ (pH 6.0).
- The cell suspension was stirred and the uptake was measured by removing a 100 ul aliquot every 2 min in the dark.
- Concentration and specific activity of GABA were 0.125 mM and 24,776 dpm/nmol, respectively.
- Concentration of L-Glu was 1.0 mM.
  Concentration of CCCP was 10 uM.
- Each value was expressed as a % of control and the mean and S.D. of 3 trials are indicated.

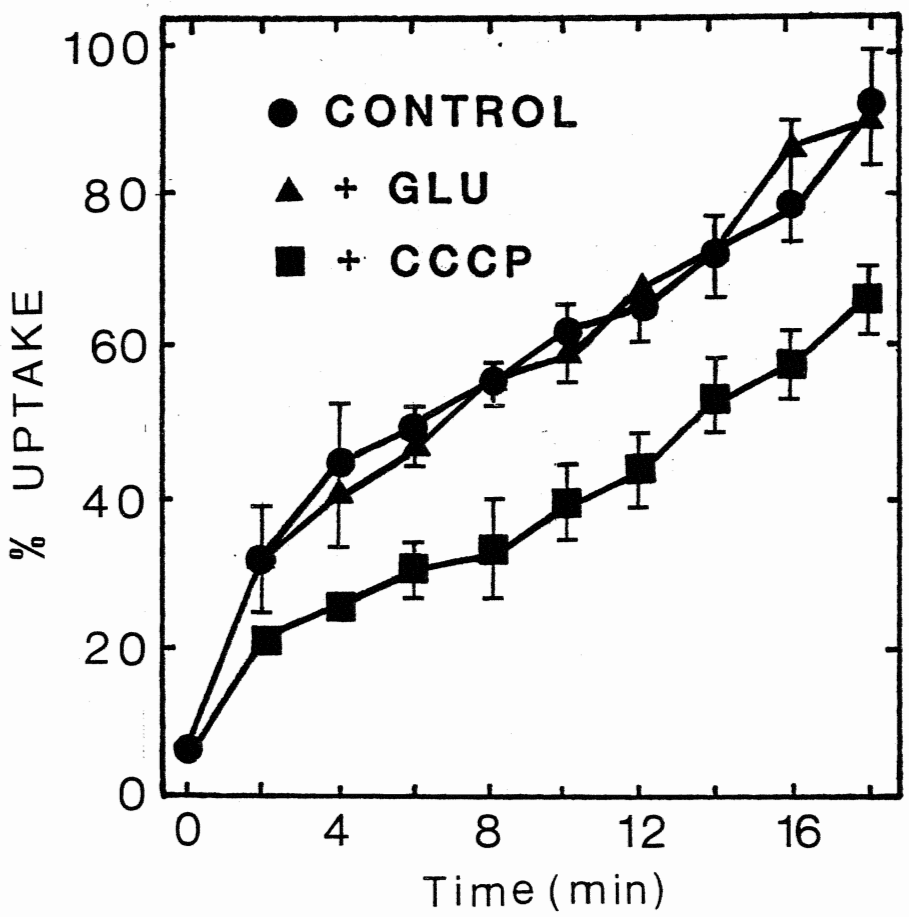
100
80
60
40
20
0
% UPTAKE
CONTROL
+ GLU
+ CCCP
0
4
8
12
16
Time (min)

Fig 23 : Effect of butyric acid and oligomycin on the uptke of GABA

- Four million cells were suspended in 1 ml of 5 mM MES/1 mM $CaSO_4$ (pH 6.0).
- The cell suspension was stirred and the uptake was measured by removing a 100 ul aliquot every 2 min in the light.
- Concentration and specific activity of GABA were 0.125 mM and 24,776 dpm/nmol.
- Concentration of butyric acid / 5.6 mM NaOH was 5 mM. Concentration of oligomycin / 2.3 mM Na_2SO_4 was 1 mg/ml.
- The mean of 3 trials is indicated.

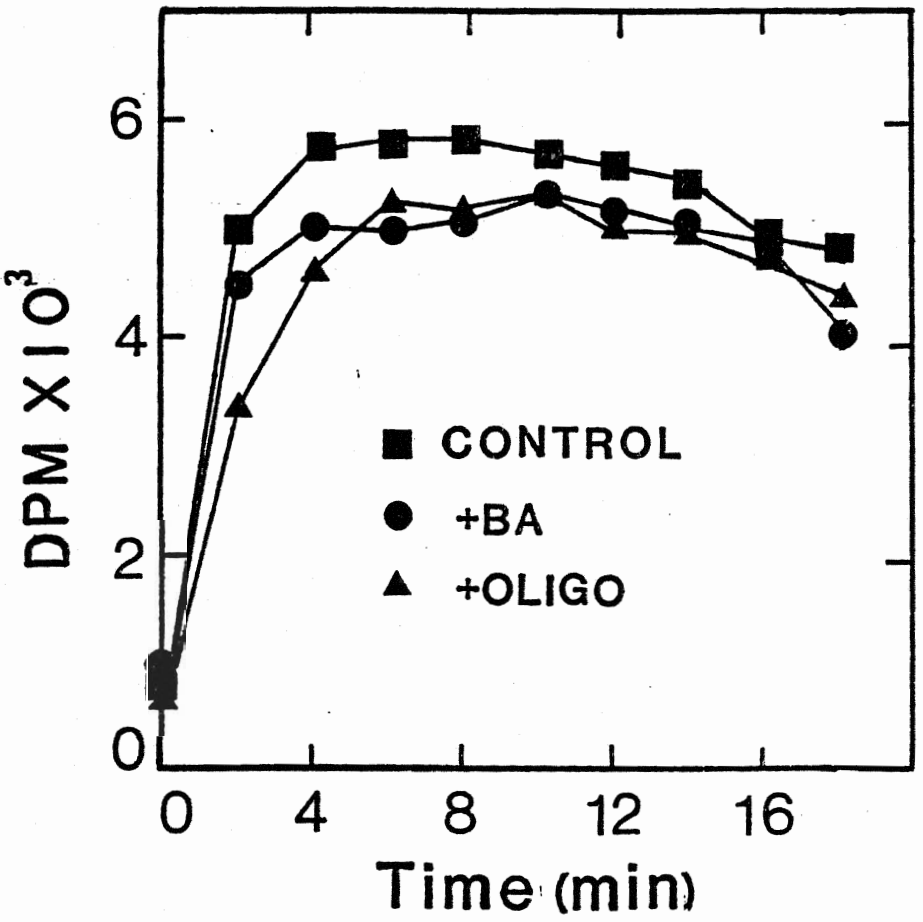
DPM X10³
6
4
2
0
0
4
8
12
16
Time (min)
CONTROL
+BA
+OLIGO

7. Net efflux of GABA

In order to characterize possible mechanisms involved in a GABA efflux process, the effect of L-Glu, butyric acid, ologomycin, and CCCP on the net efflux of GABA was measured. The net efflux of GABA was measured as the loss of radioactivity from the cells to the medium after the equilibration of GABA uptake in the light. Thus any net efflux is the result of changes in influx and/or efflux.

Cells were suspended in 5 mM MES/1 mM $CaSO_4$ (pH 6.0) and the uptake of GABA was initiated. At 6 minutes after the uptake of [^{14}C]GABA was equilibrated, 1 mM L-Glu, 20 mM K^+, or 10 uM CCCP were added. L-Glu did not affect the net GABA efflux, a result inconsistent with a coupled exchange involving L-Glu influx and GABA efflux. Potassium had no effect on the net GABA efflux, suggesting that membrane depolarization did not influence the net GABA efflux. CCCP which dissipates the H^+ electrochemical gradient across the membrane reduced the ^{14}C label inside the cells by 45 %, suggesting that it stimulates GABA efflux (Fig. 24 and 25).

Fig 24 : Effect of L-Glu and CCCP on the net GABA efflux

- Four million cells were suspended in 1 ml of 5 mM MES/1 mM $CaSO_4$ (pH 6.0).
- The cell suspension was stirred and the uptake was measured by removing a 100 ul aliquot every 2 minute in the light. At 6 minutes, 1 mM L-Glu and 10 uM CCCP were added.
- The concentration and specific activity of GABA were 0.125 mM and 24,776 dpm/nmol, respectively.
- The mean of 3 trials is indicated.

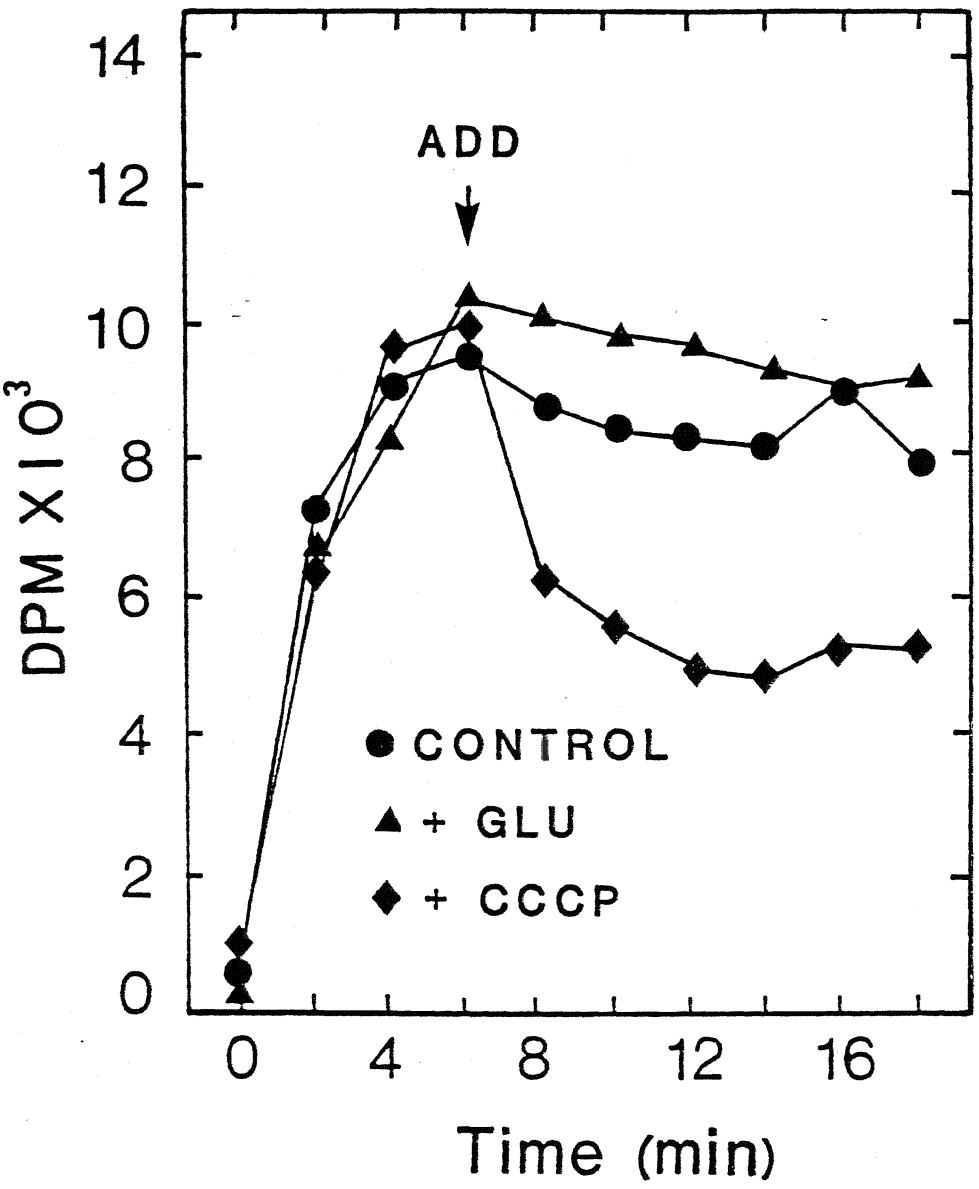
14
12
10
8
6
4
2
0
DPM X I O^3
ADD
CONTROL
+ GLU
+ CCCP
0
4
8
12
16
Time (min)

Fig 25 : Effect of K_2SO_4 on the net GABA efflux

- Four million cells were suspended in 1 ml of 5 mM MES/1 mM $CaSO_4$ (pH 6.0).
- The cell suspension was stirred and the uptake was measured by removing a 100 ul aliquot every 2 minute in the light. At 6 minutes, 10 mM K_2SO_4 was added.
- The concentration and specific activity of GABA were 0.125 mM and 24,776 dpm/nmol, respectively.
- The mean of 3 trials is indicated.

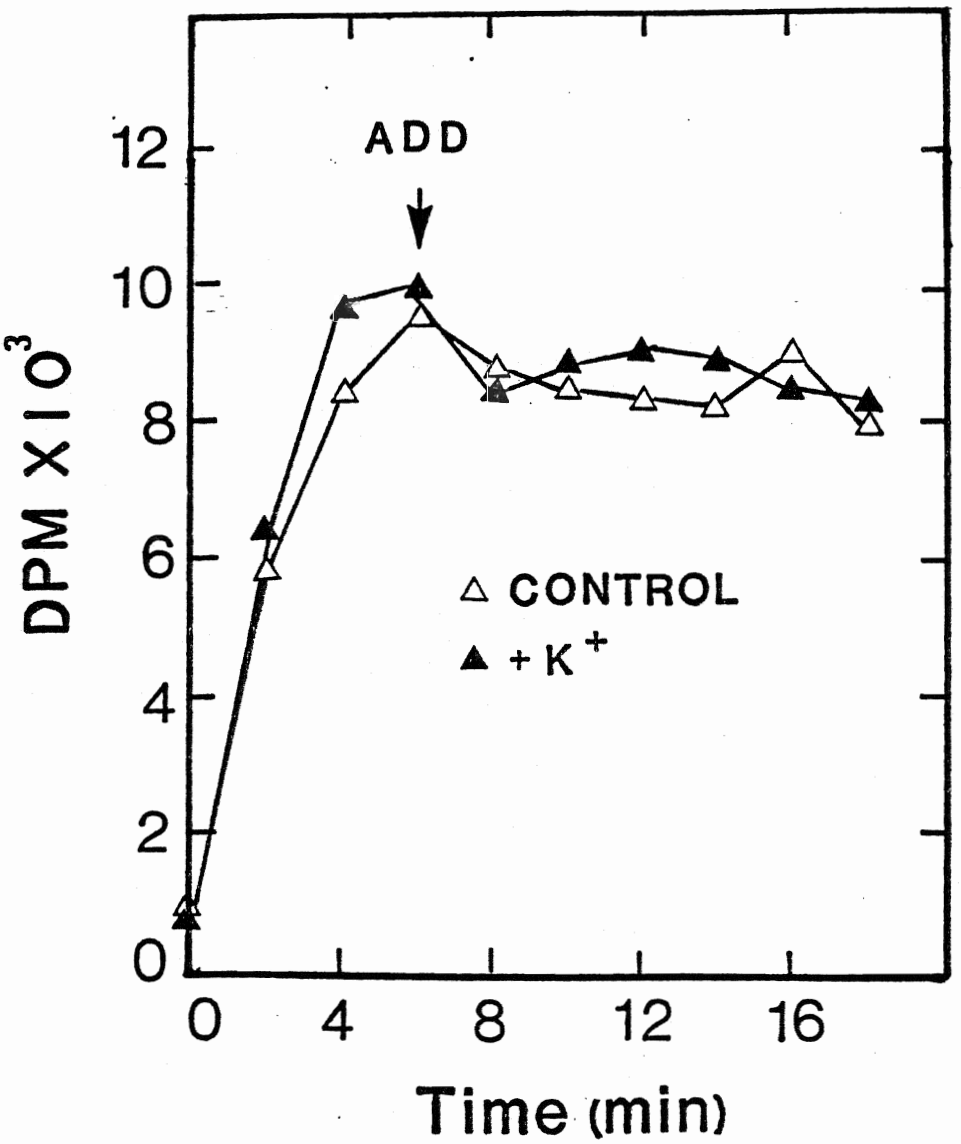
ADD
DPM X10^3
12
10
8
6
4
2
0
0
4
8
12
16
Time (min)
△ CONTROL
▲ + K$^+$

8. Unidirectional efflux of GABA

The unidirectional efflux of GABA was measured as the loss of radioactivity from the cells after washing exogenous GABA out of the medium. GABA uptake equilibrated after 6 minutes. At 6 minutes the cells were washed to remove exogenous labeled GABA and resuspended in fresh medium. The unidirectional efflux of GABA was then measured. Immediately after the washing, 69 % of the equilibrated level of radioactivity was recovered and then the radioactivity in the cells was maintained at the 50 % level. At this point addition of 1 mM L-Glu, 20 mM K^+, 5 mM butyric acid or 1 mg/ml oligomycin also had no effect on the efflux of GABA. CCCP however stimulated the net efflux of GABA and resulted in 34 % of the equilibrated level of GABA (Fig. 26,27, and 28). These results again indicate no evidence for a L-Glu/GABA antiport process. The stimulation of the GABA efflux process by CCCP may well explain labeled GABA appearance in the medium with little [U-^{14}C]L-Glu uptake when cells are treated with CCCP (Table 18). It is not clear why CCCP would stimulate the efflux of neutral GABA. It is possible however that a uniport for GABA is opened in response to a decline in ATP levels or membrane potential.

Fig 26 : Effect of L-Glu and CCCP on the unidirectional GABA efflux

- Twelve milion cells were suspended in 1 ml of 5 mM MES/1 mM $CaSO_4$ (pH 6.0).
- The cell suspension was stirred and the uptake was measured by removing a 100 ul aliquot every 2 min in the light.
- At 6 minutes, cells were washed in 1 x 15 ml of cold cell suspension medium and at 12 minutes, the uptake was measured as above.
- The concentration and specific activity of GABA were 0.125 mM and 24,776 dpm/nmol, respectively
- The concentrations of L-Glu and CCCP were 1 mM and 10 uM, respectively
- The mean of 3 trials is indicated.

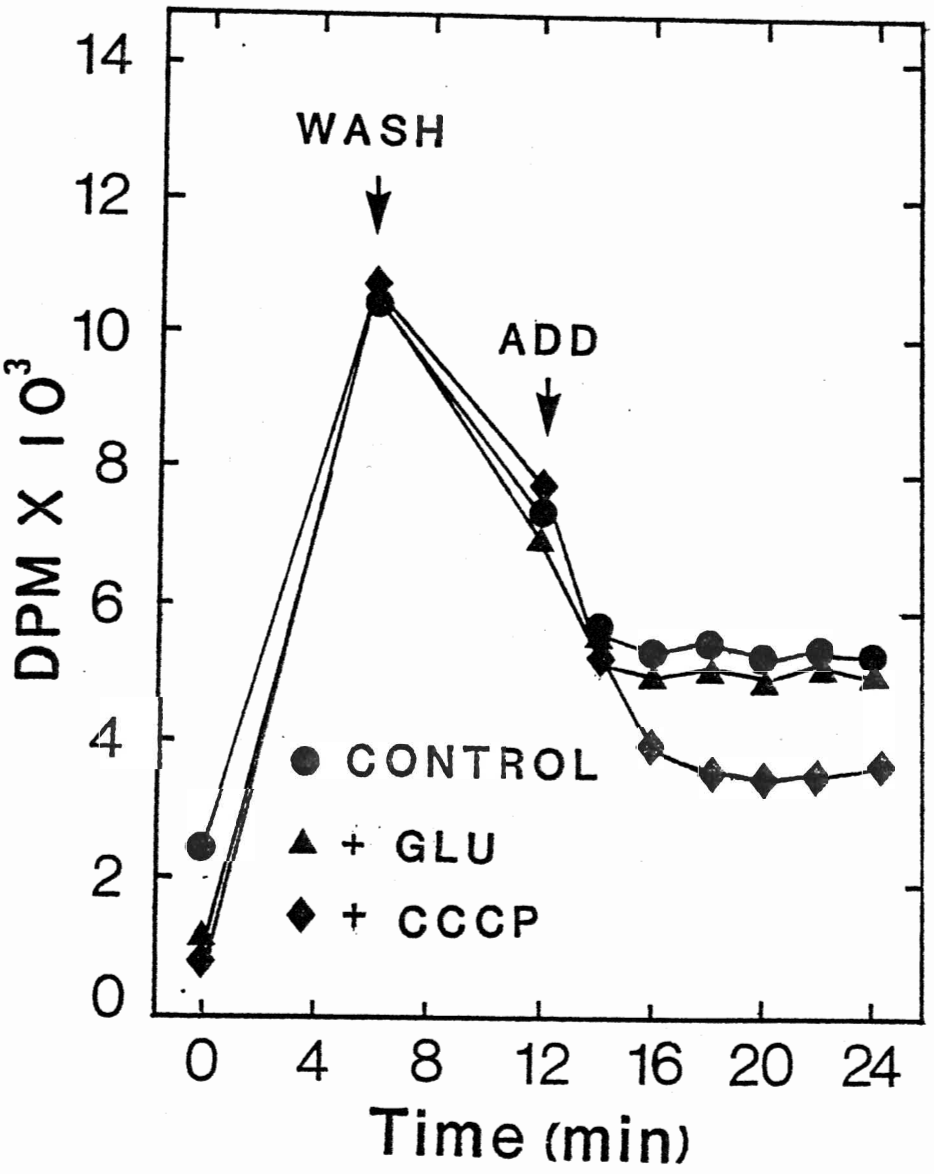
14
12
10
8
6
4
2
0
DPM X 10^3
WASH
ADD
CONTROL
+ GLU
+ CCCP
0
4
8
12
16
20
24
Time (min)

Fig 27 : Effect of K_2SO_4 on the unidirectional GABA efflux

- Twelve million cells were suspended in 1 ml of 5 mM MES/1 mM $CaSO_4$ (pH 6.0).
- The cell suspension was stirred and the uptake was measured by removing a 100 ul aliquot every 2 minute in the light.
- At 6 minutes, cells were washed in 1 x 15 ml of cold cell suspension medium and at 12 minutes, the uptake was measured as above.
- The concentration and specific activity of GABA were 0.125 mM and 24,776 dpm/nmol, respectively.
- The concentration of K_2SO_4 was 10 mM.
- The mean of 3 trials is indicated.

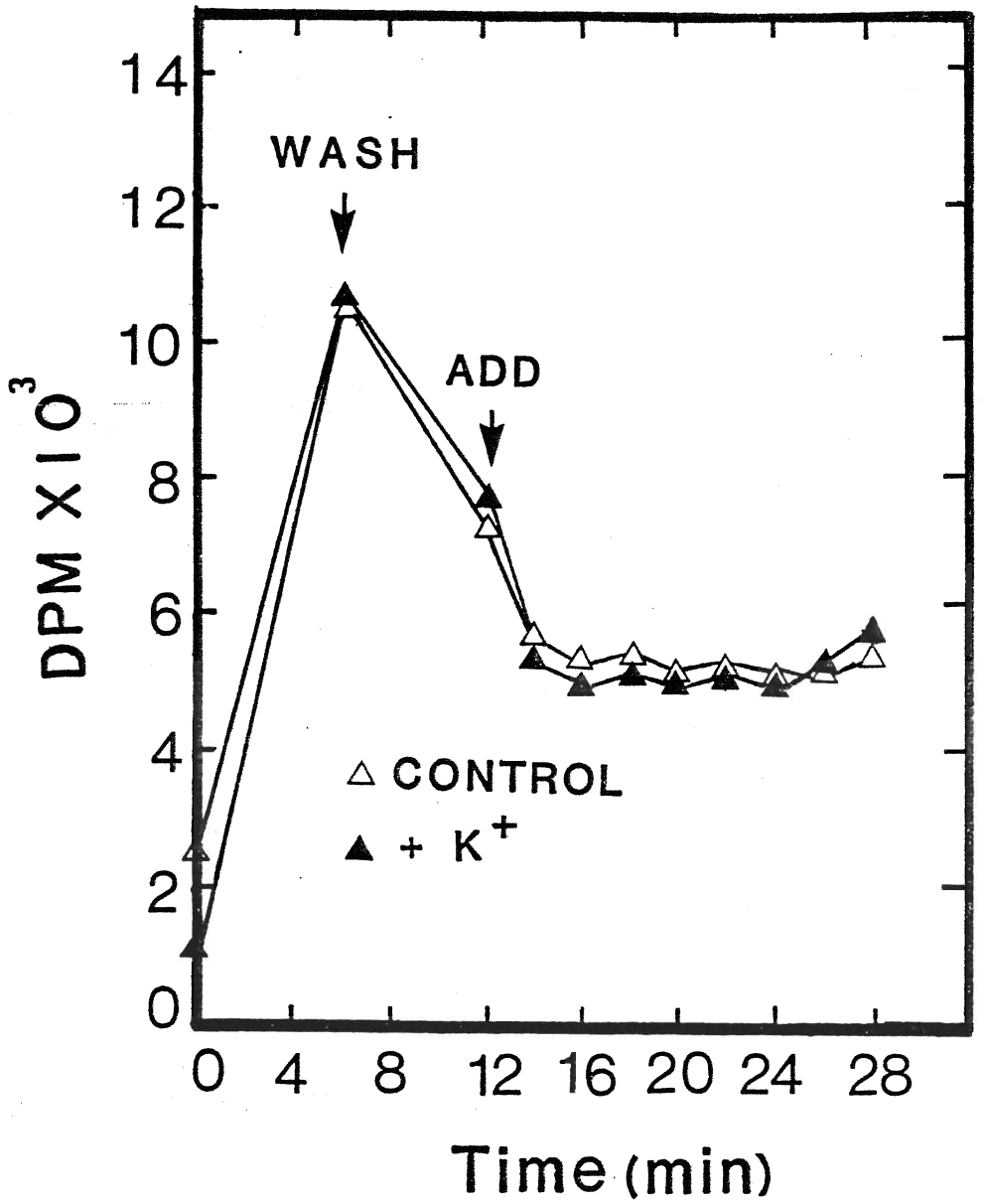
14
12
10
8
6
4
2
0
DPM X10^3
WASH
ADD
△ CONTROL
▲ + K$^+$
0 4 8 12 16 20 24 28
Time (min)

Fig 28 : Effect of butyric acid and oligomycin on the unidirectional GABA efflux

- Twelve million cells were suspended in 1 ml of 5 mM MES/1 mM $CaSO_4$ (pH 6.0).
- The cell suspension was stirred and the uptake was measured by removing a 100 ul aliquot every 2 min in the light.
- At 6 min, cells were washed in 20 ml of cold cell suspension medium and at 12 min the uptake was measured as above.
- Concentration and specific activity of GABA were 0.125 mM and 24,776 dpm/nmol.
- Concentration of butyric acid/5.6 mM NaOH was 5 mM. Concentration of oligomycin/2.8 mM Na_2SO_4 was 1 mg/ml.
- The mean of 3 trials is indicated.

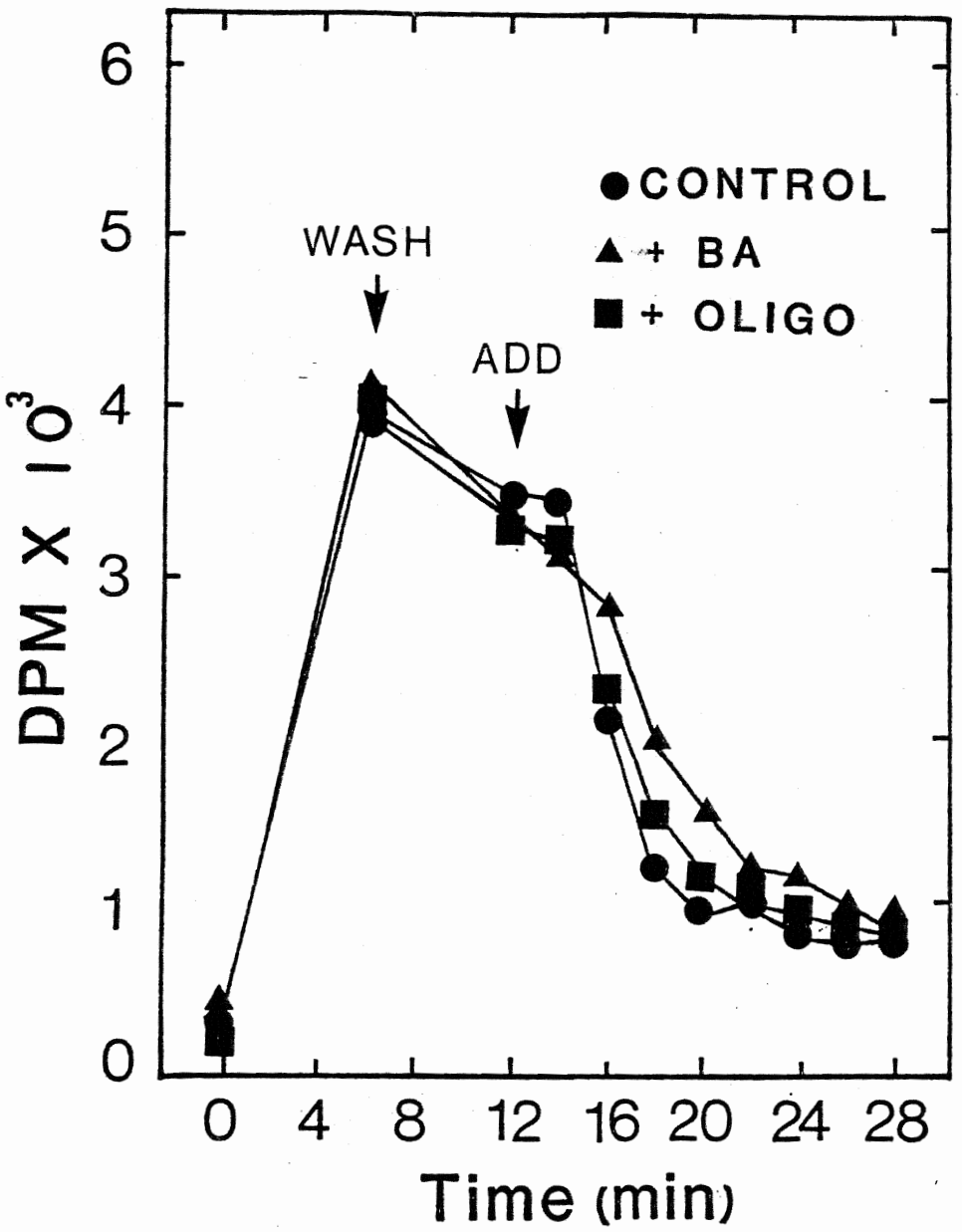
6
5
4
3
2
1
0
DPM X 10^3
WASH
ADD
● CONTROL
▲ + BA
■ + OLIGO
0
4
8
12
16
20
24
28
Time (min)

IV. L-GLUTAMATE METABOLISM STUDIES

1. Production of ^{14}C labeled GABA from [U-^{14}C]L-Glu

In order to determine whether the L-Glu to GABA conversion occurs from chemical contamination or sample preparation procedures such as cell fractionation and drying, the medium fraction was analysed after incubating [U-^{14}C]L-Glu in the presence and absence of cells. The medium was fractionated, dried and analysed by both TLC and HPLC. In the absence of cells radiolabeled GABA was not detected using either method. In contrast, when cells were present, radiolabeled GABA production was found. These results indicated that GABA production was not due to breakdown through the sample preparation procedures or contamination of the supplied radioactive L-Glu. Thus GABA production is a cell mediated process (Fig. 29, 30, 31A, and 31B). An apparent peak of radioactivity eluting at 0 to 2 minutes was found to be devoid of radioactivity and was thus an artifact.

Fig. 29 : Determination of the origin of GABA appearance in the medium : TLC

- Experiments were performed in the light and samples were analysed by TLC.
- Note :
  1. Standard ; a mixture of known L-Glu and GABA was applied.
  2. An aliqout of [^{14}C-U]L-Glu (specific activity 225 mCi/mmol) was directly loaded from stock bottle.
  3. Medium containing 5 ml of 0.1 mM [^{14}C-U]L-Glu (specific activity 49,955 dpm/nmol) in 5 mM MES/1 mM $CaSO_4$ (pH 6.0) was incubated for 10 min in the absence of cells. The dried medium was solubilized in 100 ul. Then 10 ul was loaded.
  4. Twenty million cells were incubated with 0.1 mM [^{14}C-U]L-Glu in 5 ml of 5 mM MES/1 mM $CaSO_4$ for 10 minutes. The dried medium fraction was solubilized in 100 ul of 0.1 N HCl. Then 10 ul was loaded.

  A. GABA

  B. L-Glu

  C. origin
- The chromatograph was run by duplicates.
- The solvent system was phenol/water (75/25, w/w).

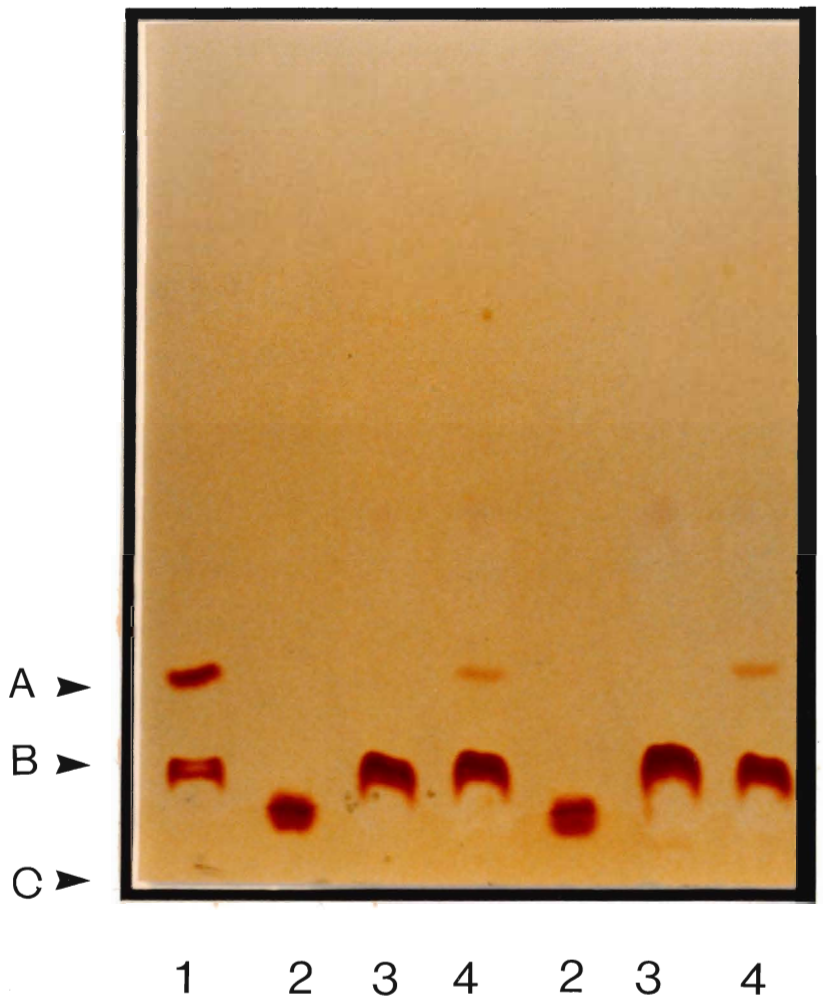
A
B
C
1
2
3
4
2
3
4

Fig 30 : Determination of the origin of GABA appearance in the medium : Autoradiography

- This is the photograph of the autoradiograph developed from the thin layer chromatogram shown in Fig. 29.
- All conditions and notes are as in Fig. 29.
- Autoradiograph was exposed at -70°C for 36 hours.
- Note : 2, 3, and 4 correspond to 2, 3, and 4, respectively, and A, B, and C correspond to A, B, and C, respectively in Fig. 29

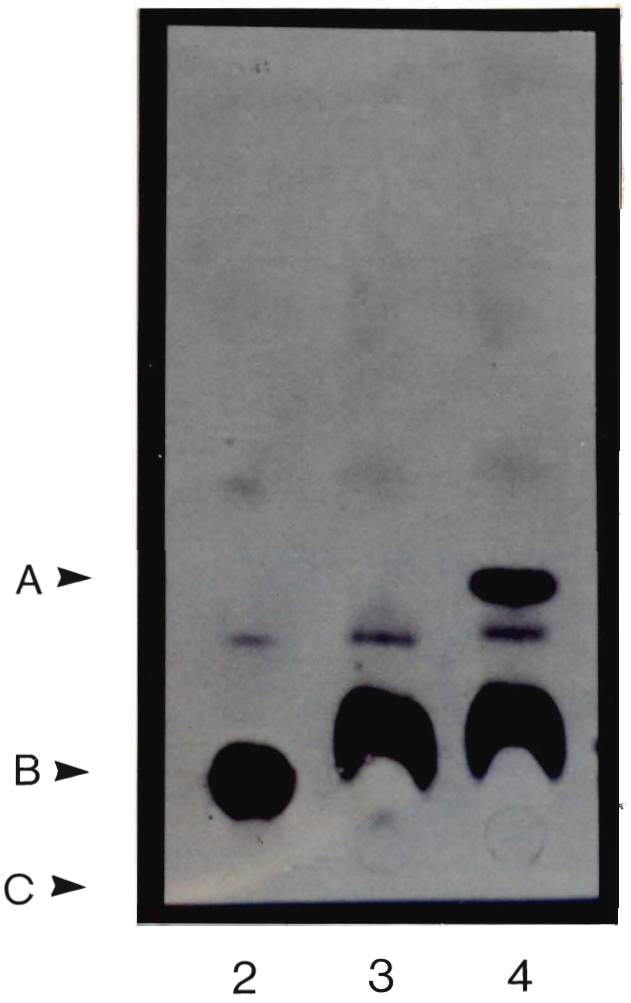
A
B
C
2
3
4

Fig 31A : Determination of the origin of GABA appearance in the medium : HPLC analysis

- This is the trace resulting from HPLC and subsequent on line scintillation counting.
- Medium containing 0.1 mM [U-^{14}C]L-Glu (specific activity 49,955 dpm/nmol) in 5 mM MES/1 mM $CaSO_4$ (pH 6.0) was incubated in the light in the absence of cells.
- The dried medium fraction was derivatized with PTC and an aliquot was injected into the HPLC apparatus.
- GABA, if present, appears at 18 minutes.

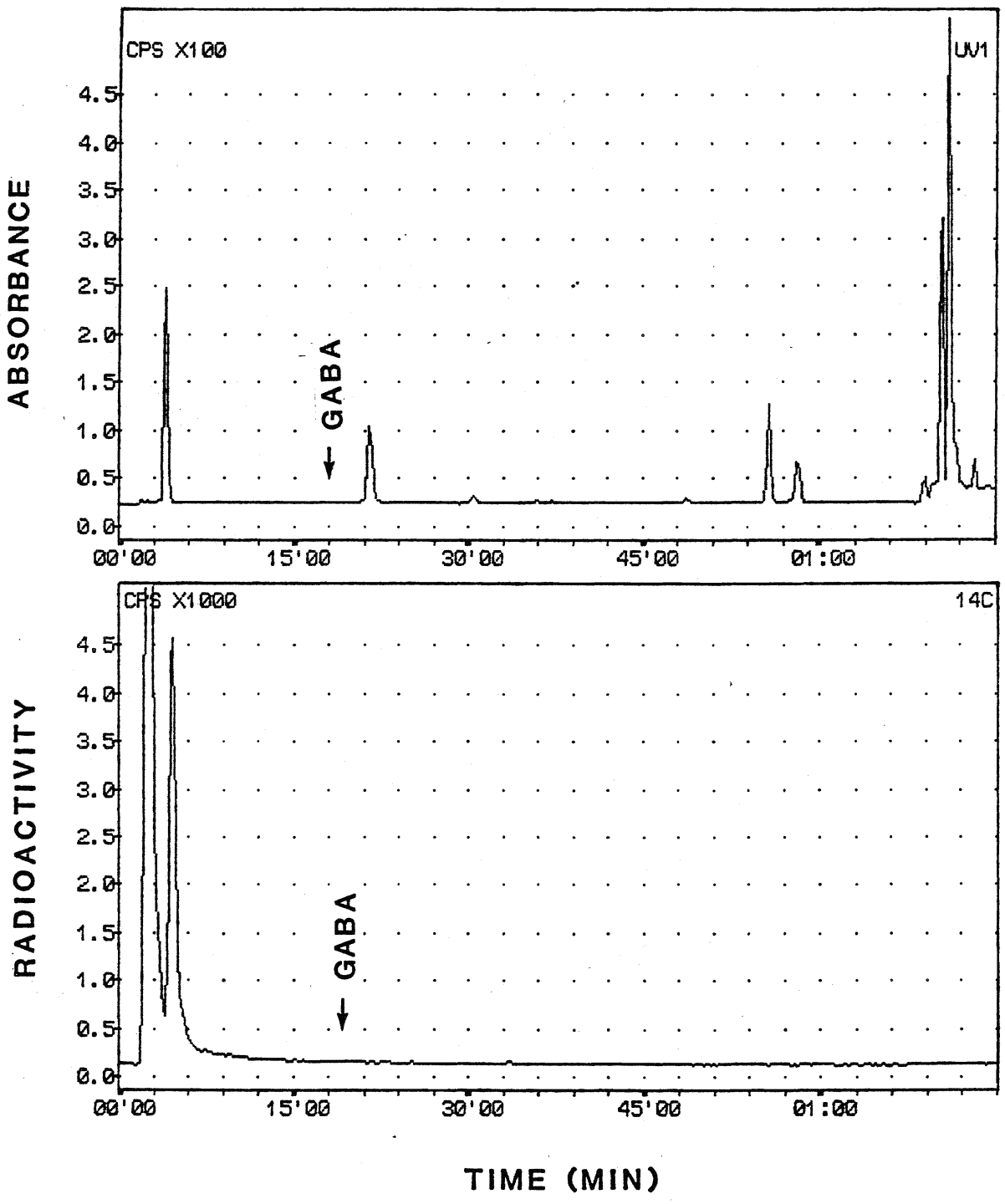
CPS X100
UV1
4.5
4.0
3.5
3.0
2.5
2.0
1.5
1.0
0.5
0.0
GABA
00'00
15'00
30'00
45'00
01:00
ABSORBANCE
CPS X1000
14C
4.5
4.0
3.5
3.0
2.5
2.0
1.5
1.0
0.5
0.0
GABA
00'00
15'00
30'00
45'00
01:00
RADIOACTIVITY
TIME (MIN)

Fig 31B : Determination of the origin of GABA appearance in the medium : HPLC analysis

- This is the trace resulting from HPLC and subsequent on line scintillation counting.
- Medium containing 0.1 mM [U-^{14}C]L-Glu (specific activity 49,955 dpm/nmol) in 5 mM MES/1 mM $CaSO_4$ (pH 6.0) was incubated in the light in the presence of cells.
- The dried medium fraction was derivatized with PTC and an aliquot was injected into the HPLC apparatus.
- GABA, if present, appears at 18 minutes.

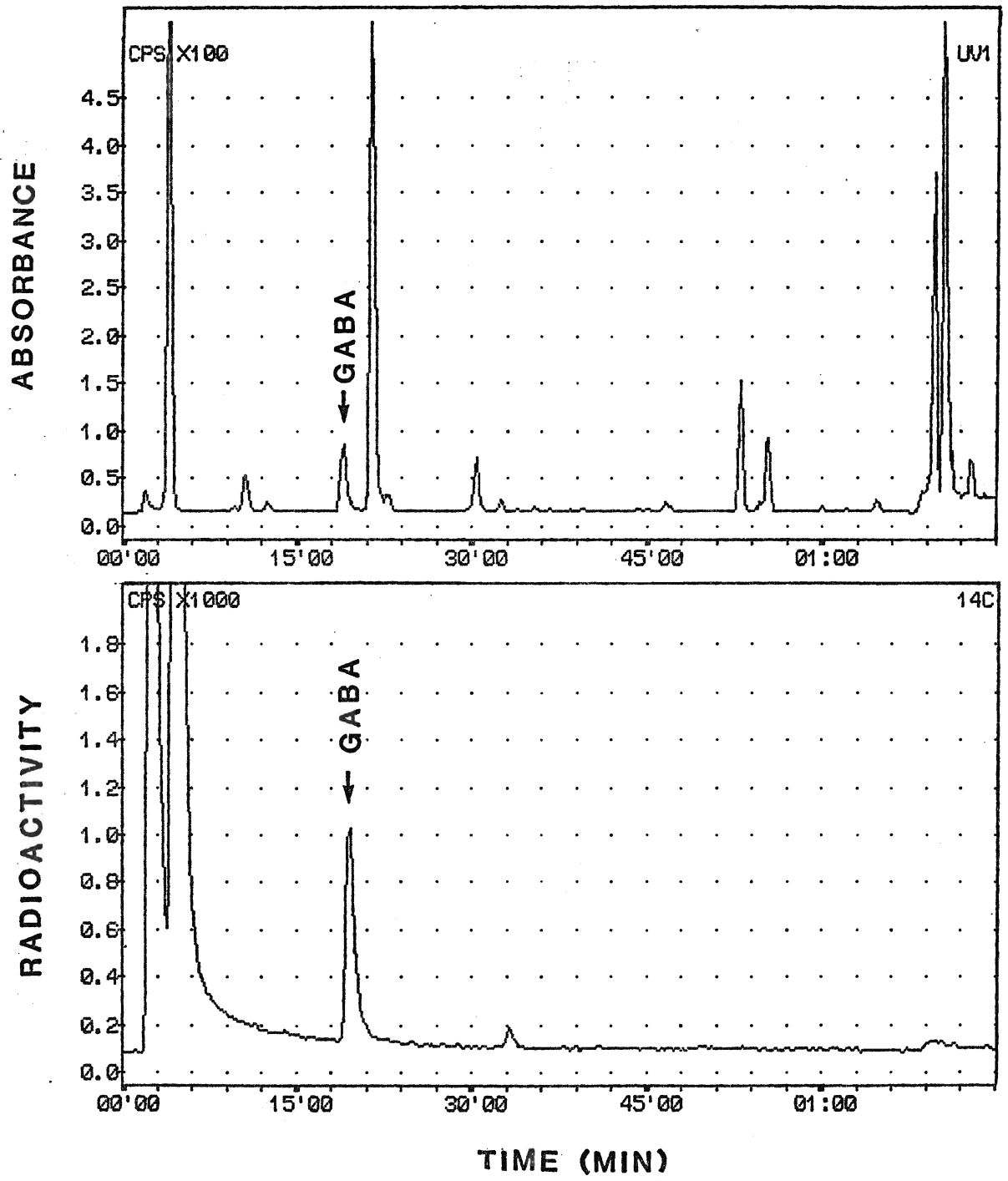
CPS X100
UV1
ABSORBANCE
4.5
4.0
3.5
3.0
2.5
2.0
1.5
1.0
0.5
0.0
GABA
00'00
15'00
30'00
45'00
01:00
CPS X1000
14C
RADIOACTIVITY
1.8
1.6
1.4
1.2
1.0
0.8
0.6
0.4
0.2
0.0
GABA
00'00
15'00
30'00
45'00
01:00
TIME (MIN)

2. Metabolism of [U-^{14}C]L-Glu

Cells were incubated with 0.1 mM [U-^{14}C]L-Glu for 10 minutes with and without illumination. Then radiolabeled metabolites in the medium and aqueous cell fractions were analysed by HPLC.

With illumination 87 % and 13 % of total label in metabolites were present in the medium and cells, respectively. Without illumination 92 % and 8 % of total radiolabeled metabolites occurred in the medium and cells, respectively. In the light the organic acid and amino acid fractions represented 12 % and 88 % of all metabolites, respectively, and 6 % and 93 %, respectively, in the dark. Therefore upto 15 times more label was found in amino acid metabolites (Table 19 and 20).

With illumination, organic acid and amino acid metabolites contained 8 % and 79 % of the label in the medium, respectively. In non-illuminated medium organic acids and amino acids contained 5 % and 87 % of label in the medium, respectively. Malate, succinate and α-KG were the major labeled organic acid metabolites in the medium in the light and dark. The amino acids were the major labeled compounds in the medium. The largest labeled amino acid metabolite was GABA. GABA represented 68 % of total metabolites and 78 % of total amino acid metabolites in the light. In the dark GABA was 59 % of total metabolites or 63 % of total amino acid metabolites. A few unidentified amino compounds in the medium represented 11 % to 28 % of total labeled metabolites in the light or dark. Thus GABA,

α-KG, malate, succinate and unidentified amino compounds were the labeled metabolites of [U-^{14}C]L-Glu found in the medium. In addition GABA was the most highly labeled metabolite of [U-^{14}C]L-Glu and represented 60 % to 70 % of total label in metabolites (Table 19 and 20).

In illuminated cells, organic acids and amino acids represented 4 % and 9 % of the total labeled metabolites, respectively. Non-illuminated cells contained organic acids and amino acids with 2 % and 6 % of the total labeled metabolites, respectively. Malate, α-KG, and succinate were the major organic acids in the illuminated and non-illuminated cells, indicating that L-Glu entered mitochondria and was oxidatively deaminated to produce α-KG and metabolised via the Krebs cycle. Ten per cent and 7 % of total label in amino compounds were present within illuminated and non-illuminated cells, respectively. The labeled amino acid metabolites within the illuminated and non-illuminated cells represented 9 % and 6 % of the total metabolites, respectively, and 67 % and 79 % of the total cellular metabolites, respectively. In particular the most highly labeled amino acid within the cells was the non-metabolised L-Glu containing 56 % of the label in amino acids in the light and dark. Thus L-Glu was entering into the cells and was present in the unmetabolised form. Intracellular GABA was a minor labeled amino acid metabolite comprising 0.39 % and 0.25 % of the label in total metabolites in the light and dark, respectively. Therefore, in the light, 68.27 % of L-Glu entering the cells was

converted to GABA and 67.88 % was then released to the medium leaving 0.39 % in the cells. In the dark 58.86 % of L-Glu entering the cells was converted to GABA and 58.61 % was present in the medium. L-Gln was present at the 0.55 % level in the illuminated cells and at the 0.12 % level in the non-illuminated cells. Thus L-Glu was also metabolised within the cytoplasm to produce L-Gln. Label in L-Gln was 4.6 times higher in the illuminated cells than in non-illuminated cells (Table 19 and 20).

From these results, it was clear that the major labeled metabolite of [U-^{14}C]L-Glu was GABA. This GABA was produced in the cytoplasm and then released to the medium. The major labeled compound in the cells was L-Glu, indicating that unmetabolised L-Glu was entering the cells. L-Glu was also metabolised to produce the Krebs acids, α-KG, malate, succinate, and OAA/citrate. These Krebs acids were found in the medium and cells. Some L-Glu was metabolised to produce L-Gln in the cell.

Table 19 and 20 : HPLC analysis of [U-^{14}C]L-Glu metabolism

- The number of cells was 20 x 10^6 .
- Cells were suspended in 5 ml of 5 mM MES/1 mM $CaSO_4$ (pH 6.0), stirred, and incubated for 10 minutes with and without illumination.
- The concentration and the specific activity of [U-^{14}C]L-Glu were 0.1 mM and 49,955 dpm/nmol or 33,903 dpm/nmol.
- The dried medium and aqueous cell fractions were derivatized with PTC and an aliquot was injected into the HPLC.
- Integration of peak area was converted to the unit of dpm/20 x 10^6 cells/10 minutes, which was then converted to the radioactivity of each metabolite expressed as a percentage of the total metabolite radioactivity.
- Each value indicates the % mean and standard error (S.E.) of 3 to 8 trials.

Table 19: HPLC analysis of [U-14C]L-Glu metabolism in the light

	Medium		Cell	
	% Mean	S.E.	% Mean	S.E.
OAA/Cit	0.00	0.00	0.80	0.35
α-KG	3.40	0.32	1.08	0.47
Malate	0.00	0.00	1.68	0.40
Malonate	0.00	0.00	0.19	0.16
Succinate	4.64	2.94	0.40	0.07
Asp	0.00	0.00	1.00	0.48
Glu	-	-	4.79	0.13
Ser	0.00	0.00	0.57	0.14
Asn/Gly	0.00	0.00	0.07	0.05
Gln	0.00	0.00	0.55	0.23
GABA	67.88	2.21	0.39	0.19
Ala	0.00	0.00	0.45	0.32
Pro	0.00	0.00	0.00	0.00
UK1	5.23	1.22	0.00	0.00
UK2	4.17	1.29	0.70	0.57
UK3	2.03	1.02	0.00	0.00
Sum	87.35		12.68	

Table 20 : HPLC analysis of [U-14C]L-Glu metabolism in the dark

	Medium		Cell	
	% Mean	S.E.	% Mean	S.E.
OAA/Cit	0.00	0.00	0.00	0.00
α-KG	2.31	0.20	0.31	0.05
Malate	0.00	0.00	0.98	0.17
Malonate	0.00	0.00	0.00	0.00
Succinate	2.20	1.31	0.40	0.07
Asp	0.00	0.00	0.00	0.00
Glu	-	-	3.55	0.61
Ser	0.00	0.00	1.44	1.08
Asn/Gly	0.00	0.00	0.00	0.00
Gln	0.00	0.00	0.12	0.10
GABA	58.61	3.83	0.25	0.03
Ala	0.00	0.00	0.12	0.10
Pro	0.00	0.00	0.15	0.12
UK1	6.56	1.17	0.00	0.00
UK2	15.20	3.09	0.70	0.57
UK3	6.54	1.88	0.00	0.00
Sum	91.42		8.03	

3. Compartmentation of GABA production

The compartmentation of GABA production was investigated by comparing the specific activities of GABA in the medium and cells after feeding [U-^{14}C]L-Glu to cells incubated in the light and dark. The specific activity of [U-^{14}C]L-Glu was 49,955 dpm/nmol. Assuming that each carbon was equally labeled, the theoretical specific activity of the GABA produced was 4/5 x 49,955 dpm/nmol or 39,964 dpm/nmol. The specific activity of GABA was obtained by dividing DPM in GABA by total nmol GABA (Table 21). The specific activity of GABA in the medium was 40,113 dpm/nmol in the light and 43,032 dpm/nmol in the dark. The specific activities were similar to or slightly greater than the theoretical specific activity. Thus the GABA was leaving the cells without mixing with the large previously synthesized pool of GABA. The specific activity of GABA in the cells was only 300 to 500 dpm/nmol. This low specific activity value was due to mixing and dilution with the large non-labeled internal GABA pool. The cellular specific activity values may be underestimated because of the rapid efflux of newly synthesized GABA. The far lower theoretical specific activity of GABA in the cells suggested that the sites of GABA production and storage were separated. GABA was produced in the cells and this newly synthesized GABA immediately left the cells without mixing with the large internal GABA pool.

Table 21 : The specific activity of GABA after feeding [U-^{14}C]L-Glu

	Medium			Cell		
	GABA	GABA	Specific Activity	GABA	GABA	Specific Activity
	nmol	DPM	DPM/nmol	nmol	DPM	DPM/nmol
L	40.58 (6.25)	1,627,780 (111,208)	40,113	56.89 (25.21)	19,204 (74)	506
D	34.57 (1.73)	1,487,619 (149,816)	43,032	30.76 (4.93)	9,663 (5,276)	314

- The specific activity of GABA was derived from HPLC analysis after [U-^{14}C]L-Glu metabolism (Table 19 an 20).
- Conditions were the same as in Table 19 and 20.
- The specific activity (DPM/nmol) was calculated by dividing DPM in GABA by nmol GABA.
- Each value is the mean and S.D. of 2 to 6 trials.

4. Labeled metabolites of [1-^{14}C]L-Glu

Metabolism of [1-^{14}C]L-Glu was investigated in illuminated and non-illuminated cell suspensions (Table 22 and 23). In the light 59 % of total labeled metabolites was present in the cells and 41 % was found in the medium. In the dark 64 % and 36 % of the total labeled metabolites were present in the medium and cells, respectively. The total organic acid and amino acid fractions contained 25 % and 75 % of total labeled metabolites, repectively, in the light, 28 % and 72 %, respectively, in the dark. In the dark the medium contained 8.8 times more label in organic acids than amino acids. Organic acids were evenly distributed between the illuminated medium and cells. The major labeled organic acid metabolites of the medium were α-KG followed by acetate. In particular α-KG represented 6 % of the total labeled metabolites in the light and 12 % in the dark. These corresponded to 50 % of total organic acid metabolites. The major labeled amino compound in the medium was the unidentified compound which represented 25 % of the total labeled metabolites both in the light and dark. This unknown amino compound was also present as a highly labeled metabolite in the medium after feeding [1-^{14}C]L-Glu to medium with cells. The major labeled amino compounds within cells was L-Glu. L-Glu represented 40 % of label in the light and 23 % in the dark. This represents further evidence for the entry of L-Glu into these cells. GABA was one of the minor labeled cellular compounds containing only 0.12 % of label in the light and 0 % in the dark.

Fig. 32 : Production of non-labeled GABA from (1-^{14}C)L-Glu

- This is the trace resulting from HPLC and subsequent on line scintillation counting.
- Twenty million cells were suspended in 5 ml of 5 mM MES/1 mM $CaSO_4$ (pH 6.0), stirred, and incubated for 10 minutes.
- The concentration and the specific activity of [1-^{14}C]L-Glu were 0.1 mM and 38,784 dpm/nmol, respectively.
- The dried medium and aqueous cell fractions were derivatized with PTC and an aliquot was injected into the HPLC.
- GABA, if present, appears at 18 minutes.

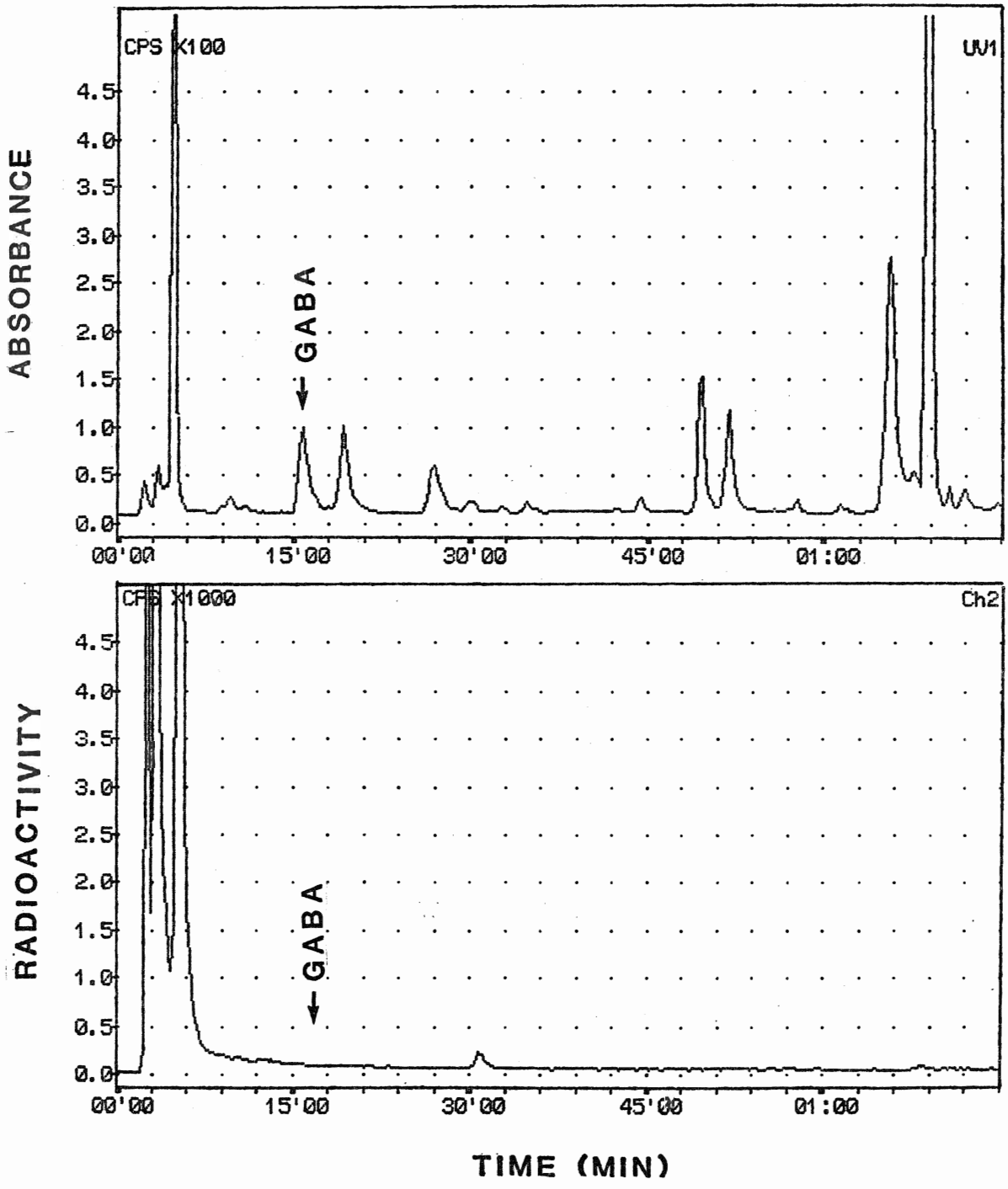
CPS X100
UV1
ABSORBANCE
4.5
4.0
3.5
3.0
2.5
2.0
1.5
1.0
0.5
0.0
GABA
00'00
15'00
30'00
45'00
01:00
CPS X1000
Ch2
RADIOACTIVITY
4.5
4.0
3.5
3.0
2.5
2.0
1.5
1.0
0.5
0.0
GABA
00'00
15'00
30'00
45'00
01:00
TIME (MIN)

Table 22 and 23 : HPLC analysis of [1-^{14}C]L-Glu metabolism

- The number of cells was 20 x 10^6 .
- Cells were suspended in 5 ml of 5 mM MES/1 mM $CaSO_4$ (pH 6.0), stirred, and incubated for 10 minutes with and without illumination.
- The concentration and the specific activity of [1-^{14}C]L-Glu were 0.1 mM and 38,784 dpm/nmol, respectively.
- The dried medium and aqueous cell fractions were derivatized with PTC and an aliquot was injected into the HPLC.
- Integration of peak area was converted to the unit of dpm/20 x 10^6 cell /10 minutes, which was then converted to the radioactivity of each metabolite expressed as a percentage of the total metabolites.
- Each value indicates the % mean of 2 trials.

Table 22: HPLC analysis of [1-14C]L-Glu metablism in the light

	Medium			Cell		
	Expt.1	Expt.2	Mean	Expt.1	Expt.2	Mean
OAA/Cit	0.36	0.00	0.18	3.16	1.73	2.45
α-KG	5.24	6.96	6.10	4.02	4.15	4.09
Malate	0.21	0.18	0.20	4.61	4.80	4.71
Malonate	1.05	2.16	1.61	1.67	1.12	1.40
Succinate	0.94	2.22	1.58	0.64	0.22	0.43
Acetate	1.42	2.61	2.02	0.12	0.17	0.15
Asp	0.00	0.00	0.00	0.00	0.00	0.00
Glu	-	-	-	44.79	33.03	38.91
Ser	0.00	2.17	1.09	0.94	1.40	1.17
Asn/Gly	0.73	1.54	1.14	0.34	1.74	1.04
Hser	0.00	0.00	0.00	4.80	0.92	2.86
GABA	0.00	0.00	0.00	0.24	0.00	0.12
Thr/Ala	0.00	0.00	0.00	0.26	0.00	0.13
UK1	22.02	28.16	25.09	0.00	0.00	0.00
UK2	0.00	1.60	0.80	0.00	0.00	0.00
Orn	0.00	0.00	0.00	0.00	0.00	0.00
Lys	1.77	1.59	1.68	0.67	1.51	1.09
Sum	33.74	49.20	41.47	66.26	50.80	58.53

Table 23:HPLC analysis of [1-14C]L-Glu metabolism in the dark

	Medium			Cell		
	Expt.1	Expt.2	Mean	Expt.1	Expt.2	Mean
OAA/Cit	1.25	0.39	0.82	0.10	0.03	0.07
α-KG	14.07	10.30	12.18	1.73	0.83	1.28
Malate	1.33	1.36	1.35	0.43	1.56	0.99
Malonate	2.79	3.78	3.29	0.28	0.39	0.33
Succinate	1.67	4.35	3.01	0.05	0.20	0.13
Acetate	3.30	5.00	4.15	0.05	0.00	0.02
Asp	0.00	0.00	0.00	0.00	0.00	0.00
Glu	-	-	-	35.08	10.92	23.00
Ser	16.78	0.00	8.39	0.00	0.00	0.00
Asn/Gly	0.97	0.00	0.49	2.69	0.00	1.35
Hser	0.00	0.00	0.00	0.00	1.28	0.64
GABA	0.00	0.00	0.00	0.00	0.00	0.00
Thr/Ala	0.00	0.00	0.00	0.00	2.85	1.42
UK1	12.97	36.60	24.79	0.00	0.00	0.00
UK2	0.00	0.00	0.00	0.00	5.39	2.69
Orn	0.00	0.00	0.00	0.00	1.80	0.90
Lys	4.16	7.54	5.85	0.29	5.45	2.87
Sum	59.30	69.32	64.31	41.70	30.68	35.69

5. Biochemical pathway of GABA production

The biochemical pathway of GABA production was investigated using both [U-^{14}C] and [1-^{14}C]L-Glu. The rationale employed was that if GABA is produced by loss 1-carbon of [U-^{14}C]L-Glu, then the GABA to be produced will be labeled. Whereas, if [1-^{14}C]L-Glu is fed, the GABA produced will not contain radioactivity. On the basis of this rationale, 0.1 mM [U-^{14}C]L-Glu (specific activity 49,955 dpm/nmol) and 0.1 mM [1-^{14}C]L-Glu (specific activity 38,784 dpm/nmol) were fed to the cells for 10 minutes. After feeding [U-^{14}C]L-Glu, 40.58 nmol GABA with 1,627,780 dpm occurred in the illuminated medium, and 34.57 nmol GABA with 1,487,619 dpm was present in the non-illuminated medium (Table 21). When [1-^{14}C]L-Glu was fed to the cells, 40.13 and 37.75 nmol GABA appeared in the illuminated and non-illuminated medium, respectively. However GABA did not contain any corresponding radioactivity. Thus GABA production occurs by the loss of 1-carbon from L-Glu.

Table 24 : The specific activity of GABA after feeding [1-^{14}C]L-Glu

	Medium			Cell		
	GABA	GABA	Specific Activity	GABA	GABA	Specific Activity
	nmol	DPM	DPM/nmol	nmol	DPM	DPM/nmol
L	40.13 (16.22)	0 (0)	0	78.70 (21.77)	34,573 (25,531)	439
D	37.75 (16.95)	0 (0)	0	36.20 (16.95)	5,162	143

- The specific activity of GABA was derived from HPLC analysis after [1-^{14}C]L-Glu metabolism (Table 22 and 23).
- Conditions were the same as in Table 22 and 23.
- The specific activity (DPM/nmol) was calculated by dividing DPM in GABA by nmol GABA.
- Each value is the mean and S.D. of 2 to 6 trials.

6. Photosynthetic fixation of CO_2 released from labeled L-Glu

The fixation of carbon-1 released as CO_2 was confirmed by comparing the uptake of [U-^{14}C]L-Glu and [1-^{14}C]L-Glu in the light and dark (Table 25). The uptake of [U-^{14}C]L-Glu and [1-^{14}C]L-Glu was higher in the light than in the dark. When cell suspensions were incubated with [U-^{14}C]L-Glu in the dark, the uptake was 73 % of uptake in the light. With [1-^{14}C]L-Glu the uptake rate in the dark was only 28 % of the rate found in illuminated cells. The much lower rates of uptake for [1-^{14}C]L-Glu in the dark can be explained by loss of radioactivity as CO_2 from carbon-1. In the light fixation of this CO_2 will result in a much larger apparent rate of uptake. Radioactivity of [1-^{14}C]L-Glu is present only in carbon-1. On decarboxylation all the label is lost and a part of this is subsequently refixed by illuminated cells. Consequently a significantly higher apparent rate of uptake will result in the light. In contrast only 1/5 of the radioactivity in [U-^{14}C]L-Glu is released on decarboxylation and therefore light has a smaller effect. Thus the higher uptake of [U-^{14}C]L-Glu and [1-^{14}C]L-Glu in the light than in the dark clearly indicated that the lost carbon-1 had been refixed in the cells.

The different labeling patterns in [U-^{14}C]L-Glu and [1-^{14}C]L-Glu also explain the different distribution of labeled metabolites between the medium and cells (Table 19, 20, 22, and 23). Because of label in carbon 2 to 5, the cellular labeled metabolites of [U-^{14}C]L-Glu were 13 % and 8 % of total

metabolites in the light and dark, respectively. The label in cellular metabolites from [1-^{14}C]L-Glu was much higher representing 59 % and 36 % in the light and dark, respectively. Thus the higher proportion of label in the cells after feeding [1-^{14}C]L-Glu is due to the release of unlabeled GABA to the medium.

Table 25 : Uptake of [U-^{14}C]L-Glu or [1-^{14}C]L-Glu in the dark as a per cent of that in the light

[U-^{14}C]L-Glu	[1- ^{14}C]L-Glu
70	30
85	18
78	22
67	43
66	
Mean (S.D.) 73 (7)	28 (9)

- Twenty million cells were suspended in 5 mM MES/1 mM $CaSO_4$ (pH 6.0).
- Cell suspensions were stirred and incubated for 10 minutes with and without illumination. After 10 minute incubation, the uptake was measured.
- The concentration and the specific activity of [U-^{14}C]L-Glu were 0.1 mM and 49,955 dpm/nmol or 33,903 dpm/nmol.
- The concentration and the specific activity of [1-^{14}C]L-Glu were 0.1 mM and 38,784 dpm/nmol, respectively.
- Each value represents a % of uptake in the light. Four to 5 trials are indicated.

7. HPLC pulse chase analysis of [U-^{14}C]L-Glu metabolites

In an attempt to confirm the metabolism of L-Glu by the Krebs cycle, time dependent consumption of metabolites of L-Glu was investigated by pulse feeding and a chase over time. The pulse feeding was performed by incubating the cells with 0.1 mM [U-^{14}C]L-Glu for 10 minutes. The labeled metabolites were then subsequently chased for 10 and 60 minutes by further incubation with 0.1 mM cold L-Glu. Each cellular fraction was then analysed and the total radioactivity was given a value of 100 %. L-Glu decreased from 56 % to 42 % to 33 % during the 10 minute pulse and subsequent 10 and 60 minute chase periods, respectively. The data suggest time dependent L-Glu metabolism. The total organic acid fraction increased from 22 % to 37 % after a 10 minute chase then to 38 % with a 60 minute chase. The total amino acid fraction minus L-Glu was relatively constant at 23 % to 23 % and 29 % for the 10 minute incubation plus 10 and 60 minute time courses. This suggested that L-Glu had been metabolised to organic acids and amino acids. Succinate increased for the 10 minute chase but decreased after 60 minutes. α-KG and malate increased during the 10 and 60 minute time course from 4 % to 7 % to 9 % and 13 % to 23 % to 27 %, respectively. In particular malate showed a large increase during the first 10 minute chase period. In addition, label in Asp, GABA, Gln, and Pro also increased over time (Table 26). The evidence demonstrates the production of Krebs acids from L-Glu.

Table 26 : HPLC pulse chase analysis of [U-^{14}C]L-Glu metabolism

- The number of cells was 20 x 10^6 .
- Cells were suspended in 5 ml of 5 mM MES/1 mM $CaSO_4$ (pH 6.0), stirred, and incubated for 10 minutes in the dark.
- The concentration and the specific activity of [U-^{14}C]L-Glu were 0.1 mM and 49,955 dpm/nmol.
- Note :

  10 min feed ; After 10 minute incubation, cells were separated from the suspension medium, washed in 1 x 15 ml of cold medium and then fractionated.

  10 min feed and 10 min / 60 min chase ; After 10 minute incubation, the cells were separated from the suspension medium. A chase for 10 or 60 minutes with cold L-Glu was initiated by suspending the cell pellet in 0.1 mM L-Glu. After a 10 or 60 minute chase, the cells were separated and fractionated.
- The aqueous cell fraction was derivatized with PTC and an aliquot was injected into the HPLC.
- Integration of peak area was converted to the unit of dpm/20 x 10^6 cells/10 minutes, which is then converted to the % of dpm in total metabolites.
- Each value indicates the % mean of 2 trials.

Table 26 : HPLC pulse chase analysis of [U-14C]L-Glu metabolism

	10 min feed	10 min feed & 10 min chase	10 min feed & 60 min chase
OAA/Cit	0	0	0
α -KG	4	7	9
Malate	13	23	27
Succinate	5	7	5
Asp	14	12	16
Glu	56	42	33
Ser	0	0	0
Gln	0	2	2
GABA	4	5	6
Ala	2	2	1
Pro	3	2	4
Sum	100	100	100

8. The influence of CCCP on [U-^{14}C]L-Glu metabolism

TLC indicated that CCCP stimulated GABA efflux after feeding [U-^{14}C]L-Glu (Table 17 and 18) or [^{14}C]GABA (Fig. 23 and 25). The effect of CCCP on GABA production and efflux was investigated using HPLC analyses of [U-^{4}C]L-Glu metabolites. CCCP inhibited the uptake of label, such that labeled metabolites could not be detected by flow through scintillation counter. However the medium fraction exhibited high levels of labeled GABA and organic acids. GABA was the most highly labeled amino acid and represented 40 % of total labeled metabolites. The second most highly labeled metabolite was the unidentified amino compound found as a product of [U-^{14}C]L-Glu or [1-^{14}C]L-Glu metabolism. Succinate was the third highest labeled metabolite in the medium (Table 27). These results indicate that CCCP stimulated GABA efflux and that newly synthesized GABA and succinate were released to the medium.

Table 27 : HPLC analysis of the influence of CCCP on [U-^{14}C]L-Glu metabolism

- The number of cells was 20 x 10^6 .
- Cells were suspended in 5 ml of 5 mM MES/1 mM $CaSO_4$ (pH 6.0), stirred.
- The concentration and the specific activity of [U-^{14}C]L-Glu were 0.1 mM and 33,903 dpm/nmol, respectively.
- The cell suspension was stirred and preincubated for 10 minutes in 10 uM CCCP in the light.
- The dried medium and aqueous cell fractions were derivatized with PTC and an aliquot was injected into the HPLC.
- Integration of peak area was converted to the unit of dpm / 20 x 10^6 cells / 10 minutes, which is then converted to the % of dpm in total metabolite.
- Each value indicates the % mean of 2 trials.

Table 27 : HPLC analysis of the influence of CCCP on [U-14C] L-Glu metabolism

	(-)CCCP		(+)CCCP	
	Medium	Cell	Medium	Cell
OAA/Cit	0	2	0	-
α-KG	3	1	2	-
Malate	0	2	1	-
Succinate	12	0	10	-
Asp	0	0	0	0
Glu	-	3	-	0
Ser	0	0	0	0
Asn/Gly	0	0	0	0
Gln	0	0	0	0
GABA	66	1	27	0
Ala	0	0	0	0
Pro	0	0	0	0
UK1	8	0	22	0
UK2	1	0	6	0
Sum	90	10	68	0

DISCUSSION

1. Origin of L-Glutmate dependent medium alkalinization and GABA appearance in the medium

The favored hypothesis to account for the active transport and accumulation of amino acids in higher plants is a H^+/amino acid symport process. The driving forces for an electrogenic H^+/amino acid symport are the amino acid concentration gradient, the H^+ chemical gradient, and the electrical gradient. The latter two are generated by the ATP driven H^+ efflux. Major criteria for the presence of a H^+ /amino acid symport system include (i) accumulation of substrate, (ii) transient alkalinization of the medium bathing cells, (iii) depolarization of the membrane, (iv) specificity of uptake, (v) saturation kinetics of uptake, and (vi) increased uptake rates with decreasing external pH (Reinhold and Kaplan 1984).

In recent years, efforts have been made to characterize the transport of L-Glu into mechanically isolated *Asparagus sprengeri* mesophyll cells. Much evidence suggests the presence of a specific H^+/L-Glu symport system in these cells (McCutcheon and Bown 1987, McCutcheon *et al.* 1988). Major evidence is as follows : (i) L-Glu induced transient alkalinization of the external medium. When L-Glu or its structural analogs L-MSO, D-Glu, L-Gln, and L-Asp were added to the cell suspension only L-Glu and L-MSO caused an immediate and transient alkalinization of the bathing medium. (ii) L-Glu uptake was stimulated by higher

external H^+ concentrations and fusiccocin (FC) which stimulates H^+ efflux (Marre 1979). It was inhibited by the protonophore, CCCP. The uptake of [U-^{14}C]L-Glu and L-Glu dependent medium alkalinization increased with increasing H^+ concentrations. Addition of 10 uM CCCP, which dissipates the H^+ electrochemical gradient (Bown 1982), inhibited the uptake of L-Glu and medium alkalinization by 95 % and 60 %, respectively. Addition of K^+ which depolarizes the membrane inhibited the L-Glu dependent medium alkalinization. Addition of fusiccocin (FC) to the cell suspension medium stimulated the rate of H^+ efflux by 111 % and the uptake of L-Glu by 55 % (McCutcheon and Bown 1987, McCutcheon *et al.* 1988).

The net influx of H^+ during a H^+/amino acid symport may cause acidification of the cytoplasm depending on the buffering capacity of the protoplasm and the operation of any homeostatic mechanisms regulating cytoplasmic pH. Using the [^{14}C] 5,5 dimethyl oxazolidine-2,4-dione (DMO) technique, decreases in the intracellular pH were detected on addition of 5 mM butyric acid, L-Glu, and L-MSO. Addition of butyric acid caused an immediate and large decrease in the equilibrium level of [^{14}C]DMO in cells. Addition of L-Glu and L-MSO gradually decreased the intracellular [^{14}C]DMO level. The decrease in intracellular [^{14}C]DMO level indicates an acidification of the cytoplasm. This result is consistent with the operation of a H^+/L-Glu symport. (The calculations of the extent of cytoplasmic pH change induced by these reagents are discussed in Discussion section 5) (McCutcheon

et al. 1988). Thus L-Glu dependent medium alkalinization can be interpreted as a loss of H^+ from the medium to the cell during H^+/L-Glu symport (Model 1A).

However the medium alkalinization could result from a decarboxylation process ($RCOO^- + H^+ \text{------>} RH + CO_2$) at the external face of the cell (Model 1B) or a H^+ symport involving an L-Glu metabolite or some combination of the two (Model 1C). The decarboxylation product of L-Glu is GABA and this reaction is catalysed by the widely distributed enzyme GAD (Spedding and Wilson 1968, Streeter and Thompson 1972b, Chou and Splittsoesser 1972, Koiwai and Noguchi 1972, Collins and wilson 1975, Inatomi and Slaughter 1975, Satyanarayan and Nair 1985, Melcher 1986, Tsushida and Murai 1987). Comparison of changes in levels of amino acids in the medium after a 10 minute incubation with 1 mM L-Glu showed that GABA levels increased by 2,743 % and 2,241 % in the light and dark, respectively (Table 5 and 6). Thus the following models (Model 1B and 1C) indicate alternative origins of L-Glu dependent medium alkalinization.

(Model 1A) H^+/L-Glu symport

(Model 1B) Decarboxylation of L-Glu in the extracellular phase and consequent H^+ consumption

(Model 1C) H^+/GABA symport subsequent to GABA production in the medium

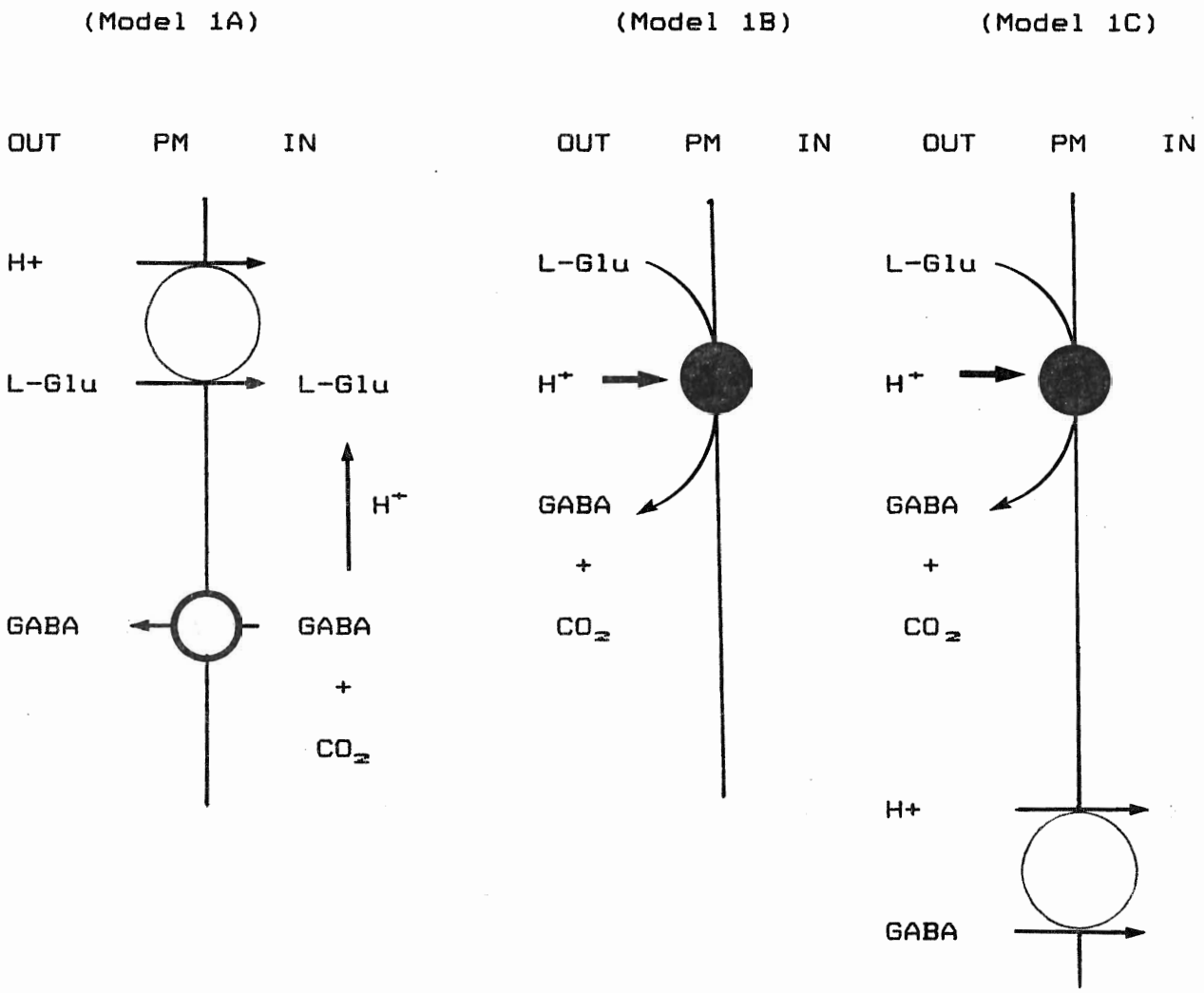

All three models give rise to medium alkalinization, CO_2 evolution, and GABA appearance in the medium.

In order to determine whether the huge increase in GABA levels in the medium was due to extracellular events, the possibilities of extracellular GABA production were examined. GABA may appear by breakdown or contamination of L-Glu during sample preparation procedures in a process independent of the cells. GABA appearance in the medium did not occur when labeled

L-Glu was incubated in the absence of cells. It did appear when cells were present (Fig. 30, 31A, and 31B). Thus GABA production was definitely a cell mediated process, not due to breakdown or contamination of L-Glu. The intracellular production of GABA was investigated by determining the uptake of labeled L-Glu and the corresponding GABA production in the medium as influenced by K^+ and CCCP (Table 18). Twenty mM K^+ and 10 uM CCCP inhibited the uptake of 0.5 mM [U-14 C]L-Glu by 17 % and 95 %, respectively, and the corresponding GABA appearance in the medium by 17 % and 50 %, respectively, indicating that GABA is produced inside the cells. It is unlikely that K^+ and CCCP would inhibit extracellular GABA production. It appears that GABA production is diminished because these agents inhibit membrane transport into the cell. HPLC analysis also demonstrated that the most highly labeled compound in the cell was L-Glu, demonstrating L-Glu uptake into the cells. In addition small levels of GABA were found in the cell. It is also important to note that GABA appearance in the medium also occurred in the absence of L-Glu (Table 5 and 6) demonstrating that GABA efflux from the cells does occur. These results clearly indicate that L-Glu entered the cells and was subsequently decarboxylated to GABA which was then released to the medium.

The simultaneous measurements of the L-Glu dependent medium alkalinization and the $^{14}CO_2$ evolution upon addition of [U-^{14}C]L-Glu demonstrated that the medium alkalinization was immediate and reached a maximal value after 45 minutes. In

contrast $^{14}CO_2$ evolution exhibited a lag period for the first 5 minutes and then increased linearly for 100 minutes. However L-MSO which causes alkalinization did not stimulate the CO_2 evolution (McCutcheon *et al.* 1988). Thus the evidence suggests that the alkalinization is not due to decarboxylation. In contrast the data suggest that alkalinization is due to a specific H^+/L-Glu symport. Consequently the (Model 1B) was excluded.

However it was still possible that GABA in the medium might enter via a symport and thereby cause medium alkalinization. Addition of 5 mM GABA did not cause medium alkalinization. Thus there is no evidence for H^+/GABA symport process causing the medium alkalinization (Fig. 15). Again (Model 1C) is excluded.

Thus the origin of L-Glu dependent medium alkalinization was not due to the extracellular decarboxylation of L-Glu or H^+/GABA symport but due to the H^+/L-Glu symport process.

2. Stoichiometry of the H^+/L-Glutamate symport system

A carrier mediated H^+/substrate (amino acids and sugars) symport hypothesis (model a) suggests that a membrane transporter or carrier (E) binds H^+ (H). Binding of H^+ to the carrier raises the affinity to the substrate (S), so that a ternary complex forms (ESH) at the outer surface of the membrane. This charged ternary complex is transported across the membrane by the electrical gradient where S and H^+ dissociate. The pH gradient across the membrane stimulates the uptake by enhancing the formation of the ternary complex at the outer surface and the dissociation of the complex at the inner surface (Reinhold and Kaplan 1984).

(Model 2A : from Reinhold and Kaplan, 1984)

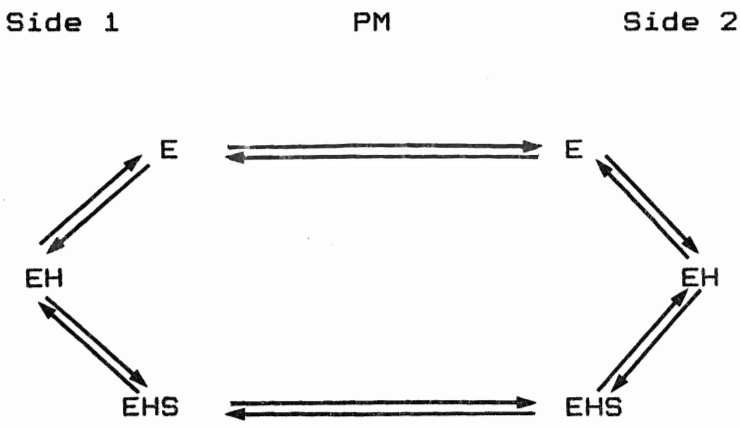

The ratio of nH^+ to one substrate carried by the symport is a whole number and called the stoichiometry. The stoichiometry is usually obtained from simultaneous measurements of the rate of

solute dependent medium alkalinization and the rate of solute uptake (Cockburn 1975, Hutchings 1978, Robinson and Beevers 1981, Wyse and Komor 1984, McCutcheon *et al.* 1988).

In order to determine the stoichiometry of H^+/L-Glu transport in *Asparagus* mesophyll cells, the L-Glu dependent medium alkalinization, uptake of [U-^{14}C]L-Glu, and $^{14}CO_2$ evolution were simultaneously measured (McCutcheon *et al.* 1988). The stoichiometry was then calculated by dividing rate of medium alkalinization by the rate of uptake of [U-^{14}C]L-Glu uptake. The total uptake rate of [U-^{14}C]L-Glu represented the rate of uptake of [U-^{14}C]L-Glu plus the rate of $^{14}CO_2$ evolution. As a result, the minimal stoichiometry obtained was 3 : 1 with 0.5 mM L-Glu in the light. The maximal stoichiometry of H^+ : L-Glu uptake was 7.7 : 1 with 10 mM L-Glu in the dark. The stoichiometry was higher in the dark than in the light and increased with increasing concentrations of L-Glu (McCutcheon *et al.* 1988). Work done by Wyse and Komor (1984) suggested that three different transport systems are present in sugarcane cells, specific for basic, neutral, and acidic amino acids. The transport of neutral amino acids was coupled to the uptake of 0.71 to 0.98 H^+ (1 H^+) per 1 amino acid molecule. One K^+ left the cells for charge compensation. Basic amino acids such as L-Arg were transported with 0.27 H^+ (0 H^+), suggesting a uniport. There was a charge compensating K^+ efflux. The uptake of the acidic amino acids, L-Asp and L-Glu, in their anionic form was coupled to the uptake of 1.89 to 2.09 H^+ (2 H^+) and the release of 1 K^+ per 1 amino acid

molecule for charge compensation. Thus an electrogenic stoichiometry of 2 H^+/L-Glu was suggested. On the basis of measured membrane depolarization in oat coleoptiles, Kinraide and Etherton (1980) also suggested that the transport of acidic amino acids involved 1 H^+ and 1 other cation. Four strains of yeast, *Saccharomyces*, grown with L-Glu transported extra protons with the uptake of L-Glu. *S. cerevisiae* absorbed L-Glu with 3 H^+ per 1 L-Glu molecule and 1 to 2 K^+ left the cells (Cockburn 1975). Thus compared to the stoichiometries in other systems, the stoichiometry of 3 to 7 H^+ per 1 L-Glu transported in *Asparagus* mesophyll cells was disconcertingly high.

It is now clear that the high stoichiometry resulted from an underestimation of L-Glu uptake due to the efflux of the major metabolite GABA. TLC of medium resulting from the incubation of cells with 0.5 mM [U-^{14}C]L-Glu revealed that GABA in the medium contained 6.2 times more radioactivity than the total uptake of the cells (Table 18). HPLC analysis of L-Glu metabolites demonstrated that about 87 % to 92 % of the total labeled metabolites was found in the illuminated or non-illuminated medium (Table 19 and 20). Thus the H^+/L-Glu stoichiometry can be lowered by a factor of 6 upto 9. A more accurate H^+/L-Glu stoichiometry can be obtained by dividing the rate of medium alkalinization by the rate of uptake of L-Glu, the $^{14}CO_2$ evolution plus the rate of efflux of L-Glu metabolites such as GABA and other amino acids and organic acids. The extent of 0.5 mM L-Glu uptake and GABA appearance in the medium were

simultaneously measured for 10 minutes in the light (Table 18). The uptake of 0.5 mM [U-^{14}C]L-Glu was 3,683 dpm/10^6 cells/10 minutes. The corresponding GABA appearance in the medium was 22,894 dpm/10^6 cells/10 minutes. Therefore the total uptake of [U-^{14}C]L-Glu was 3,683 plus 22,894 or 26,577 dpm/10^6 cells/10 minutes. Because the specific activity of L-Glu was 3,151 dpm/nmol, the total uptake of L-Glu was converted to 8.43 nmol L-Glu/10^6 cells/10 minutes (Table 18). The rate of 0.5 mM L-Glu dependent medium alkalinization measured in separate experiments was 0.82 nmol H^+/10^6 cells/minute in the light (Table 16). Since $^{14}CO_2$ evolution during the metabolism of L-Glu in the light is small, the loss of radioactivity as $^{14}CO_2$ was negligible. Consequently, the H^+/L-Glu stoichiometry obtained from the separate measurements was 0.9 : 1. Simultaneous measurement of alkalinization, L-Glu uptake, and GABA efflux also indicate a 1 : 1 stoichiometry (Bown unpublished data). HPLC analysis of 0.1 mM [U-^{14}C]L-Glu metabolism in illuminated cell demonstrated that 92 % of label taken up was lost to the medium after 10 minute incubation. This resulted from loss of organic acids and amino acids as well as GABA. Consequently the stoichiometry was lowered to 0.7 : 1. Thus different approaches suggest an overall stoichiometry somewhere between 0.7 : 1 and 1 : 1.

In castor bean (*Ricinus communis*) cotyledons, the uptake of [^{14}C]L-Gln was simultaneously measured with the proton uptake. The stoichiometry was 0.33 with 1 mM L-Gln and decreased to 0.32 and 0.28 as the concentrations of L-Gln increased to 2 mM

and 4 mM, respectively (Robinson and Beevers 1981). Also the stoichiometry of H^+/sucrose transport in castor bean cotyledons was 0.370 with 1 mM sucrose and decreased to 0.0048 with 100 mM sucrose (Hutchings 1978).

These low stoichiometries found by other workers have been explained in two ways ; (i) a recirculation of H^+ taking place due to ATP driven H^+ efflux, (ii) substrate entry with the unprotonated form of the carrier.

(i) The recirculation of H^+ : A H^+/substrate symport process increases the H^+ concentration of the cytoplasm. Consequently the increase in concentration of the pump substrate stimulates ATP driven H^+ efflux. In addition the depolarization of the membrane due to electrogenic symport may stimulate homeostatic regulation of the membrane potential by stimulating electrogenic H^+ extrusion. Therefore H^+ influx in cotransport with L-Glu may increase the rate of H^+ efflux resulting in rates of H^+ influx lower than the true rate of H^+ influx. Thus the true stoichiometry of the H^+/L-Glu symport may be 2 : 1.

(ii) Two conformational states of the symport carrier : As mentioned, the transport is mainly effected via the ternary complex (ESH) (Reinhold and Kaplan 1984). However the binary ES complex may traverse the membrane under certain conditions. This is called a 'slip pathway' (Model 2B)(Reinhold and Kaplan 1984).

(Model 2B : from Reinhold and Kaplan 1984)

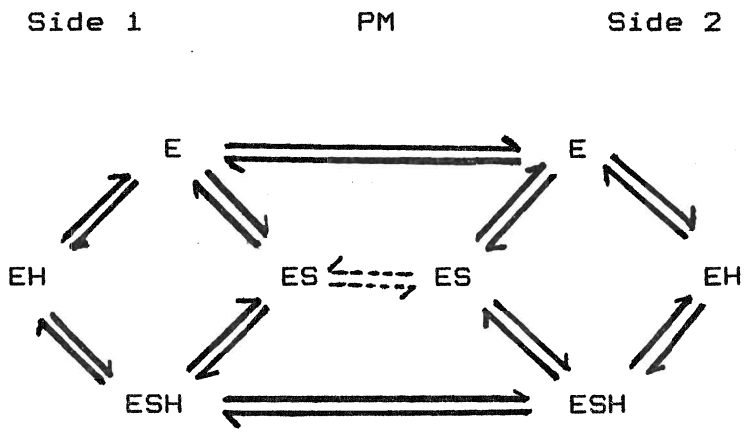

i.e. ESH is formed either via ES or via EH. E and ESH are the principal species which cross the membrane from side 1 to side 2. However the binary complex ES may traverse the membrane under certain conditions. Thus the transport of S may occur via the ternary complex ESH or the binary complex ES. This suggests two conformational states of the symport carrier. *i.e.* a high affinity, protonated form operating at low substrate levels and high H^+ concentrations and a low affinity, unprotonated form operating at high substrate levels and low H^+ concentrations. It is not necessary that the same carrier is involved in both ES and ESH formation as indicated by the model. Therefore the existence of an unprotonated carrier would explain the declining stoichiometry of H^+/sucrose and L-Gln with increasing substrate concentrations and increasing pH (Hutchings 1978).

Since the stoichiometry has not been measured with increasing concentrations of L-Glu, it is not yet known whether

the stoichiometry declines with the increase in L-Glu. However evidence indicates that the stimulation of H^+ pumping may result in an apparent stoichiometry of H^+/L-Glu less than 2. Oligomycin eliminated H^+ efflux and consequently allowed for the determination of the rate of H^+ efflux before and after the addition of L-Glu. It appears that the rate of H^+ efflux measured with illuminated and non-illuminated cells was stimulated by the addition of 2 mM L-Glu by 57 % and 49 %, respectively. In addition 1.5 mM butyric acid and acetic acid stimulated the rate of H^+ pumping by 100 % (Bown unpublished data). Weak permeant acids can across the plasma membrane in the uncharged form and dissociate to acidify the cytoplasm (Sanders and Slayman 1982, Marre *et al.* 1983). The decreases in [^{14}C]DMO levels on addition of L-Glu and butyric acid indicate that L-Glu and butyric acid cause the acidification of the cytosol (McCutcheon *et al.* 1988). Therefore the evidence indicates that weak acids and H^+/L-Glu symport acidify the cytosol and stimulate the ATP driven H^+ pump. Thus a net stoichiometry of H^+/L-Glu of approximately 1 may be due to stimulated H^+ pumping. Therefore considering that the net stoichiometry of H^+/L-Glu symport is 1 : 1, the actual stoichiometry may be 2 : 1.

A process transporting $L\text{-}Glu^-$ with 1 H^+ is electroneutral and therefore will not cause the depolarization of the membrane. If $L\text{-}Glu^-$ is transported with 2 H^+ , the membrane will be depolarized due to the net entry of one positive charge. Twenty millimolar K^+ inhibited the uptake of L-Glu by 17 %

presumably by depolarizing the membrane. Similarly lipophilic cation inhibited uptake (Bown, unpublished data). These results indicate that the H^+/L-Glu symport is electrogenic. Many authors suggest that during electrogenic symport electroneutrality is maintained by the most mobile cation, K^+ (Cockburn 1975, Wyse and Komor 1984, Komor *et al.* 1989). However despite repeated attempts addition of L-Glu did not stimulate K^+ efflux from *Asparagus* cells (McCutcheon and Bown 1987). When cytoplasmic pH was continuously measured by pH-sensitive microelectrode, the electrogenic uptake of glucose, L-Arg, L-Ala, and L-Glu in *Riccia* rhizoid cells did not cause acidification of the cytoplasm, but rather caused alkalinization of the cytoplasm (Johannes and Felle 1987). These authors suggested that depolarization of the membrane stimulated H^+ pumping such that the cytoplasm became alkaline and the membrane was repolarized. The simultaneous measurements of H^+ and K^+ fluxes, cytoplasmic pH, respiration, and cellular ATP level suggested three consecutive phases on addition of glucose to *Chlorella*. Phase 1 was characterized by the immediate uptake of H^+, K^+ efflux, and the loss of other ions to a small degree. Phase 2 was observed 5 seconds after the addition of Glucose and demonstrated the stimulation of H^+-ATPase, a slow-down of K^+ efflux, and net acidification of the external medium together with a decrease in cellular ATP level and an increase in respiration. Phase 3 occurred after 1 minute and demonstrated a slow rate of H^+ uptake and K^+ efflux and slight membrane depolarization. In addition the buffering

capacity masked the influx of H^+ and resulted in no change in cytoplasmic pH (Komor *et al.* 1989).

These results clearly suggest that H^+ efflux or H^+ efflux in combination with K^+ or other cation efflux maintains the electroneutrality. A stimulation of H^+ efflux may maintain electroneutrality during electrogenic H^+/L-Glu symport in *Asparagus* mesophyll cells.

3. The biochemical pathway and compartmentation of GABA production

Pathways of L-Glu metabolism were investigated by incubating cells with [U-^{14}C]L-Glu in the light and dark. After a 10 minute incubation, the medium was separated from cells and both medium and aqueous cell fractions were analysed by HPLC. Eighty per cent to 90 % of total radioactivity taken up into the cells was recovered in amino acids or organic acids. This result is consistent with the utilization of L-Glu mostly to produce amino acids and organic acids in cultured tobacco cells (Koiwai and Noguchi 1972), wheat leaves (Walker *et al.* 1984), and pea seedlings (Melcher 1986). Eighty-seven per cent to 92 % of the labeled metabolites was present in the medium fraction, and 8 % to 13 % was present in the cell fraction (Table 19 and 20). GABA was always the most highly labeled metabolite and contained 60 % to 70 % of labeled metabolites in the light or dark. In the cellular fraction, L-Glu was a major labeled compound, indicating that L-Glu entered the cells. Malate and succinate were the major labeled organic acid metabolites in the illuminated and non-illuminated cells and medium. Label in malate and succinate was greater in non-illuminated cells than in illuminated cells. The utilization of L-Glu was followed by determining the time course of conversion of L-Glu into amino acids and organic acids during 10 minute and 60 minute chase with cold L-Glu (Table 26). After a 10 minute incubation with [U-^{14}C]L-Glu, cellular L-Glu represented 56 % of total label within the cell. The

radioactivity in L-Glu progressively decreased over time from 56 % to 42 % at 10 minutes and 33 % at 60 minutes. The radioactivity appeared in succinate and malate. The data are consistent with the utilization of L-Glu by the Krebs cycle. The incubation of *Vicia faba* leaves with labeled L-Glu in the presence of malonate caused an accumulation of succinate (Jordan and Givan 1979). This result also supports the utilization of L-Glu via the Krebs cycle. Therefore it is suggested that *Asparagus* mesophyll cells metabolised L-Glu mainly to GABA. A small fraction of L-Glu is metabolised via the Krebs cycle to produce succinate, malate, and α-KG.

Previous studies on the metabolism of L-Glu also demonstrated that GABA was a major metabolite of L-Glu (Streeter and Thompson 1972b, Koiwai and Noguchi 1972). Cultured tobacco cells were incubated with L-Glu. The labeled metabolites were then analysed without separation of the cells from the bathing medium. Amino acids and organic acids represented 63 % and 26 % of total labeled metabolites, respectively. GABA was the most highly labeled metabolite and represented 32 % of total labeled metabolites. L-Glu inside the cells contained 28 % of total label. Succinate, malate, and α-KG each contained 3 % to 5 % of the total label (Koiwai and Noguchi 1972). In intact excised radish leaves labeled L-Glu was rapidly converted to GABA (Streeter and Thompson 1972b). However the degree of metabolic conversion of L-Glu to GABA seems to vary with the tissue and experimental systems employed. Previous studies on the

metabolism of L-Glu in leaves of *Vicia faba* and wheat indicated that the major metabolite in the light was L-Gln and suggested that illuminated leaves metabolised L-Glu mainly to L-Gln via the GS reaction in the chloroplasts. In the dark or in the presence of MSO, the major metabolite of L-Glu was GABA (Jordan and Givan 1979, Walker *et al.* 1984). When L-Glu was fed to intact illuminated tobacco leaves, L-Glu was metabolised mainly to Pro followed by L-Gln and GABA. GABA represented 6 % of total labeled amino acids (Mizusaki *et al.* 1964). In illuminated and non-illuminated pea seedlings, major labeled metabolites were Hser and L-Gln. Only 1 % of labeled L-Glu was converted to GABA (Melcher 1986). These reports are in contrast with the rapid metabolism of L-Glu to GABA in illuminated and non-illuminated *Asparagus* and radish leaf cells.

In radish leaves a longer incubation with L-Glu showed the decrease of radioactivity in GABA and subsequent increase of label in succinate (Streeter and Thompson 1972b). This suggests the metabolism of L-Glu via the GABA shunt to the Krebs cycle. The GABA shunt indicates that GABA is converted to succinic semialdehyde which is then metabolised to succinate. Thus the GABA shunt facilitates the entry of L-Glu carbon into Krebs cycle acids (Dixon and Fowden 1961, Streeter and Thompson 1972b, Satyanarayan and Nair 1986b). Although the detection of Krebs acids is consistent with the metabolism of L-Glu by the GABA shunt, succinic semialdehyde could not be detected in these studies. The levels of succinic semialdehyde are reported to be

8 nmol/gm fresh wt. in potato (Satyanarayan and Nair 1986b) or 30 nmol/gm fresh wt. in radish leaves (Streeter and Thompson 1972b). The very low succinic semialdehyde levels suggest that free succinic semialdehyde does not accumulate in the cell but is rapidly converted to succinate.

The biochemical conversion of L-Glu to GABA was determined by feeding [1-^{14}C]L-Glu and [^{14}C]L-Glu (Fig. 31B, Table 19, 20, 22, and 23). When [U-^{14}C]L-Glu was fed to cell suspensions, labeled GABA appeared in the medium. However incubation of cells with [1-^{14}C]L-Glu resulted in the production of unlabeled GABA (Fig. 32, Table 22 and 23). This result clearly indicates that GABA is produced by the decarboxylation of carbon-1 of L-Glu. In *Vicia faba* leaves L-Glu was also decarboxylated to form GABA by loss of carbon-1 (Walker *et al.* 1984).

The specific activity of GABA in the medium was very similar to the theoretical specific activity of GABA calculated assuming the loss of 20 % of ^{14}C label from L-Glu. A 10 minute incubation of cells with [U-^{14}C]L-Glu demonstrated that the specific activity of GABA in the medium was 140 times greater than that in cells. A 10 minute incubation of cells with [U-^{14}C]L-Glu in the presence of CCCP resulted in little uptake into the cells. However the GABA appearance in the medium was 50 % of GABA production of the control (Table 18), indicating that the newly synthesized GABA is rapidly released to the medium. The very low specific activity values of cellular GABA is understood

as the dilution of a small labeled GABA pool by a large previously synthesized pool of unlabeled GABA. Thus the specific activity values of GABA suggest that a large internal GABA pool is sequestered from the site of production. Evidence for compartmentation of GABA has also been obtained from *in vivo* and *in vitro* experiments with leaves, petals, and cotyledons of soybean, *Hippeastrum* and *Tulipa* (Wagner 1979, Yamaki 1982, Secor and Schrader 1984). It was suggested that the large internal pool of GABA was sequestered and thereby was not available for export from soybean mesophyll cells (Secor and Schrader 1984). However there is conflicting evidence for the compartmentation of GABA. Direct analysis of amino acid in vacuoles and protoplasts indicates that GABA is primarily extravacuolar in leaves, petals, and cotyledons of *Hippeastrum*, *Tulipa*, and Apple (Wagner 1979, Yamaki *et al* 1982).

Thus on the basis of the pathway of L-Glu metabolism and specific activity of GABA, a scheme involving the metabolic compartmentation of GABA and other metabolites may be integrated into a single model in *Asparagus* cells (Model 3A). L-Glu enters the cells and is mainly converted to GABA in a reaction catalysed by GAD. Further metabolism of GABA involves the GABA shunt. A minor fraction of L-Glu is oxidatively deaminated to α-KG and further metabolised via the Krebs cycle. Most of the newly synthesized GABA is exported passively to the medium. One pool of GABA is associated with the utilization of GABA via the GABA shunt. The other storage pool of GABA is sequestered within a

separate compartment.

(Model 3A) Compartmentation of L-Glutamate metabolism

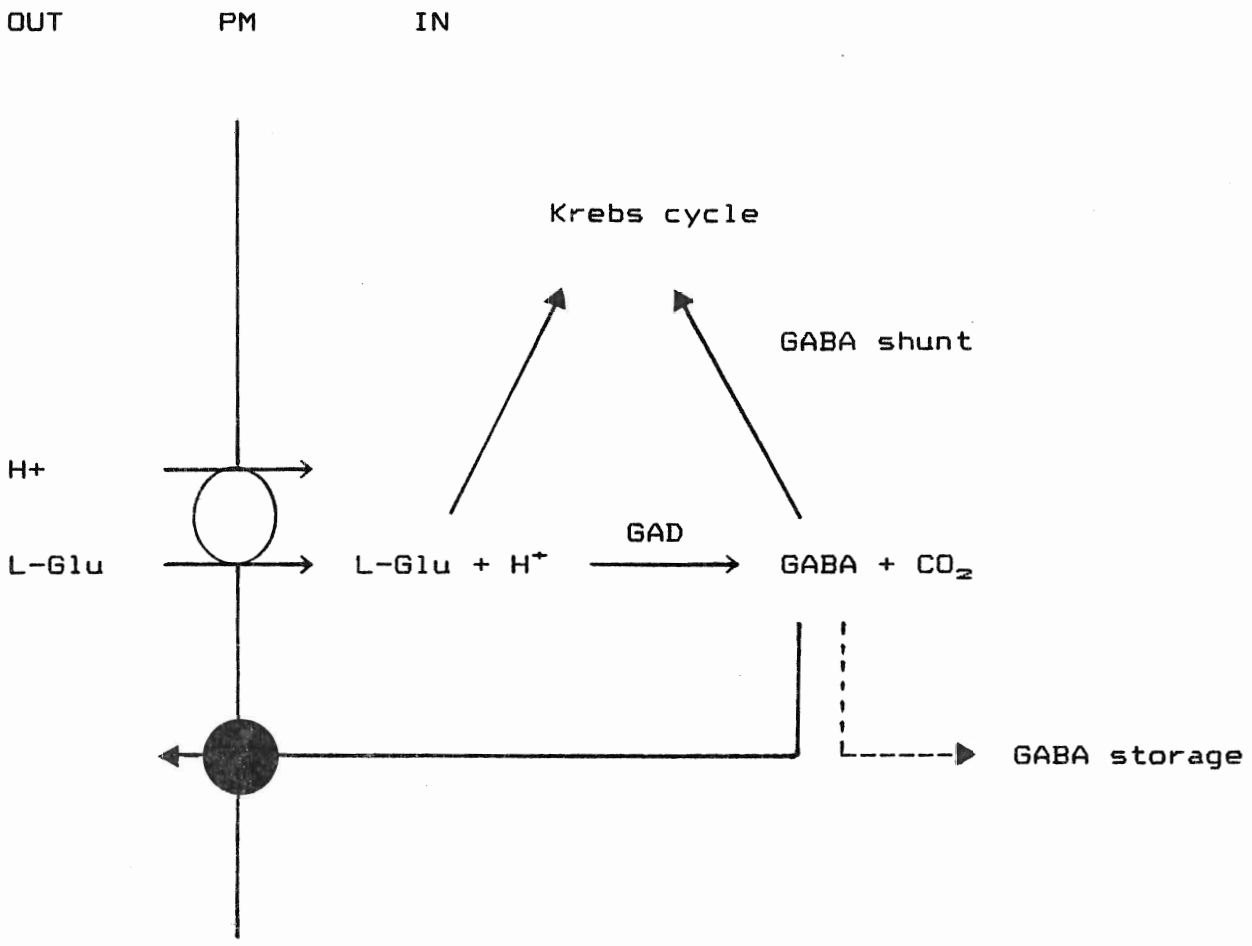

4. Mechanisms of GABA efflux

Since the H^+/L-Glu symport resulted in rapid GABA efflux to the medium, a reversible antiport model for fluxes of L-Glu and GABA was postulated (Model 4A).

(Model 4A) L-Glutamate/GABA antiport

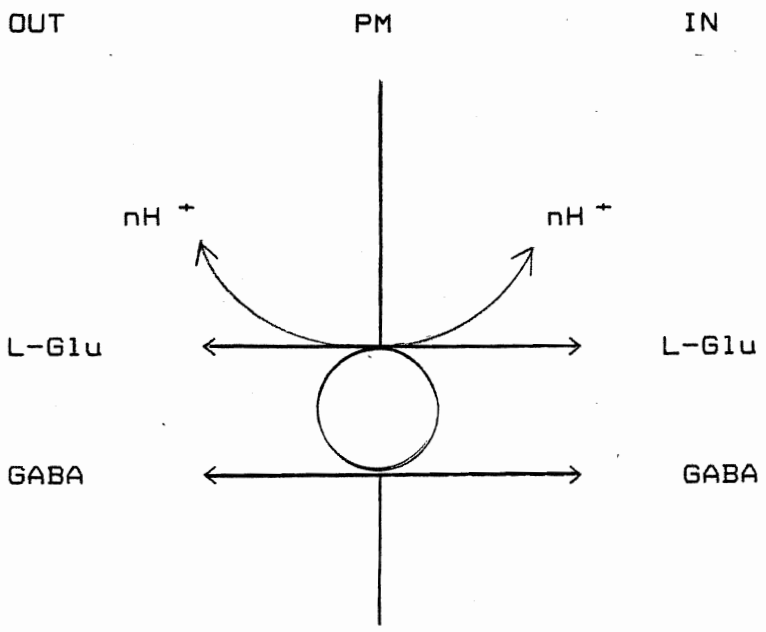

This reversible revolving door model suggests that one carrier mediates the coupled movement of both L-Glu and GABA in opposite directions. According to the model, influx of L-Glu is coupled to the influx of protons and efflux of GABA. Exogenous GABA may inhibit L-Glu dependent medium alkalinization by driving the system in the opposite direction and stimulating L-Glu efflux. Similarly the influx of GABA may be reversed by L-Glu. Thus a

series of experiments were conducted to test for the presence of an L-Glu/GABA antiport process and to demonstrate mechanism of GABA transport.

Preincubation with 5 mM GABA for 10 to 20 minutes inhibited the initial rate of 5 mM L-Glu dependent medium alkalinization by 20 % and 30 % in the dark and light, respectively (Table 13). However preincubation with 5 mM GABA stimulated the initial rate of 1 mM L-Glu dependent medium alkalinization by 50 % and 61 % in the light and dark, respectively (Table 14). Thus the effect of GABA on L-Glu dependent H^+ influx appeared to vary with the L-Glu concentration. The influence of 5 mM GABA on the uptake of labeled 0.5 mM L-Glu also varied. When the experiments were conducted in a buffer system (MES, pH 6.0) with illumination, GABA inhibited the 0.5 mM L-Glu uptake by 19 % (Fig. 17A). However in a non-buffered medium ($CaSO_4$) GABA stimulated 0.5 mM L-Glu uptake by 69 % (Fig. 17B). Again exogenous GABA stimulated or inhibited 0.5 mM L-Glu uptake depending on the medium. It should be noted that in these experiments the rate of GABA efflux was not measured. However stimulation of L-Glu symport by GABA is not consistent with the antiport model. Experiments were also performed to determine the influence of L-Glu on the flux of GABA. GABA fluxes were measured as influx, net efflux, and unidirectional efflux. Incubation with a molar excess of L-Glu did not affect GABA influx in the light and dark (Fig. 21 and 22), net GABA efflux in the light (Fig. 24) or unidirectional

GABA efflux (Fig. 26). The data clearly indicate that L-Glu does not stimulate GABA efflux, and therefore do not support the antiport model.

Potential factors influencing GABA transport were investigated. In the light the uptake of GABA label quickly equilibrated at 4 minutes. In the dark, however, the uptake of GABA was slower and increased linearly until 24 minutes. At 4 minutes the extent of GABA uptake in the light was 3 times that in the dark (Fig. 20). To determine whether membrane potential influenced GABA efflux, a high concentration of K^+ was employed. Twenty mM K^+ did not affect either the net or unidirectional GABA efflux (Fig. 25 and 27). Similarly neither GABA influx nor unidirectional GABA efflux was affected by oligomycin (Fig. 23 and 28), indicating that GABA influx and effflux were not dependent on metabolic energy. Weak acids enter cells in the uncharged form and dissociate to cause acidification of the cytoplasm (Marre *et al.* 1983). GAD has been shown to be stimulated by acidic pH value and the optimal pH was around 5.8 (Streeter and Thompson 1972b, Tsushida and Murai 1987, Bown *et al.* 1988). Thus the acidification of the cytoplasm may stimulate the L-Glu to GABA conversion and subsequently increase the release of GABA to the medium. However butyric acid had no effect on the influx or efflux of GABA (Fig. 23 and 28). CCCP which dissipates the H^+ electrochemical gradient by increasing membrane permeability for H^+ inhibited the influx of GABA in the light (58 %) and dark (29 %) (Fig. 21 and 22) and stimulated

the net and unidirectional efflux of GABA in the light also (Fig. 24 and 26). HPLC analysis of the CCCP effect on [U-^{14}C]L-Glu metabolism demonstrated that GABA was a major labeled metabolite and appeared in the medium even though there was little label in the cell (Table 27). Thus data indicate that CCCP stimulates GABA efflux. Recently experiments were performed with isolated soybean leaf cells to determine the mechanism involved in amino acid efflux processes (Secor and Schrader 1984). One mM *p*-chloromercuriphenyl sulfonic acid (PCMS) stimulated the specific net efflux of GABA. Because PCMS inactivates proteins containing sulfhydryl group, the authors suggested that GABA is transported by a sulfhydryl-dependent transporter which is specific for GABA.

In isolated *Asparagus* mesophyll cells GABA efflux seems to be specific. Ala and GABA were the major pools in these cells. The internal pool of Ala was 2.2 and 3.3 times larger than that of GABA in the light and dark, respectively. After a 10 minute incubation, 1 % to 3 % of the total amount of Ala and 6 % to 8 % of the total amount of GABA appeared in the external medium. However after 10 minute incubation with 1 mM L-Glu 2 % to 3 % of the total amount of Ala was present in the medium. Whereas 60 % to 70 % of the total GABA appeared in the medium (Table 3, 4, 5, and 6). Similar trends were observed after a 60 minute incubation with L-Glu. Calculation of intracellular concentrations of Ala and GABA indicated that the concentration gradients for Ala and GABA were outwardly directed (Table 7, 8, 9, and 10). However only GABA was exported, indicating that the

efflux of GABA is a specific and controlled process. Amino acid composition in intact tissue and tissue debris demonstrated that GABA was the most and second most prevalent amino acid (Table 11). However GABA was less abundant in isolated mesophyll cells (Table 11). This may result from GABA also export during cell isolation.

Results with isolated cells indicate that (i) there is no evidence for a L-Glu/GABA antiport, (ii) the concentration gradient for GABA favors efflux, (iii) neither membrane potential nor metabolic energy affects the flux of GABA, (iv) CCCP stimulates the GABA efflux, and (v) GABA export is specific. Thus the mechanism for efflux of GABA may be a passive process mediated by a uniport. However it is not clear whether GABA efflux occurs from cells in intact tissue. GABA efflux could be a response to cell isolation.

5. Regulation of internal pH

A H^+ symport system for substrate uptake is supported by alkalinization of the medium surrounding the cells on substrate addition. It is, therefore, generally assumed that a H^+ symport process will cause cytoplasmic acidification. Assuming that active cytoplasmic pH regulation mechanisms are absent, a theoretical pH change in response to a symport can be calculated from three values (i) protoplasmic buffering (ii) cell volume, and (iii) rate of H^+ influx. In isolated *Asparagus* mesophyll cells : (i) The protoplasmic buffering capacity is 15 µmol Eq. H^+/ml ptotoplasm/pH unit (Table 17). (ii) On addition of 5 mM L-Glu, the rate of H^+ influx is 3.35 and 2.97 nmol H^+/10^6 cells/minute in the light and dark, respectively (Table 13). (iii) The cell volume is 4.68 µl/10^6 cells (Table 2). From these values, the rate of cytoplasmic acidification can be calculated to be 2.87 and 2.53 pH unit per 1 hour in the light and dark, respectively. If the cytosolic volume is 20 % of cell volume (Espie and Colman 1981), and H^+ remains in the cytosol then the cytosolic pH change will be approximately 14 pH units per hour.

The DMO technique for measurement of cytoplasmic pH has been estabilished as a reliable method (Spanswick and Miller 1977, Espie and Colman 1981, Reid and Smith 1988). Using the [^{14}C]DMO distribution between the medium and cells at an external pH of 5.5 (McCutcheon *et al* 1988) and cell volume data (Table 2), the cytoplasmic pH in *Asparagus* mesophyll cells was calculated to

be 6.69 to 6.70. This value is within the range of the intracellular pH values (7.02 at external pH 5.57 in the light, 6.18 at external pH 5.46 in the dark) obtained by Espie and Colman (1981) in *Asparagus* mesophyll cells. During a 10 minute and a 20 minute incubation with 5 mM L-Glu, McCutcheon's data demonstrated that the DMO level decreased inside the cells. Calculation of the resulting cytoplasmic pH resulted in values of 6.41 and 6.38 with a 10 minute and a 20 minute incubation, respectively. Thus calculations suggest that the cytoplasmic pH decrease was 0.28 to 0.32 pH unit on addition of 5 mM L-Glu (Appendix). This actual cytoplasmic pH change is far smaller than the theoretical pH change when active pH regulatory mechanisms are assumed to be absent.

In recent years, efforts have been made to measure cytoplasmic pH in a wide variety of plant systems, employing intracellular pH-sensitive microelectrodes, distribution of weak acids and bases and ^{31}PNMR spectroscopy. The use of 3 independent measuring techniques gave cytoplasmic pH values in close agreement and suggested that the cytoplasmic pH is slightly alkaline and maintained within remarkably narrow limit (pH microelectrode : Spanswick and Miller 1977, Bertl and Felle 1985, Reid and Smith 1985, Johannes and Felle 1987 ; DMO technique : Walker and Smith 1975, Smith and Walker 1976, Spanswick and Miller 1977, Raven and Smith 1978, Espie and Colman 1981 ; ^{31}PNMR : Reid *et al.* 1985, Torimitsu *et al.* 1984, Wray *et al.* 1985).

When the external pH was changed from pH 3 to 10, the

cytoplasmic pH was relatively insensitive to external pH change and was tightly regulated at a slightly alkaline pH (Spanswick and Miller 1977, Torimitsu *et al.* 1984, Reid *et al.* 1985, Wray *et al.* 1985, Bertl and Felle 1987, Johannes and Felle 1987, Reid and Smith 1988). In addition to changes in external pH, cytoplasmic pH values were measured after treating with acids-loads such as butyric acid and propionic acid (Guern *et al* 1986, Sanders and Slayman 1982). It is presumed that weak acids acidify the cytosol by penetrating the plasma membrane as the free acid before dissociating. The majority of results indicate that the initial drop of cytoplasmic pH in the first minutes of exposure to weak acids is followed by recovery to reach a plateau phase regardless of tissue types or acids applied (Guern *et al.* 1986, Sanders and Slayman 1982). In addition when the cytoplasmic pH was continuously recorded by pH-sensitive microelectrodes during glucose (Glc), Arg, Ala, and L-Glu transport into *Riccia* rhizoid cells, a cytoplasmic alkalinization (0.1 to 0.3 units) occurred and then reached a new steady state (Johannes and Felle 1987). Because H^+ symport process are expected to acidify the cytoplasm, these data suggest the presence of pH regulating mechanisms. Thus the pattern of cytoplasmic pH changes clearly suggest that regardless of external pH changes, exposure to weak acids or H^+ symport, the cytoplasmic pH is regulated at a slightly alkaline pH.

Generally physiological pH-perturbing processes comprise biochemical and biophysical processes. Biochemical pH-

perturbation results from biosynthetic metabolism accompanied by consumption or production of protons. Biophysical pH-perturbing processes involve fluxes of protons across the biological membranes. This biophysical proton flux is often associated with the activation or deactivation of H^+ pumping ATPase, H^+ symport with substrates and passive H^+ leakage. It is expected that the balance between biochemical and biophysical events regulates the cytoplasmic pH over short or long time periods. Short-term pH regulation indicates rapid mechanisms regulating proton concentration after acute pH changes and includes (i) physiocochemical buffering, (ii) proton export to the outside or cell organelles and (iii) metabolism consuming or producing protons (Felle 1988).

(i) Physicochemical buffering : The protoplasmic buffering capacity of plant cells is recorded as 15 µmol Eq. H^+/ml protoplasm/pH unit in *Asparagus* (Table 17), 20 to 25 µmol Eq H^+ /ml protoplasm/pH unit in *Acer* (Mathieu et al. 1986) and *Chlorella* (Raven and Smith 1978), and 30 to 35 µmol Eq H^+ /ml protoplasm/pH unit in *Neurospora* (Sanders and Slayman 1982) at neutral pH values. Considering the large H^+ uptake during the H^+/L-Glu symport process (43 and 38 µmol H^+/ml protoplasm/hour in the light and dark, respectively), the buffering capacity of 15 umol Eq. H^+/ml cytoplasm/pH unit is not sufficient to maintain cytoplasmic pH. Similarly in *Acer*, the extent of the contribution of protoplasmic buffering capacity to the regulation of cytoplasmic pH during the recovery period from a propionic

acid load is less than 20 % (Guern *et al.* 1986). Therefore the buffering capacity of the cells is insufficient to maintain a constant cytoplasmic pH.

(ii) Biophysical pH-stat : The presence of an ATP driven H^+ pump ATPase has been established in a wide variety of plant systems. Elimination of H^+ efflux with oligomycin allowed for the determination of the influence of L-Glu on the rate of H^+ efflux. On adoition of 2 mM L-Glu, the rate of H^+ efflux was stimulated by 57 % and 49 % in the light and dark, respectively. Acetic acid and butyric acid stimulated the rate of H^+ efflux by 100 %. Both these results indicate that cytoplasmic acidification of *Asparagus* cells can be regulated by a stimulation of H^+ efflux (Bown unpublished data). When Glc, Arg, Ala, and Glu were tranported into *Riccia* rhizoid cells by electrogenic H^+ symport, the H^+ pump was stimulated by depolarization. Cytoplasmic alkalinization resulted. It is, therefore, suggested that the plasma membrane H^+ pumping ATPase alone can be responsible for the regulation of cytoplasmic pH (Johannes and Felle 1987).

Other data however indicate that the H^+ pump alone may have a little effect on the regulation of cytoplasmic pH. The specific inhibition of the H^+ pump by orthovanadate had little effect on cytoplasmic pH in *Acer* and *Neurospora* (Sanders and Slayman 1982, Mathieu *et al.* 1986)). Calculations of the quantitative importance of the H^+ pump at the plasma membrane showed that 60 % of the protons taken up into the *Acer* cells was

removed by the H^+ pump during the recovery period from a propionic acid-load (Mathieu et al. 1986). In *Chlorella* it is also suggested that the extent of acidity compensation by the pump alone may have a little effect on the regulation of cytoplasmic pH (Komor et al. 1989). Thus H^+ efflux alone at the plasma membrane is not sufficient to maintain cytoplasmic pH.

(iii) Biochemical pH-stat : The biochemical pH-stat proposed by Davies suggests that the cytoplasmic pH in plant cells is regulate by the balance between production and consumption of acidic carboxyl groups which in turn is regulated by enzymes forming and removing carboxyl groups. Thus two pH-dependent enzymes forming and removing carboxyl group from a shared metabolite act as a pH-stat (Davies 1986).

GABA production catalyzed by GAD involves the decarboxylation of L-Glu and the consumption of H^+. GAD has a cytosolic location, an optimal pH around 5.8 and is PLP dependent (Streeter and Thompson 1972b, Satyanarayan and Nair 1985, Tsushida and Murai 1987). In *Asparagus*, the optimal pH of GAD is 5.8, and activity increased dramatically as the pH declined from 7 to 6 (Bown *et al.* 1989). GABA and succinate, metaboltes of the GABA shunt pathway did not inhibit *in vitro* GAD activity (Bown unpublished data), indicating that these products do not regulate GAD. Two mM aminoxyacetate (AOA) however inhibited *in vitro* GAD acitvity in the presence and absence of PLP. In addition, the same concentration of AOA completely inhibited simultaneously measured L-Glu dependent medium alkalinization, L-Glu uptake, and

GABA production in the medium (Bown unpublished data). Inhibition by AOA of *in vitro* and *in vivo* GAD activity and L-Glu dependent medium alkalinization indicates that L-Glu symport activity is dependent on L-Glu decarboxylation. The H^+ influx during H^+/L-Glu symport decreases the cytoplasmic pH. It is suggested that as a consequence, the activity of GAD increases producing GABA. Thus cytoplasmic pH returns to the balance point. The results indicate that GABA production is stimulated by cellular acidosis and functions as a biochemical pH-stat mechanism. Recent reports also suggest that L-Glu decarboxylation to GABA functions as a cytoplasmic pH regulating process during cellular acidosis resulting from anoxia (Reid *et al.* 1985, Tsushida and Murai 1987, Reggiani *et al.* 1988, Menegus *et al.* 1989).

The results indicate that in *Asparagus* mesophyll cells acidification of cytoplasmic pH resulting from the H^+/L-Glu symport is resisted by protoplasmic buffering, stimulation of H^+ efflux, and a decarboxylation process. Calculations indicate that the protoplasmic buffering capacity alone is insufficient to regulate protoplasmic pH. Protons resulting from the H^+/L-Glu symport are probably removed by a stimulated H^+-ATPase, indicating operation of biophysical pH-stat. In addition the pH-dependent GAD activity suggests that L-Glu decarboxylation process is also important in resisting acidosis. Concurrent inhibition of L-Glu uptake, medium alkalinization and GABA producton by AOA demonstrated that L-Glu decarboxylation is

necessary for long term L-Glu dependent medium alkalinzation. It appears that L-Glu decarboxylation functions in pH regulation.

A model is proposed on the basis of all the results obtained with the *Asparagus* system (Model 5A). ATP driven proton pumping at the plasma membrane establishes an inwardly directed proton electrochemical gradient across the membrane. L-Glu enters the cell with 2 H^+. One H^+ is pumped out by the plasma membrane H^+-ATPase and the other H^+ is consumed during GABA production inside the cells. Sixty per cent to 70 % of L-Glu entering the cells is metabolised to produce GABA. Most of the newly synthesized GABA is immediately released to the medium.

The model indicates that the driving forces for electrogenic H^+/L-Glu symport are maintained. The driving forces are the electrical gradient, the proton gradient, and the L-Glu gradient. The electrical gradient is maintained by ATP driven electrogenic H^+ efflux. The proton gradient is maintained by H^+ efflux and GAD activity. The L-Glu gradient is maintained by L-Glu decarboxylation. Thus the long period of L-Glu dependent medium alkalinization can be explained by the maintenance of these symport driving forces.

(Model 5A) L-Glutamate symport, GABA efflux, and the regulation of intracellular pH

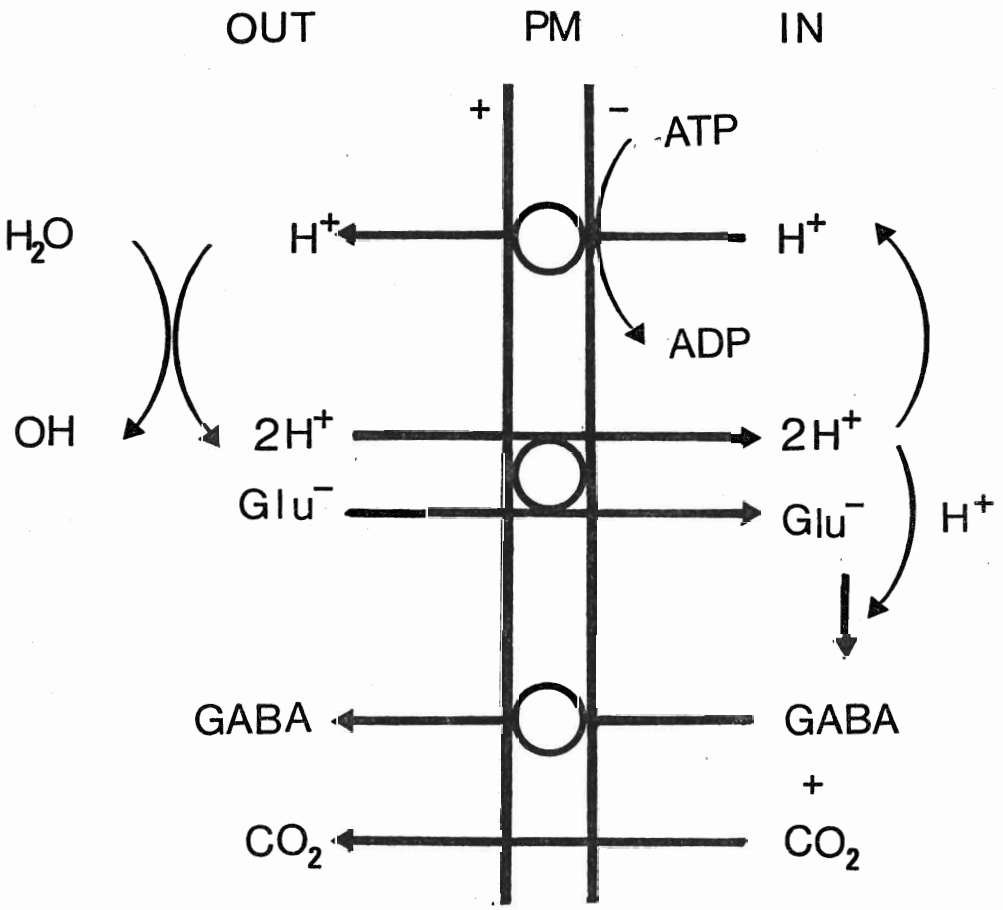

6. Possible roles of L-Glu to GABA conversion and GABA accumulation in intact cladophylls

Many authors have suggested that GABA is accumulated in response to mechanical stress and injury (Wallace *et al.* 1984, Melcher 1986). However the data presented indicate that in intact *Asparagus* tissue a H^+/L-Glu symport protein is located at the plasma membrane (McCutcheon and Bown 1987), GAD is present (Bown *et al.* 1989), and GABA levels are high (Table 11). Thus GABA production is considered to be a physiological process occurring in intact *Asparagus* cladophyll, independent of stress.

On a % molar basis L-Glu was a minor amino compound in the xylem sap (Table 12). However L-Glu and GABA were the second and third most abundant amino acids in mesophyll cells (Table 11), indicating that L-Glu may be delivered to mesophyll cells without being retained in vascular tissues. Similar patterns of L-Glu distribution to maintain mesophyll cells were found in *Lupinus albus* and *Populus deltoides* (McNeil *et al.* 1979, Vogelmann *et al.* 1985).

Slender cytoplasmic bridges called plasmodesmata interconnect neighboring cells (Fig. 9C, 9D, 10 and 11). The plasmodesmata provides a symplastic path for continuous transport of substances via the cytoplasm. Plasmodesmata were abundant between border mesophyll cells and vascular parenchyma but rare between mesophyll cells (Fig. 9C, 9D, and 10). The lowest plasmodesmatal frequency was also found between mesophyll cells in *Amaranthus retroflexus* (Fisher and Evert 1982), *Beta vulgaris*

(Evert and Mierzwa 1986), *Populus deltoides* (Russin and Evert 1986), and *Themeda triandra* (Botha and Evert 1988). Thus the symplastic route appears to be a minor pathway in the transfer of solute between the palisade mesophyll cells and the vascular bundle. Ultrastructural studies of *Asparagus* mesophyll cells showed that plasma membranes in these cells were highly invaginated and thus have increased surface area (Fig. 11). In addition an L-Glu symport system is located in the plasma membrane. Thus L-Glu supplied from the xylem may be taken up into the mesophyll cells via an apoplastic route which terminate at the symport.

Presumably L-Glu delivered via the xylem to mesophyll cells is converted to GABA in a reaction catalysed by GAD. The continuous supply of H^+/L-Glu by this process may result in GABA accumulation. GABA accumulation in turn may contribute to the regulation of cytoplasmic pH and the adjustment of the osmoticum. The roles of GABA in regulating cytoplasmic pH or the osmotic potential have been previously suggested (Menegus *et al.* 1984, Reggiani *et al.* 1988, Menegus *et al.* 1989).

Generally mature leaves are supplied with N via the xylem and export N in the phloem to young leaves and fruit. The balance for net import of GABA in xylem and export in phloem indicated that it was always delivered to leaves in excess of the amounts consumed in growth and/or phloem export in *Lupinus albus* (Atkins *et al.* 1983). GABA was usually a minor component in xylem sap (Sharkey and Pate 1974, 1975, Pate *et al.* 1981, 1984,

Shelp 1987) but absent (Fukumorita and Chino 1982) or very little in phloem (Hayashi and Chino 1986), indicating that GABA is not translocated into the stem phloem from leaves. Unlike other neutral amino acids (Asn, Gln, Val, Thr, Ser) GABA carbon was found in other amino compounds in the phloem, indicating that GABA is metabolised in mesophyll cells prior to translocation (Pate 1986). Thus GABA may be stored temporarily in mesophyll cells as a C and N source for later utilization and eventually passed to the phloem for transport to other parts of the plant.

CONCLUSIONS

The origin of L-Glu dependent medium alkalinization and the production and transport of GABA were investigated in mechanically isolated *Asparagus sprengeri* mesophyll cells.

1. L-Glu entered the cells prior to decarboxylation. There was no evidence for a H^+/GABA symport or L-Glu/GABA antiport. The evidence indicate that the origin of L-Glu dependent medium alkalinization is a H^+/L-Glu symport process.
2. The biochemical pathway of GABA production occurs through loss of carbon-1 of L-Glu.
3. The data indicate that the mechanism of GABA efflux is a specific and passive uniport.
3. Sixty to 70 % of L-Glu entering the cells leaves as GABA. Newly synthesized GABA is exported to the medium without mixing with a storage pool of GABA.
4. L-Glu was a minor amino acid in the xylem sap, but a major amino acid in mesophyll cells. It is suggested that L-Glu is supplied via the xylem to mesophyll cells.
5. GABA was always a major amino acid in xylem sap, intact cladophylls, and isolated mesophyll cells.

APPENDIX

1. Calculation of cytoplasmic pH measured by [^{14}C]DMO distribution

- Two million cells were suspended in 1 ml of 20 mM KPi buffered (pH 5.5) at 30°C. Thirty uM DMO was added and equilibrated for 20 minutes. At 20 minutes 5 mM L-Glu, L-Asp, L-MSO, and butyric acid were added and the uptake of measured for a further 20 minutes.
- The specific activity of [^{14}C]DMO was 1.1935 x 10^{5} or 1.2 x 10^{5} dpm/nmol and the pKa of DMO is 6.3.
- [^{14}C]DMO inside the cells after a 10 and 20 minute incubation periods

	10 min incubation		20 min incubation	
	[^{14}C]DMO DPM	[DMO] uM	[^{14}C]DMO DPM	[DMO] uM
Control	102,000	91	100,000	89
L-Glu	64,000	57	66,000	59
L-Asp	88,000	78	90,000	80
L-MSO	68,000	61	76,000	68
Butyric acid	44,000	39	46,000	41

- Calculation of cytosolic pH value

Control (i) : $pHo = pKa + \log ([DMO^-]o/[DMOH]o)$

$5.5 = 6.3 + \log (16/100)$

$[DMO^-]o = 30\ uM \times 16/100 = 4.8\ uM$

$[DMOH]o = 30\ uM \times 84/100 = 25.2\ uM$

$[DMO^-]i = 89 - 25.2 = 63.8\ uM$

$pHi = 6.3 + \log (63.8/25.2) = 6.7$

(ii) : $Ci/Co = 1 + 10^{(pHi-pKa)} / 1 + 10^{(pHo-pKa)}$

$89\ uM/3\ uM = 1 + 10^{(pHi-6.3)} / 1 + 10^{(5.5-6.3)}$

$pHi = 6.69$

	10 min		20 min	
	(i)	(ii)	(i)	(ii)
Control	6.70	6.69	6.72	6.70
L-Glu	6.43	6.41	6.40	6.38
L-Asp	6.64	6.62	6.62	6.61
L-MSO	6.53	6.51	6.45	6.43
Butyric acid	6.09	6.07	5.89	6.00

REFERENCES

Atkins, C.A. and Pate, J.S. (1983) Nitrogen uptake, transport, and utilization *in* Nitrogen Fixation Vol. 3. Legumes, pp.249-298, Broughton, W.J. Ed. pp. 249-298 Clarendon Press, Oxford

Atkins, C.A., Pate, J.S., and McNeil, D.L. (1980) Phloem loading in fruiting shoots of a legume J. Exp. Bot. 31, 1509-1520

Atkins, C.A., Pate, J.S., Peoples, M.B., and Joy, K.W. (1983) Amino acid transport and metabolism in relation to the nitrogen economy of a legume leaf Plant Physiol. 71, 841 -848

Baldy, P. (1976) Metabolism du Γ-aminobutyrate chez *Agaricus bisporus* Planta 130,275-281

Bertl, A. and Felle, H. (1985) Cytoplasmic pH of root hair cells of *Sinapis alba* recorded by a pH-sensitive microelectrode J. Exp. Bot. 36, 1142-1149

Bollard, E. (1960) Transport in the xylem Ann. Rev. Plant Physiol. 11, 141-166

Boller, T. and Wiemken, A, (1986) Dynamics of vacuolar compartmentation Ann. Rev. Plant Physiol. 37, 137-164

Borstlap, A.C., Meenks, J.L.D., Eck, W.F., and Bicker, J.T.E. (1986) Kinetics and specificity of amino acid uptake by the duckweed *Spirodela polyrhiza* (L.) Schleiden J. Exp. Bot. 37,1020-1035

Botha, C.E.J. and Evert, R.F. (1988) Plasmodesmatal distribution and frequency in vascular bundles and contiguous tissues of the leaf of *Themeda triandra* Planta 173, 433-441

Bown, A.W. (1982) An investigation into the roles of photosynthesis and respiration in H^+ efflux from aerated suspensions of *Asparagus* mesophyll cells Plant Physiol. 70, 803-810

Bown, A.W. and Nicholls, F. (1985) An investigation into the role of photosynthesis on regulating ATP levels and rates of H^+ efflux in isolated mesophyll cells Plant Physiol. 79, 928-934

Bown, A.W., Chung, I., Snedden, W., and Shelp, B. (1989) Specific glutamate cotransport into mesophyll cells and efflux of the major metabolite 4-aminobutyric acid In press

Briskin, D.P. and Poole R.J. (1983) Characterization of a K^+-stimulated adenosine triphosphatase associated with the plasma membrane of red beet Plant Physiol. 71, 350-355

Briskin, D.P. and Poole R.J. (1984) Characterization of the solubilized plasma membrane ATPase of red beet Plant Physiol. 76, 26-30

Cameron, D.S. and Cossins E.A. (1967) Studies of intermediary metabolism in germinating pea cotyledons Biochem. J. 105, 323-331

Chapman, J.S. and Meeks, J.C. (1983) Glutamine and glutamate transport J. Bacteriol. 156, 122-129

Cheng, Y., Linko, P., and Milner, M. (1960) On the nature of glutamic acid decarboxylase in wheat embryos Plant Physiol. 35, 68-71

Cheung, Y.N.S. and Nobel, P.S. (1973) Amino acid uptake by pea leaf fragments Plant Physiol. 52,633-637

Chou, K. and Splittstoesser, W.E. (1972) Changes in amino acid content and the metabolism of Γ-aminobutyrate in *Cucurbita moschata* seedling Physiol. Plant. 26, 110-114

Cockburn, M., Earnshaw, P., and Eddy, A.A. (1975) The stoichiometry of the absorption of protons with phosphate and L-glutamate by yeasts of the genus *Saccharomyces* Biochem. J. 146, 705-712

Collins, D.M. and Wilson, A.T. (1975) Embryo and endosperm metabolism of barley seeds during early germination J. Exp. Bot. 26, 737-740

Cossins, E.A. (1964) Formation and metabolism of lactic acid during germination of pea seedlings Nature 203, 989-990

Cooper, D.R., Hill-Cottingham, D.G., and Shorthill, M.J. (1972) Gradients in the nitrogenous constituents of the sap extracted from apple shoots of different ages J. Exp. Bot. 23, 247-254

Cooper, P. and Selman, I.W. (1974) An analysis of the effects of tobacco mossaic virus on growth and the changes in the free amino compounds in young tomato plants Ann. Bot. 38, 625-638

Davies, D.D. (1986) The fine control of cytoplasmic pH Physiol. Plant. 67,702-706

Desmaison, A.M. and Tixier, M. (1986) Amino acid content in germinating seeds and seedlings from *Castanea sativa* L. Plant Physiol. 81, 692-695

Diener, T.O. (1960) Free amino acids and amides in healthy and virus-infected cherry and peach leaves Phytopathol. 50,

141-145

Dickson, R.E. (1979) Xylem translocation of amino acids from roots to shoots in cottenwood plants Can. J. For. Res. 9, 374-378

Dixon, R.O.D. and Fowden, L. (1961) Γ-aminobutyric acid metabolism Ann. Bot. 25, 513-530

Draper, S.R. (1972) Amino acid associated with low temperature treatment of *Lolium perenne* Phytochem. 11, 639-641

Effer, W.R. and Ranson, S.L. (1967) Respiratory metabolism in buckwheat seedlings Plant Physiol. 42,1042-1052

Espie. G.S. and Colman, B. (1981) The intracellular pH of isolated photosynthetically active *Asparagus* mesophyll cells Planta 153, 210-216

Evert, R.F., Eschrich, W., Eichhorn, S.E., and Limbach, S.T. (1973) Observations on penetration of barley leaves by the aphid *Rhopalosiphum maidis* (Fitch) Protoplsma 77, 95-110

Evert, R.F. and Mirerzwa, R.J. (1986) Pathway(s) of assimilate movement from mesophyll cells to sieve tubes in the *Beta vulgaris* leaf *in* Plant Biology Vol. 1. Phloem Transport Cronshaw, J., Lucas, W.J., and Giaquinta, R.T. Eds. pp. 419 -432, Alan R. Liss, Inc

Felle, H. (1988) Short-term pH regulation in plants Physiol. Plant. 74, 583-591

Fellow, R.J., Egli, D.B., and leggett, J.E. (1978) A pod leakage technique for phloem translocation studies in soybean (*Glycine max* [L.] Merr) Plant Physiol. 62, 812-814

Fife, J.M., Price, F.E., and Fife, D.C. (1962) Some properties of phloem exudate collected from root of sugar beet Plant Physiol. 37, 791-792

Fisher, D.G. and Evert, R.F. (1982) Studies on the leaf of *Amaranthus retroflexus* (Amaranthaceae) : Morphology and anatomy Am. J. Bot. 69, 1133-1147

Fisher, J.D. and Hodges, T.K. (1969) Monovalent ion stimulated adenosine triphosphatase from oat roots Plant Physiol. 44, 385-395

Fisher, J.D., Hansen, D., and Hodges T.K. (1970) Correlation between ion fluxes and ion - stimulated adenosine triphosphatase activity of plant roots Plant Physiol 46,

812-814

Flinn, A.M. and Pate, J.S. (1970) A quantitative study of carbon transfer from pod and subtending leaf to the ripening seeds of the field pea (*Pisum arvense* L.) J. Exp. Bot. 21, 71-82

Freny, J.R. and Gibson, A.H. (1975) Accumulation of 4 -aminobutyrate in *Trifolium subterraneum* root nodules : effect of *Rhizobium trifolii* strain on aminotransferase activity Aust. J. Plant Physiol. 2, 663-668

Fukumorita, T. and Chino, M. (1982) Sugar, amino acid, and inorganic contents in rice phloem sap Plant and Cell Physiol. 23, 273-283

Gaff, D.F. and Okong'O-Ogola, O. (1971) The use of non-permeating pigment for testing the survival of cells J. Exp. Bot. 22,756-758

Glauert, A.M. (1981) Fixation, dehydration and embedding of biological specimens *in* Practical methods in electron microscopy Vol. 3. Glauert, A.M. Ed. North-Holland

Guern, J., Mathieu, Y., Pean, M., Pasquier, C., Beloeil, J.C., and Lallemand, J.Y. (1986) Cytoplasmic pH regulation in *Acer pseudoplatanus* cells Plant Physiol. 82, 840-845

Hall, S.M. and Baker, D.A. (1972) The chemical composition of *Riccinus* phloem exudate Planta 106, 131-140

Hall, S.M., Baker, D.A., and Milburn, J.A. (1971) Phloem transport of ^{14}C labeled assimilates in *Riccinus* Planta 100, 200-207

Hanks, R.W. and Feldman, A.W. (1966) Quantitative changes in tree and protein amino acids in leaves of healthy, *Radopholus similis*-infected, and recovered grapefruit seedlings Phytopathol. 56,261-264

Hartmann, T. and Ehmke, A. (1980) Role of mitochondrial glutamate dehydrogenase in the reassimilation of ammonia produced by glycine-serine transformation Planta 149, 207 -208

Harvarstein, L.S. and Nissen, P. (1981) Stimulation of plasmalemma adenosine triphosphatase from oat roots by inorganic and organic cations : concentration - dependence, selectivity, and sites Plant Physiol. 68, 597-604

Hayashi, H. and Chino, M. (1986) Collection of pure phloem sap form wheat and its chemical composition Plant and Cell Physiol. 27, 1387-1393

Higinbotham, N., Graves, J.S., and Davis R.F. (1970) Evidence for ion transport pump in cells of higher plants J. Membrane Biol. 3, 210-222

Hockings, P.J. (1980) The composition of phloem exudate and xylem sap from tree tobacco (*Nicotiana glauca* Grah.) Ann. Bot. 45, 633-643

Hodges, T.K., Leonard, R.T., Bracker, C.E., and Keenan, T.W. (1972) Purification of an ion-stimulated adenosine triphoshatase from plant roots : association with plasma membrane Proc. Natl. Acad. Sci. USA 69, 3307-3311

Hutchings, V.M. (1978) Sucrose and proton cotransport in *Riccinus* cotyledons Planta 138, 229-235

Inatomi, K. and Slaughter, J.C. (1975) Glutamate decarboxylase from barley embryos and roots : general properties and the occurrence of these enzymic forms Biochem. J. 147, 479-484

Johannes, E. and Felle, H. (1987) Implication of cytoplasmic pH, protonmotive force, and amino acid transport across the plasmalemma of *Riccia fluitans* Planta 172, 53-59

Jordan, B.R. and Givan, C.V. (1979) Effects of light and inhibitors on glutamate metabolism in leaf discs of *Vicia faba* L. Plant Physiol. 64, 1043-1047

Keifer, D.W. and Spanswick, R.M. (1979) Correlation of adenosine triphosphate levels in *Chara corallina* : the activity of the electrogenic pump Plant Physiol. 76, 26-30

Khavkin, E.E. (1964) Age variations of the free amino acids and accumulation of Γ-ABA in the leaves of leguminous plants Fiziologiya Rast. 11, 862-866

King, J. (1969) The isolation, properties, and physiological role of lactic dehydrogenase from soybean cotyledons Can. J. Bot. 48, 533-540

King, R.W. and Zeevaart, J.A.D. (1974) Enhancement of phloem exudation from cut petioles by chelating agents Plant Physiol. 53, 96-103

Kinraide, T.B. and Etherton, B. (1980) Electical evidence for different mechanisms of uptake for basic, neutral, and acidic amino acids in oat coleoptiles Plant Physiol. 65, 1085-1089

Kitasato, H. (1968) The influence of H^+ on the membrane potential and ion fluxes of *Nitella* J. Gen. Physiol. 52, 60-86

Koiwai, A. and Noguchi, M. (1972) Metabolism of glutamate and Γ-aminobutyrate in cultured tobacco cells Plant and cell physiol. 13,395-399

Komor, E., Cho, B.H., Schricker, S., and Schobert, C. (1989) Charge and acidity compensation during proton-sugar symport in Chlorella : the H^+-ATPase does not fully compensate for the sugar-coupled proton influx Planta 177, 9-17

Lahdesmaki, P. (1968) The amount of Γ-amino butyric acid and the activity of glutamic acid decarboxylase in aging leaves Physiol. Plant 21, 1322-1327

Lane, T.R. and Stiller, M. (1970) Glutamic acid decarboxylase in *Chlorella* Plant Physiol. 45, 558-562

Layzell, D.B. and LaRue, T.A. (1982) Modeling C and N transport to developing soybean fruits Plant Physiol 70, 1209-1298

Leblova, S., Zima, J., and Perglerova, E. (1976) Conversion of pyruvate under natural and artificial anaerobiosis in maize Aust. J. Plant Physiol. 3,755-761

Marre. E. (1979) Fusicoccin : a tool in plant physiology Ann. Rev. Plant Physiol. 30, 273-288

Marre, M.T., Romani, G., and Marre, E. (1983) Transmembrane hyperpolarization and increase of K^+ uptake in maize roots treated with permeant weak acids Plant Cell and Envir. 6, 617-623

Mathieu, Y., Guern, J., Pean, M., Pasquier, C., Beloeil, J.C., and Lallemand, J.Y. (1986) Cytoplasmic pH regulation in *Acer pseudoplatanus* cells Plant Physiol. 82, 846-852

Matile, P. (1978) Biochemistry and function of vacuoles Ann. Rev. Plant, Physiol. 29, 193-213

Nauen, W. and Hartmann, T. (1980) Glutamate dehydrogenase from *Pisum sativum* L. Planta 148, 7-16

McClure, P.R. and Israel, D.W. (1979) Transport of N in the xylem of soybean plants Plant Physiol. 64, 411-416

McCutcheon S.L. and Bown A.W. (1987) Evidence for a specific glutamate/H^+ cotransport in isolated mesophyll cells Plant Physiol. 83, 691-697

McCutcheon S.L., Ciccarelli, B.W., Chung, I., Shelp, B.J., and Bown, A.W. (1988) L-Glutamate-dependent medium alkalinization by *Asparagus* mesophyll cells Plant Physiol. 88, 1042-1047

McNeil, D.L., Atkins. C.A., and Pate, J.S. (1979) Uptake and utilizatin of xylem-borne amino compounds by shoot organs of a legume Plant Physiol. 63, 1076-1081

Melcher, I.M. (1986) Glutamate metabolism in intact seedlings and seedling segments of peas New Phytol. 103, 685-688

Menegus, F., Cattaruzza, L., Chersi, A., and Fronza, G. (1989) Difference in the anaerobic lactate-succinate production and in the changes of cell sap pH for plants with high and low resistance to anoxia Plant Physiol. 90, 29-32

Menegus, F., Brambilla, I., and Bertani, A. (1984) Nutrient translocation pattern and accumulation of free amino acids in rice coleoptile elongation under anoxia Physiol. Plant. 61, 203-208

Micallef, B.J., Shelp, B.J., and Ball, R.O. (1989) Quantification of ^{14}C-labeled amino acids by reverse-phase high performance liquid chromatography J. Liq. Chromatogr. 12, 1281-1300

Milloning, G. (1961) A modified procedure for lead staining of the thin sections J. Biophys. Biochem. 11, 736-739

Missen, A.W. and Wilson, A.T. (1970) The metabolism of *Sinapis alba* seeds in water under anaerobic conditions Phytochem. 9, 1473-1478

Mitchell, W.J., Booth, I.R., and Hamilton, W.A. (1979) Quantitative analysis of proton-linked transport system Biochem. J. 184, 441-449

Mizusaki, S., Noguchi, M., and Tamaki, E, (1964) Studies on nitrogen metabolism in tobacco plants Arch. Biochem. Biophys. 105, 599-605

Nelson, C.D. (1962) The translocation of organic compounds in plants Can. J. Bot. 40, 757-770

Nicholls, D.G. (1982) Bioenergetics : An introduction to the chemiosmotic theory Academic Press

Oghoghorie, C.G.O. and Pate, J.S. (1972) Exploration of the nitrogen transport system of a nodulated legume using ^{15}N Planta 104, 35-49

O'Neill, S.D. and Spanswick, R.M. (1984a) Solubilization and reconstitution of a vanadate - sensitive H^+-ATPase from the plasma membrane of *Beta vulgaris* J. Membrane Biol. 79, -243

O'Neill, S.D. and Spanswick, R.M. (1984b) Characterization of native and reconstituted plasma membrane H^+-ATPase from the plasma membrane of *Beta vulgaris* J. Membrane Biol. 79, 245-256

Pate, J.S. (1975) Exchange of solutes between phloem and xylem and circulation in whole plant *in* Encyclopedia of Plant Physiology, New Series, Vol. 1. Zimmermann, M.H. and Milburn, J.A. Eds. pp. 451-473, Spriger-Verlag, Berlin

Pate, J.S. (1980) Transport and partitioning of nitrogenous solutes Ann. Rev. Plant. Physiol. 31, 313-340

Pate, J.S. (1983) Distribution of metabolites *in* Plant Physiology A Treatise Vol. VIII : Nitrogen metabolism pp. 335-401, Academic Press

Pate, J.S. (1986) Nutrient and metabolites of fluides recovered from xylem and phloem : significance in relation to long -distance transport in plants *in* Transport and transfer process in plants pp. 253-281

Pate, J.S., Atkins, C.A., Herridge, D.F., and Layzell, D.B. (1981) Synthesis, storage and utilization of amino compounds in white lupin (*Lupinus albus* L.) Plant Physiol. 67, 37-42

Pate, J.S., Atkins, C.A., Hamel, K., McNeil, D., and layzell, D. (1979) Transport of organic solutes in phloem and xylem of a nodulated legume Plant Physiol. 63, 1082-1088

Pate, J.S., Gunning, B.E.S., and Milliken, F.F. (1970) Function of transfer cells in the nodal regions of stems, particularly in relation to the nutrition of young seedlings Protoplasma 71, 313-334

Pate, J.S., Layzell, D.B., and McNeil, D.L. (1979) Modeling the transport and utilization of carbon and nitrogen in nodulated legume Plant Physiol. 63, 730-737

Pate, J.S. and O'Brien, T.P. (1968) Microautoradiographic study of the incorporation of labeled amino acids into insoluble compounds of the shoot of a higher plants Planta 78, 60-71

Pate, J.S., Peoples, M.B., and Atkins, C.A. (1984) Spontaneous phloem bleeding from cryopunctured fruits of a ureide -producing legume Plant Physiol. 74, 499-505

Pate, J.S., Sharkey, P.J., and Lewis, O.A.M. (1974) Phloem bleeding from legume fruit - a technique for study of fruit nutrition Planta 120, 229-243

Pate, J.S., Sharkey, P.J., and Lewis, O.A.M. (1975) Xylem to phloem transfer of solutes in fruiting shoots of legumes, studies by a phloem bleeding technique Planta 122, 11-26

Pate, J.S., Walker, J., and Wallace, W. (1965) Nitrogen -containing compounds in the shoot system of *Pisum arvense* L. Ann. Bot. 29, 469-491

Pate, J.S. and Wallace, W., and van Die, J. (1964) Petiole bleeding sap in the examination of the circulation of nitrogenous substances in plants Nature 204, 1073-1074

Perlin, S.D. and Spanswick, R.M. (1981) Characterization of ATPase activity with corn leaf plasma membrane Plant Physiol. 68, 521-526

Rasi-Caldogno, F., Pugliarello, M.C., and De Michelis, M.I. (1985) Electrogenic transport of protons driven by the plasma membrane ATPase in membrane vesicles from radish Plant Physiol. 77, 200-205

Raven, J.A. and Smith, F.A. (1978) Effect of temperature and external pH on the cytoplasmic pH of *Chara corallina* J. Exp. Bot. 29,853-866

Reggiani, R., Cantu, C.A., Brambillka, I., and Bertani, A. (1988) Accumulation and interconversion of amino acids in rice roots under anoxia Plant and Cell Physiol. 29, 981-987

Reid, R.J., Field, L.D., and Pitman, M.G. (1985) Effects of external pH, fusicoccin and butyrate on the cytoplasmic pH in barley root tips measured by ^{31}P-nuclear magnetic spectroscopy Planta 166, 341-347

Reinhold, L. and Kaplan, A. (1984) Membrane transport of sugars and amino acids Ann. Rev. Plant Physiol. 35, 45-83

Reinold, E.S. (1963) The use of lead citrate at high pH as an electron opaque stain in electron microscopy J. Cell. Biol. 17, 208

Roberts, J.K.M., Callis, J., Jardetzky, O., Walbot, V., and Freeling, M. (1984) Cytoplasmic acidosis as a determinant of flooding intolerance in plants Proc. Natl. Acad. Sci. USA 81, 6029-6033

Robinson, S.P., and Beevers, H. (1981) Evidence for amino acid

: proton cotransport in *Riccinus* cotyledons Planta 152, 527-533

Rubinstein, B. and Tatter, T.A. (1980) Regulation of amino acid uptake into oat mesophyll cells J. Exp. Bot. 31, 269-279

Russin, W.A. and Evert, R.F. (1985) Studies on the leaf of *Populus deltoides* (Salicaceae) : Morphology and anatomy Am. J. Bot. 72, 487-500

Sanders, D. and Slayman, C.L. (1982) Control of intracellular pH :predominant role of oxidative metabolism, not proton transport, in the eukaryotic microorganism *Neurospora* J. Gen. Physiol. 80, 377-402

Satyanarayan and Nair, P.M. (1985) Purification and characterization of glutamate decarboxylase from *Solanum tuberosum* Eur. J. Biochem. 150, 53-60

Satyanarayan, V. and Nair, P.M. (1986a) Enhanced operation of 4-aminobutyrate shunt in Γ-irradiated potato tubers Phytochem. 25, 1801-1805

Satyanarayan, V. and Nair, P.M. (1986b) The 4-aminobutyrate shunt in *Solanum tubersum* Phytochm. 25, 997-1001

Sauer, N., Komor, E., and Tanner, W. (1983) Regulation and characterization of two inducible amino-acid transport system in *Chlorella vulgaris* Planta 159, 404-410

Secor, J. and Schrader, L. (1984) Characterization of amino acid efflux isolated soybean cells Plant Physiol. 74, 26-31

Selman, I.W. and Cooper, P. (1978) Changes in the free amino compounds in young tomato plants in light and darkness with particular reference to Γ-aminobutyric acid Ann. Bot. 423, 627-636

Serrano, R. (1984) Purification of the proton pumping ATPase from plant plasma membranes Biochem. Biophys. Res. Comm. 121, 735-740

Sharkey, P.J. and Pate, J.S. (1975) Selectivity in xylem to phloem transfer of amino acids in fruiting shoots of white lupin (*Lupinus albus* L.) Planta 127, 251-262

Shaw, M. and Coletelo, N. (1961) The physiology of host-parasite relations Can. J. Bot. 39, 1351-1372

Shelp, B.J. (1987) The composition of phloem exudate and xylem sap from broccoli (*Brassica oleracea* var. *italica*) supplied with NH_4^+, NO_3^- or NH_4NO_3 J. Exp. Bot. 38, 1619-1636

Sherwin, T. and Simon, E.W. (1969) The appearance of lactic acid in *Phasaeolus* seeds germinating under wet conditions J. Exp. Bot. 20, 776-785

Shimmen, T. and Tazawa, M. (1981) Dependency of H^+ efflux on ATP in cells of *Chara australis* Plant and Cell Physiol. 22, 1007- 1023

Singh, D. and Smalley, E.B. (1969) Changes in amino acid and sugar constituents of the xylem sap of American elm following inoculation with *Ceratocytis ulmi* Phytopathol. 59, 891-896

Slayman, C.L., Christopher, Y.H.Lu., and Shane, L. (1970) Correlated changes in membrane potential and ATP concentrations in *Neurospora* Nature 226, 274-276

Slayman, C.L., Long, W.S., and Lu, C.Y.H. (1973) The relationship between ATP and electrogenic pump in the plasma membrane of *Neurospora crassa* J. Membrane Biol. 14, 305-338

Smith, F.A. and Walker, N.A. (1976) Chloride transport in *Chara corallina* and the electrochemical potential difference for hydrogen ions J. Exp. Bot. 27, 451-459

Spanswick, R.M. and Miller, A.G. (1977) Measurement of the cytoplasmic pH in *Nitella translucens* : comparison of values obtained by microelectrode and weak acid methods Plant Physiol. 59, 664-666

Spedding, D.J. and Wilson, A.T. (1968) Studies of the early reactions in the germination of *Sinapis alba* seeds Phytochem. 7,897-901

Streeter, J.G. and Thompson, J.F. (1972a) Anaerobic accumulation of Γ-aminobutyric acid and alanine radich leaves (*Raphanus sativus* L.) Plant Physiol. 49, 572-578

Streeter, J.G. and Thompson, J.F. (1972b) *In vivo* and *In vitro* studies on Γ-aminobutyric acid metabolism with the radish plant (*Raphanus sativus* L.) Plant Physiol. 49, 579-584

Suzuki, M. (1981) L-Leucine transport in isolated protoplasts of *Vinca* suspension culture : characterization of uptake Plant and Cell Physiol. 22,1269-1278

Sze, H. (1985) H^+-translocating ATPases : advances using membrane vesicles Ann. Rev. Plant Physiol. 36, 175-208

Torimitsu, K., Yazaki, Y., Nagasuka, K., Ohta, E., and Sakata, M. (1984) Effect of external pH on the cytoplasmic and vacuolar pHs in mung bean root-tip cells Plant and Cell Physiol. 25, 1403-1409

Tsushida, T, and Murai, T. (1987) Conversion of glutamic acid to Γ-aminobutyric acid in tea leaves under anaerobic conditions Agric. Biol. Chem. 51, 2865-2871

Turgeon, R, (1973) Leaf development and phloem transport in *Cucurbita pepo* : transition from import to export Planta 113, 179-191

Turgeon, R. and Webb, J.A. (1976) Leaf development and phloem transport in *Cucurbita pepo* : maturation of the minor veins Planta 129, 265-26

Vandewalle, I. and Olssen, R. (1983) The Γ-aminobutyric acid shunt in germinating *Sinapis alba* seeds Plant Sci. Lett. 31, 269-273

Vogelmann, T.C., Dickson, R.E., and Larson, P.R. (1985) Comparative distribution and metabolism of xylem-borne amino compounds and sucrose in shoots of *Populus deltoides* Plant Physiol 77, 418-428

Wagner, G.J. (1979) Content and vacuole/extravacuole distribution of neutral sugars, free amino acids, and anthocyanin in protoplasts Plant Physiol. 64, 88-93

Wagner, G.J. and Murleady, P. (1983) Characterization and solubilization of nucleotide-specific Mg^{+2}-ATPase and Mg^{+2} -pyrophosphatasae of tonoplast Biochim. Biophys. Acta. 728, 267-280

Waldron, J.C. (1976) Nitrogen compounds transported in the xylem of sugar cane Aust. J. Plant Physiol. 3, 415-419

Walker, K.A., Givan, C.V., and Keys, A. (1984) Glutamic acid metabolism and the photorespiratory nitrogen cycle in wheat leaves Plant Physiol. 75, 60-66

Walker, N.A. and Smith, F.A. (1975) Intracellular pH in *Chara corallina* measured by DMO distribution Plant Sci. Lett. 4, 125-132

Wallace, W. and Pate, J.S. (1965) Nitrate assimilation in higher plants with special refernece to cocklebur (*Xanthium pennsylvanicum* Wallr.) Ann. Bot. 31, 213-228

Wallace, W., Secor, J., and Schrader, L.E. (1984) Rapid accumulation of Γ-aminobutyric acid and alanine in soybean leaves in response to an abrupt transfer to lower temperature, darkness, or mrchanical manipulation Plant Physiol. 75, 170-175

Wallsgrove, R.M., Tuner, J.C., and Hall, N.P., Kendel, A.C., and Bright, S.W. (1987) Barley mutant lacking chloroplast glutamine synthetase-biochemical and genetic analysis Plant Physiol. 83, 155-158

Wickremasinghe, R.L. and Swain, T. (1965) The accumulation of Γ-aminobutyric acid in bean callus tissue Phytochem. 4, 687-691

Wilding, M.D., Stahmann. M.A., and Smith, D. (1960) Free amino acids in alfalfa as related to cold hardiness Plant Physiol. 35, 726-732

Wooding, F.B.P. and Northcote, D.H. (1965) An anomalous wall thickening and its possible role in the uptake of stem-fed tritiated glucose by *Pinus pines* J. Ultrast. Res. 12, 463-472

Wray, V., Schiel, O., Berlin, J., and Witte, L. (1985) Phosphorus-31 nuclear magnetic resonance investigation of the *in vivo* regulation of intracellular pH in cell suspension cultures of *Nicotiana tabacum* Arch. Biochem. Biophys. 236, 731-740

Wyse, R.E. and Komor, E. (1984) Mechanism of amino acid uptake by sugarcane suspension cells Plant Physiol. 76, 865-870

Yamaki, S.(1982) Distribution of sorbitol, neutral sugars, free amino acids, malic acid, and hydrolytic enzymes in vacuoles of apple cotyledons Plant and Cell Physiol. 23, 881-889

Yamaya, T., Oaks, A., and Matsumoto, H. (1984) Characteristics of glutamate dehydrogenase in mitochondria prepared from corn shoots Plant Physiol. 76, 1009-1013

Yamaya, T., Oaks, A., Rhodes, D., and Matsumoto, H. (1986) Synthesis of $[^{15}N]H_4^+$ and [^{15}N]Glycine by mitochondria isolated from pea and corn shoots Plant Physiol. 81, 754-757

Ziegler, H. (1975) Nature of transported substances *in* Encyclopedia of Plant Physiology, New Series, Vol. 1. Zimmermann, M.H. and Milburn, J.A. Eds. pp. 59-100 Springer-Verlag, Berlin

Zimmermann, M.H., and Ziegler, H. (1975) List of sugars alcohols in sieve tube exudate *in* Encyclopedia of Plant Physiology, New Series, Vol. 1. Zimmermann, M.H. and Milburn, J.A. Eds. pp.480-503 Spriger-Verlag, Berlin